Experimental determination of the critical loci for {*n*-C_6H_{14} or CO_2 + alkan-1-ol} mixtures. Evaluation of their critical and subcritical behavior using PC-SAFT EoS.

Laura Gil, Sofía Blanco, Clara Rivas, Eduardo Laga, Javier Fernández, Manuela Artal*, Inmaculada Velasco

Departamento de Química Física, Facultad de Ciencias, Universidad de Zaragoza,

50009 Zaragoza, Spain

■ ABSTRACT

Vapor-liquid critical locus (x, T_c, P_c) has been determined, in the whole range of mole fractions, for the systems {*n*-hexane + methanol, or + ethanol, or + propan-1-ol, or + butan-1-ol} and {CO_2 + methanol, or + ethanol, or + propan-1-ol, or + butan-1-ol}.

A comprehensive bibliographic review for the vapor-liquid equilibrium (VLE) and the critical locus of these systems has been performed, and they have been modelled with PC-SAFT EoS. The three parameters that characterize the segments of pure compounds have been rescaled from their critical point values. In all cases, the classical mixing rules and temperature-dependent binary interaction parameters $k_{ij}(T) = k_{ij}^0 + k_{ij}^1 T$ have been used.

The average deviations obtained for the *n*-hexane + alkan-1-ol binary mixtures are: for critical loci, mean relative deviation in critical temperature $MRD(T_c)$ = 0.47 % and in critical pressure $MRD(P_c)$ = 3.38 %; for VLE, mean relative deviation in bubble pressure $MRD(P)$ = 2.90 % and absolute deviation for the solvent mole fraction in the vapor phase $\Delta y_{C_6H_{14}}$ = 0.031.

The average deviations obtained for the CO_2 + alkan-1-ol binary mixtures are: $MRD(T_c)$ = 1.91 % and $MRD(P_c)$ = 5.93 %; $MRD(P)$ = 7.07 % and Δy_{CO_2} = 0.022.

Keywords: Critical points; alkan-1-ol; *n*-hexane; carbon dioxide; PC-SAFT.

**Corresponding Author*

E-mail address: martal@unizar.es.

1. Introduction

Supercritical media exhibit two important and interesting properties as opposed to simple liquid solvents: (i) The values of densities can vary continuously from those typical of liquids to those typical of gases. By working at temperatures slightly higher than the critical temperature, it is possible to reach a broad range of densities by simply changing temperature and pressure conditions. (ii) The second property of supercritical fluids (SCF) is also related to the very high compressibility of the fluid near the critical point region. In this "compressible regime", the very high susceptibility of the solvent density to small variations of pressure generates strong density fluctuations at the microscopic level [1-3]. The presence of such microscopic density fluctuations in the solvent is therefore expected to have significant effects on the molecular arrangement and dynamics of the solute in such compressible SCF solutions. In particular, attractive solutes are expected to induce a region of local solvent density that can be greater than the density of the bulk solvent [4,5]. Additionally, the extent of this density enhancement is, at least partly, driven by the relative strength of solute-solvent versus solvent-solvent interactions.

Supercritical carbon dioxide ($scCO_2$) is often regarded as a "green" solvent because it is recyclable, has low toxicity, and is a nonflammable fluid. It can be used in the control of reaction rates, in the developing of efficient separation processes, and in the manufacturing of various kinds of special materials due to its easy tunability of solvent properties. However, although CO_2 is the most commonly used supercritical fluid, it is not the only one. In recent years, several industrial processes that use other types of fluids in the supercritical state have been developed. For example, supercritical hexane has been used as a reaction media in several processes such as hydrodeoxygenation of biocrude [6], Fischer-Tropsch (FT) synthesis [7,8], SynGas process [9,10], etc.

However, these fluids are only capable of dissolving polar and ionic materials to a very small extent, a fact which greatly limits their industrial use. To circumvent this disadvantage, some other polar compounds, such as small-chain alcohols, can be added as cosolvents to enhance the capacity of these fluids to dissolve this type of materials. Therefore, in order to understand this behavior it is essential to determine the exact type of molecular interactions present in non polar SCF - alcohol (cosolvent) systems. This study can be approached from a thermodynamic point of view through the experimental determination of the critical loci of these systems, and by means of modelling the behavior of these fluids in the upper limit of the gas-liquid phase equilibrium.

When using an alkane as a SCF together with an alcohol, the only non-dispersive interaction present in the mixture is the alcohol - alcohol hydrogen bonding, which can lead to different types of molecular aggregates. On the other hand, those interactions emerging when alcohols act as cosolvents in the $scCO_2$ media are much more complex. In addition to the non-dispersive interactions and the hydrogen bonds among alcohol molecules, there exist some other specific interactions: carbon atom of CO_2 - oxygen atom of alcohol and CO_2 - alcohol hydrogen bonding (between an oxygen atom of CO_2 and the hydrogen atom of the hydroxyl group). To develop this study, it is necessary to take into account the nature of CO_2.

Although CO_2 was originally considered to be a non-polar solvent comparable to alkanes because of its low dielectric constant and zero dipole moment, this view is slowly changing. The charge separation and electronic structure of CO_2 (the carbon atom in a CO_2 molecule is electron deficient, whereas the oxygen has two lone pairs of electrons) generate a significant quadrupole moment and allow it to act, depending on its environment, either as a Lewis acid (LA) or as a Lewis base (LB). These conditions can induce a dipole moment in the CO_2 molecule. In the above situation, the carbon atom behaves as an electron acceptor from a neighboring molecule, whereas the oxygen atom plays as an electron donor. The miscibility of cosolvents such as alcohols in CO_2 is closely linked to this aspect of the carbon dioxide molecule. In general, sp^3 oxygen atoms are better electron donors than sp^2 oxygen atoms. Therefore, in CO_2 - alcohol mixtures, oxygen atoms from an alcohol are also expected to participate in a LA - LB interaction (electron donor - acceptor, EDA, complex) similar to that of the CO_2 - carbonyl group. Danten et al. [11] and van Ginderen et al. [12] show how the interaction between CO_2 and sp^3 oxygen of methanol is energetically almost as favorable as those calculated by Raavendran and Wallen [13] for the CO_2 - acetaldehyde or methyl acetate mixtures.

As mentioned above, the CO_2 oxygen atoms could participate in hydrogen bonding with molecular systems carrying electron-deficient hydrogen atoms: Raavendran and Wallen´s ab initio calculations [13,14] revealed that in CO_2 + acetaldehyde or + methyl acetate systems, the CO_2 oxygen participates in a cooperative C-H…O hydrogen bond, apart from the EDA interaction.

Raman spectroscopic studies of acetaldehyde and CO_2 mixtures [15] showed the presence of both interactions: EDA complex, corresponding to the carbonyl stretching band red-shifting, and a blue-shifting attributed

to the cooperative C-H…O hydrogen bond between the aldehyde C-H and the CO_2 oxygen. Fujii et al. [16] used IR spectroscopy to reveal the formation of conventional hydrogen bonds between an oxygen atom of CO_2 and hydroxyl (OH) groups. Saharay and Balasubramanian [17] carried out Car-Parrinello molecular dynamics simulation studies of a system containing ethanol (EtOH) and CO_2. They concluded that carbon dioxide and ethanol can interact with each other by forming an EDA complex or through the formation of a hydrogen bond. Xu et al. [18] analyzed and compared, using Monte Carlo simulations, the following three interactions in some EtOH + CO_2 mixtures: EtOH - EtOH hydrogen bonding, EtOH - CO_2 hydrogen bonding and EtOH - CO_2 EDA bonding.

In our current investigation, the critical loci of mixtures containing *n*-hexane or carbon dioxide + alkan-1-ols have been determined experimentally along the whole composition range. Likewise, an exhaustive review of the critical locus and vapor-liquid equilibrium of these systems has been carried out with the aim of modelling its thermodynamic behavior, both in critical and subcritical conditions.

2. Model

In this work, the PC-SAFT model, developed by Gross and Sadowski [19,20] has been used. In this model, molecules are conceived to be chains composed of spherical segments in which the pair potential for the segment of a chain is given by a modified square-well potential. When the molecules exhibit various attractive interactions, the equation of state is given as the sum of the ideal-gas contribution, a hard-chain term, a contribution for the dispersive attraction and several terms for associating, dipolar and quadrupolar interactions. The form of the PC-SAFT equation of state written in terms of the Helmholtz energy, a, is:

$$a = a^{id} + a^{hc} + a^{dis} + a^{assoc} + a^{polar} \tag{1}$$

$$a = a^{id} + a^{hc} + a^{dis} + a^{assoc} + (a^{QQ} + a^{DD} + a^{QD})$$

For the pure compounds a maximum of 5 parameters are needed: the segment number, *m*, the segment diameter, σ, the segment energy parameter, ε, the volume of association, $\kappa^{A_iB_i}$, and the energy of association, $\varepsilon^{A_iB_i}$. *m*, σ and ε ("geometric parameters") are needed for every molecule. $\kappa^{A_iB_i}$ and $\varepsilon^{A_iB_i}$ ("association parameters") are only needed if the molecule is self-associated and therefore the association scheme of the compound should be established. Due to their physical meaning, the association parameters ($\kappa^{A_iB_i}$, $\varepsilon^{A_iB_i}$) could be

estimated from molecular orbital calculations or based on experimental values of the enthalpy and entropy of hydrogen bonding [21-23]. Thus, only three parameters (m, σ, ε) remain to be fit to vapor pressures and liquid densities. These parameters provide an accurate representation for both volumetric and vapor-liquid equilibrium properties, but they always overestimate the values for the critical properties. Other SAFT versions have been proposed to describe the critical area at the expense of using more adjustable parameters [24,25]. On the other hand, Cismondi et al. [26] present a rescaling of PC-SAFT pure-compounds parameters from critical temperature and pressure (T_c and P_c), for which the critical point is matched. We also rescaled the PC-SAFT pure-compounds parameters for the CO_2 + alkane mixtures in previous works [27,28], and we were able to represent the volumetric and critical mixture properties without major deviation.

Following this approach, both properties, VLE phase equilibria and critical locus of each studied mixture, are going to be represented through a single set of pure-compounds parameters. We calculated the pure CO_2 geometric parameters (m, σ, ε) in a previous work [27]. For pure *n*-hexane and pure alkan-1-ols these parameters (m, σ, ε) have been rescaled from their critical points using the method described by Heidemann et al. [29], employing the objective function:

$$OF = \left[\left(\frac{T_c^{\exp} - T_c^{\mathrm{cal}}}{T_c^{\exp}}\right)^2 + \left(\frac{P_c^{\exp} - P_c^{\mathrm{cal}}}{P_c^{\exp}}\right)^2\right] \tag{2}$$

where “exp” and “cal” superscripts refer to the experimental and calculated values, respectively.

The association parameters ($\kappa^{A_iB_i}$ and $\varepsilon^{A_iB_i}$) for the pure alcohols have been extracted from Gross and Sadowski [20], where the association scheme 2B (molecule with two association sites, 1-electron donor and 1-electron acceptor) [30] was used. CO_2 has been considered as a non self-associated molecule [27,28].

When dealing with mixtures, classical mixing rules have been used and temperature-dependent binary interaction parameters $k_{ij}(T) = k_{ij}^0 + k_{ij}^1 T$ have been introduced. Several authors [31-35] have shown that the use of a temperature-dependent binary interaction parameter is justified if the modelling temperature range is wide or the mixtures are very asymmetric, either in size or interactions. Critical loci calculations were carried out using the method described by Heidemann et al. [29]. For VLE we have used bubble point calculations, which obtain bubble

pressure and vapor-phase composition from liquid-phase composition at a given temperature. The estimation of the $k_{ij}(T)$ parameters from VLE data has been performed using the objective function:

$$OF = \sum_{i=1}^{N} \left(\frac{P_i^{\exp} - P_i^{\text{cal}}}{P_i^{\exp}} \right)^2 \quad (3)$$

3. Experimental Section

3.1. Materials.

The compounds were used as received withuot further purification. Table 1 shows their purity, their water content, the suppliers and our experimental values for T_c and P_c, as well as those recommended by the National Institute of Standars and Technology (NIST) [36].

3.2. Apparatus and procedures.

The experimental setup used in this work is the same as that described in previous studies [37]. The flow apparatus was designed by ARMINES at the École Nationale Supérieure des Mines de Paris (France) and manufactured by TOP-INDUSTRIE. The apparatus allows critical property measurements (P_c and T_c) of pure compounds and mixtures up to 700 K and 20 MPa. These measurements are carried out by observing the critical opalescence (a video is available in the online version) in a sapphire transparent cell. Similar facilities have been used in previous works of Soo et al. [38], Horstman et al. [39-42], Guilbot et al. [43], and Juntarachat et al. [44,45]. The uncertainties in the critical temperature and the critical pressure for pure compounds are [37]: repeatability in the critical temperature ≤ 0.14 K, repeatability in the critical pressure ≤ 0.011 MPa, and the confidence intervals are *c.i.*(T_c) < 0.1 K and *c.i.*(P_c) < 0.01 MPa. For the mixtures, the repeatabilities in critical temperature and pressure are ≤ 0.15 K and ≤ 0.013 MPa, and the confidence intervals calculated are *c.i.*(T_c) < 0.32 K and *c.i.*(P_c) < 0.034 MPa. Finally, for the mixtures studied in this work a mean value uncertainty in the mole fraction, $u(x_j)$ = ± 0.0015 has been obtained.

3.3. Experimental results.

n-hexane + alkan-1-ol systems

Experimental results (x, T_c, P_c) for the critical locus of the systems *n*-hexane + alkan-1-ol (methanol, ethanol, propan-1-ol, butan-1-ol) are given in Table 2 and Figures 1a, 1b, 1c. Each mixture was studied over the whole range of compositions, with at least twenty-one experimental points (including pure compounds ones) at mole fraction intervals of approximately 0.05.

All the systems display an uninterrupted (gas + liquid) critical locus which connects the critical points of the pure components. This indicates that the fluids belong either to Type I or Type II fluid phase behavior, according to the classification of van Konynenburg and Scott [46]. Several authors [47-50] report partial miscibility for *n*-hexane + methanol mixtures, a fact which implies that they are Type II fluids. For the rest of the systems, no indication of partial miscibility has been found in the literature. *n*-hexane + methanol, or + ethanol or + propan-1-ol present a minimum temperature point in the critical locus curve. This is characteristic of systems whose components have small differences in T_c and form positive (minimum boiling) azeotropes extending up to their critical region [51]. The lower the number of carbon atoms in the alkan-1-ol (the closer its T_c to that of the *n*-hexane) the deeper the minimum is. Simultaneously, as the number of carbon atoms in the alkan-1-ol increases (and with it, its T_c), the minima in critical temperature points shift to richer compositions in *n*-hexane. The mixture containing butan-1-ol, whose T_c is the highest, does not present a temperature minimum. The P_c-x projections of the systems are monotonic functions.

In the literature there exist few data on the critical points of *n*-hexane + alkan-1-ol studied mixtures [38,50,52-63], and more than half of the references do not provide the three variables x, P_c and T_c, or do not cover the whole range of compositions or neither of them. The whole set of experimental data (from this work and literature) is represented in Figures SF1 - SF6. These figures and the comparison between our experimental results and those from literature are included in the Supplementary Data.

CO_2 + alkan-1-ol systems

The experimental results (x, T_c, P_c) for the critical locus of the systems CO_2 + alkan-1-ol (methanol, ethanol, propan-1-ol and butan-1-ol) are given in Table 3 and Figures 2a, 2b, 2c. Each mixture was studied over the whole range of compositions, with at least twenty-one experimental points (including pure compounds ones) at mole fraction intervals of approximately 0.05.

From our results we deduce a fluid phase behavior of Type I or Type II for these mixtures, according to the classification of van Konynenburg and Scott [46], although many discrepancies have been found in the literature about the exact corresponding type. Lam et al. [64] indicate that the lightest alkan-1-ol exhibiting LLV immiscibility with CO_2 is propan-1-ol. Likewise, Polishuk et al. [65], from experimental results of several authors, assign CO_2 + methanol and CO_2 + ethanol to Type I and CO_2 + butan-1-ol to Type II. Secuianu et al. [66-68] attribute the mixtures containing methanol and ethanol to Type I as well, and include CO_2 + propan-1-ol in Type III. Nevertheless, Roman-Ramírez et al. [31] report that CO_2 + methanol or + ethanol or + propan-1-ol belong to Type II while Peters and Gauter [69] state that the four systems (CO_2 + methanol, or + ethanol, or + propan-1-ol, or + butan-1-ol) are Type II.

The critical loci curves have neither maxima nor minima in temperature, although all of them present a point of maximum critical pressure. This behavior is typical of those systems whose components differ greatly in physical and chemical properties but do not form azeotropes [51]. Ethanol, propan-1-ol and butan-1-ol have lower P_c than CO_2 and such P_c values reduce as the number of C atoms in the alkan-1-ol increases. This results in these mixtures exhibiting higher critical pressure values the higher the number of carbon atoms present in the alkan-1-ol. P_c of methanol is higher than that of CO_2 and the maximum critical pressure value for the mixture lays between CO_2 + propan-1-ol and CO_2 + butan-1-ol ones. The compositions at the maximum critical pressure points are located in the CO_2-rich zone, and they shift to regions richer in CO_2 as the number of carbon atoms in the alkan-1-ol increases.

Critical point data of CO_2 + methanol [54,70-81] and CO_2 + ethanol [73,75-78,82-93] mixtures are abundant in the literature, but they are scarcer for mixtures with propan-1-ol [68,73,75,78,88,94] or butan-1-ol [73,75,78,95,96]. 90% of the references do not give the three variables x, P_c and T_c, or do not cover the whole range of compositions or neither of them. The whole set of experimental data (this work and literature) is represented in Figures SF7 - SF10.

These figures and the comparison between our experimental results and those from literature are included in the Supplementary Data.

The agreement between the authors is in general better in the P_c-T_c projection than in the T_c-x and P_c-x planes. This fact becomes much more evident for the CO_2 + methanol or + ethanol systems. Errors in the determination of the real composition of the critical mixtures could be attributed to the difficulty in achieving a homogeneous mixture. To overcome this problem in our current investigation, we have carried out all our experimental measurements by paying special attention to several aspects of the setup: the pump flows have been adjusted according to the viscosities and densities of the chemicals, and the length of the tubing conducting the mixture to the cell has been increased. Another contribution to the aforementioned disagreements could also be found in the different sources, purities and water contents of the chemicals used by the different authors.

4. Discussion

4.1. n-hexane + alkan-1-ol systems

Mixtures that contain a polar component and an alkane show a transitional behavior between non-associating and associating mixtures. The specific interactions (polar and hydrogen bonding) exhibited between alcohol molecules are strongly affected when surrounded even by a single alkane molecule in their proximity. As a result, modelling of *n*-hexane + alcohol mixtures should be based preferentially on theories with strong molecular origin that contain a quantitative account of the pertinent intermolecular forces between like and unlike molecules such as PC-SAFT EoS. In this work, *n*-hexane + alkan-1-ol systems have been modelled over the whole composition range and over the temperature and pressure ranges which are reported in Table 4.

Table 5 shows the geometric pure-compounds paramenters for *n*-hexane + alkan-1-ol mixtures rescaled in this work, as well as the association parameters for pure alkan-1-ols with a 2B association scheme, taken from reference [20].

For the mixtures, classical mixing rules have been used and only one temperature dependent binary interaction parameter $k_{ij}(T) = k_{ij}^0 + k_{ij}^1 T$ has been introduced to model both VLE and critical locus of each system.

We have used for modelling about 1970 VLE experimental values from the literature [48,50,52,55-57,97-130] and 245 critical experimental values from this work and other literature data [38,50,52-63]. Unpublished data from Laga [63], determined with the same apparatus that we used in our investigation, are included. Tables 6 and 7 show the number of experimental points and the corresponding authors for both critical loci and VLE, as well as the comparison of PC-SAFT results with experimental data by means of the values of the mean relative deviations, *MRD*, for critical temperature, critical pressure and bubble pressure, obtained from equation 4,

$$MRD(X) = \frac{100}{N}\sum_{n=1}^{N}\left|\frac{X_n^{\mathrm{exp}} - X_n^{\mathrm{calc}}}{X_n^{\mathrm{exp}}}\right| \tag{4}$$

where *X* refers to a generic variable and *N* is the number of experimental points. For VLE, the absolute deviations for the solvent mole fraction in the vapor phase $\Delta y_{\mathrm{C_6H_{14}}}$ (eq. 5) are also included.

$$\Delta y = \frac{1}{N}\sum_{n=1}^{N}\left|y_n^{\mathrm{exp}} - y_n^{\mathrm{cal}}\right| \tag{5}$$

Figures 1a, 1b and 1c show the experimental and calculated critical loci for these systems and Figures 3 and 4 show VLE (experimental and calculated) for *n*-hexane + methanol or + ethanol mixtures. The corresponding figures for the rest of the VLE systems are included in the Supplementary Data (Figures SF11 - SF14).

As it can be seen, there is a good agreement between experimental values and those calculated by using a single set of pure-compounds parameters and only one temperature-dependent binary interaction parameter for the two kind of properties of each mixture. The mean values of the deviations are: $MRD(T_c)$ = 0.47 % and $MRD(P_c)$ = 3.38 % for the critical locus and $MRD(P)$ = 2.90 % and $\Delta y_{\mathrm{C_6H_{14}}}$= 0.031 for the VLE.

The modelling has been carried out using temperature-independent binary interaction parameters k_{ij} as well. Tables ST1 and ST2 (Supplementary Data) show values for $k_{ij}(T)$ and k_{ij} as well as *MRD* and Δy for each system in both calculations. As it can be observed, the values obtained for critical loci do not differ greatly from those calculated with $k_{ij}(T)$ as expected due to the fact that critical temperatures of both components are similar. However, the results for VLE are worse than those obtained with $k_{ij}(T)$.

Some studies of the performance of different SAFT types in alkane - alkanols mixtures have been published

[32,33,131-137]. None of the authors carried out their studies in a wide range of temperatures, neither do they calculate simultaneously the VLE and the critical locus of the systems. Table ST3 (Supplementary Data) shows the deviations obtained by the preceeding authors and those obtained by us. As it can be observed, our deviations are similar to those obtained by other authors even though we have modelled with only one binary interaction parameter both the critical locus and the VLE over the whole composition range and over a wide range of temperature.

4.2. CO_2 + alkan-1-ol systems

We have used PC-SAFT EoS to model the systems CO_2 + alkan-1-ol as well, but the scheme to represent these mixtures has to differ from that used to represent *n*-hexane + alkan-1-ol mixtures, since these systems present different types of interactions and thus very different behavior from the preceeding mixtures (Figures 1a, 1b, 1c and 2a, 2b, 2c).

In these systems, beside the dispersive interactions and alcohol - alcohol hydrogen bonding, there are other specific interactions: carbon atom of CO_2 - oxygen atom of alcohol and CO_2 - alcohol hydrogen bonding (between an oxygen atom of CO_2 and the hydrogen atom of the hydroxyl group). The association theories belonging to the SAFT family explicitly account for self- and cross-association, or solvation phenomena, due to the Lewis acid - Lewis base interaction. When modeling systems containing CO_2 and alcohols, the important question of what model to choose arises. There are many studies in the literature on this topic. Some of them [34,138] conclude that the solvation/association effect for CO_2 must be included, whereas others [31] remark that the introduction of polar contributions in the model (PCSAFT-Q, PCSAFT-D, PCSAFT-QD) do not improve it substantially. Finally, other authors [33,94,95,133,139,140,143] utilize other models from which some of them obtain better results, but at the expense of increasing the number of parameters. None of these studies performes an exhaustive correlation from bibliographic VLE and critical data. Table ST4 (Supplementary Data) shows the deviations obtained by the preceeding authors (when numeric values are available) and those obtained by us. As it can be observed, our deviations are similar to those obtained by other authors even though we have modelled the critical locus and the VLE over the whole composition range and over a wide range of temperature.

On the other hand, simulation studies show the influence of temperature, pressure and composition on the interactions in these mixtures. Xu et al. [18] have studied the microscopic structure and molecular interactions of mixtures containing supercritical carbon dioxide and ethanol (EtOH) using Monte Carlo simulations and they have calculated the average number of bonding for each type of present interaction (EtOH – EtOH hydrogen bonding, EtOH - CO_2 hydrogen bonding and EtOH - CO_2 EDA bonding) as a function of temperature, pressure and mole fraction. The average number of EtOH - EtOH hydrogen bonding (which is the highest) increases significantly with ethanol mole fraction, however it also decreases significantly with temperature and pressure; the average number of EtOH - CO_2 hydrogen bonding (the lowest), decreases slightly with ethanol mole fraction, does not vary with temperature and increases slightly with pressure; finally, for EtOH - CO_2 EDA bonding, the average number of these interactions shows a similar behavior to the average number of EtOH - CO_2 hydrogen bonding though its values are slightly higher.

Fulton et al. [144] use Fourier transform infrared (FTIR) spectroscopy to study the aggregation of a series of small alcohols in supercritical CO_2 and supercritical ethane; they conclude that the specific interaction CO_2 quadrupole - alcohol dipole is not present in the alkane-alcohol system and that the solubility of the alcohol in CO_2 greatly increases. Likewise, they affirm that this interaction also perturbs the monomer-aggregate equilibria towards the monomer form of the alcohol. Thus, at a temperature of 313 K, 20 MPa pressure and an alcohol (methanol, ethanol and butan-1-ol) mole fraction from 0.03 to 0.15, the monomeric alcohol concentration in CO_2 is around three times of that in ethane.

In this work, the systems have been studied over the whole composition range and over the temperature and pressure ranges which are reported in Table 4. The number of experimental points from the literature as well as the corresponding authors for both critical loci [54,68,70-92,94-96] and VLE [66-68,71,74-77,79,85-92,95,96,145-195] are shown in Tables 8 and 9. All the experimental data (around 2250 VLE and 350 critical values) were used in the modelling, except those for VLE marked with an asterisk in Table 9 (46 values), due to their very high deviations.

Table 10 shows the rescaled geometric pure-compounds parameters for CO_2 (previous work [27]) and alkan-1-ols (this work) as well as the utilized association scheme and the pure-compounds association parameters.

In these systems classical mixing rules have been used and due to their complexity (different types of specific interactions), the wide range of temperatures studied and the different behavior of the supercritical systems, it has been necessary to adjust one temperature-dependent binary interaction parameter $k_{ij}(T) = k_{ij}^0 + k_{ij}^1 T$ for each of the two properties studied, VLE and critical locus, for a given system. These values, together with the mean deviations obtained, *MRD* (eq. 4), for the critical temperature, critical pressure and bubble pressure are collected in Tables 8 and 9. For VLE, the absolute deviations for the solvent mole fraction in the vapor phase $\Delta y_{\mathrm{CO_2}}$ (eq. 5) are also included.

Regarding the association, we find a similar behavior to that observed by Fulton et al. [144]. When modeling $\mathrm{CO_2} + n - \mathrm{C}_m\mathrm{H}_{2m+1}\mathrm{OH}$ ($m \neq 1$) mixtures with a given association scheme for the alcohols (2B for instance) results are unsatisfactory, either for VLE or for the critical locus. The net balance of the three types of specific interactions that appear competing in these systems, in addition to the occasionally opposed effects of temperature, pressure and composition, has led us to choose a scheme without association of hydrogen bonding and without cross-association to represent CO_2 + ethanol or + propan-1-ol or + butan-1-ol systems.

Nevertheless, CO_2 + methanol behavior is different. The critical locus of this system could be represented without great deviations with the same scheme as above (*MRD*(T_c) = 1.9 % and *MRD*(P_c) = 6.1 %), but the representation of its VLE is unsatisfactory. Since methanol has higher self-association energy (Table 5) and dielectric constant than any of the other three alcohols (methanol: 33.0; ethanol: 25.3; propan-1-ol: 20.8; butan-1-ol: 17.8) [196], we have to take into account all the present interactions in this mixture. For this reason we have chosen a scheme where the molecule of methanol is considered both as a donor and as an acceptor centre (2B scheme), and the CO_2 as a two-electron donor (with two negative sites which are only active when mixed with a molecule with at least one positive or neutral site), 2C scheme [197].

As we have considered pure CO_2 as a non self-associated molecule, it is not possible to calculate its volume and energy of association. The Dortmund approximation based on the Kleiner and Sadowski method has been chosen [198] to calculate the mixture association parameters:

$$\varepsilon^{A_iB_j} = \frac{\varepsilon^{assoc}}{2} \qquad \kappa^{A_iB_j} = \kappa^{assoc} \tag{6}$$

where ε^{assoc} and κ^{assoc} are respectively the energy of association and the volume of association of the associated compound, in our case methanol.

With this association scheme it is only necessary one temperature-dependent binary interaction parameter $k_{ij}(T) = k_{ij}^0 + k_{ij}^1 T$ to represent both VLE and critical locus. These values, together with the mean deviations obtained, *MRD* (eq. 4), for the critical temperature, critical pressure and bubble pressure are collected in Tables 8 and 9. For VLE, the absolute deviations for the solvent mole fraction in the vapor phase Δy_{CO_2} (eq. 5) are also included.

Figures 2a, 2b and 2c show the experimental and calculated critical loci for these systems and Figures 5 and 6 the VLE (experimental and calculated) for CO_2 + methanol or + ethanol mixtures. The corresponding figures for the rest of the VLE systems are included in the Supplementary Data (Figures SF15 - SF16).

There is a good agreement between experimental and calculated values of these properties. The obtained deviations are: *MRD*(T_c) = 1.91 % and *MRD*(P_c) = 5.93 %, *MRD*(P) = 7.07 % and Δy_{CO_2} = 0.022.

The modelling has been carried out using temperature-independent binary interaction parameters k_{ij} as well. Tables ST1 and ST2 (Supplementary Data) show values for $k_{ij}(T)$ and k_{ij} as well as *MRD* and Δy for each system in both calculations. As it can be seen, the improvement is noticeable when using temperature-dependent binary interaction parameters, as expected due to the different values of the critical temperatures of the pure components (assymetric mixtures).

Finally, we have represented the ternary critical locus [54] and VLE [199] for *n*-C_6H_{14} + CO_2 + CH_3OH, both found in the literature. For this purpose, we have used the parameters obtained in this work for the binary interactions CO_2 - CH_3OH and *n*-C_6H_{14} - CH_3OH , and for the interaction CO_2 - alkane we have used those parameters obtained by us in earlier reports [27], k_{ij} = 0.09. The calculated deviations for the critical locus of the ternary mixture (*MRD*(T_c) = 3.5 % and *MRD*(P_c) = 7.1 %) are similar to those obtained for the corresponding binary mixtures determined by the same author, a fact that indicates that the presence of a third component does not modify the binary interaction between the other two, and that significant ternary interactions do not exist in the mixture. The calculated deviation for the VLE of the ternary mixture is *MRD*(P) = 8.26%.

5. Conclusions

In this work, the critical locus of the mixtures $n-\mathrm{C_6H_{14}} + n-\mathrm{C}_m\mathrm{H}_{2m+1}\mathrm{OH}$ and $\mathrm{CO_2} + n-\mathrm{C}_m\mathrm{H}_{2m+1}\mathrm{OH}$ $(m = 1-4)$, has been determined experimentally over the entire range of compositions. The measurements were carried out using an experimental setup that includes a flow apparatus for the determination of critical temperature and pressure (P_c, T_c), using a critical opalescence method. All the systems display an uninterrupted (gas + liquid) critical locus connecting the critical points of the pure components.

$n-\mathrm{C_6H_{14}} + n-\mathrm{C}_m\mathrm{H}_{2m+1}\mathrm{OH}$ $(m = 1-3)$ systems present a minimum in the T_c-x projection, which is more pronounced the lower the number of carbon atoms in the alcohol is. Simultaneously, we observed that the minimum shifts to richer compositions in *n*-hexane as the number of carbon atoms in the alcohol (and thus its T_c) increases. In the P_c-x projection, all the lines are monotonic.

In $\mathrm{CO_2} + n-\mathrm{C}_m\mathrm{H}_{2m+1}\mathrm{OH}$ $(m = 1-4)$ systems, the critical locus curves have neither maximum nor minimum points in temperature and all of them present a point of maximum critical pressure located in the CO_2-rich zone, shifting to regions richer in CO_2 as the number of carbon atoms of the alcohol increases.

In this work, a comprehensive bibliographic review of the phase equilibrium of the systems containing *n*-hexane + alkan-1-ol (methanol, ethanol, propan-1-ol, butan-1-ol, pental-1-ol and hexan-1-ol) and CO_2 + alkan-1-ol (methanol, ethanol, propan-1-ol and butan-1-ol) has been undertaken with the aim of modelling their thermodynamic behavior under critical and subcritical conditions. For this, PC-SAFT EoS has been used. The geometrical parameters for the pure compounds have been rescaled from the values of their critical points. In all cases, classical mixing rules and temperature-dependent binary interaction parameters $k_{ij}(T) = k_{ij}^0 + k_{ij}^1 T$ have been used.

In this manner, approximately 2215 points (VLE and critical loci) have been modelled for the $n-\mathrm{C_6H_{14}} + n-\mathrm{C}_m\mathrm{H}_{2m+1}\mathrm{OH}$ $(m = 1-6)$ systems in a temperature range from 263 to 588 K. The results show that these systems are well represented by PC-SAFT EoS when using a 2B association scheme for the alcohols and only one temperature-dependent binary interaction parameter for both VLE and critical locus of each system. The deviations obtained are *MRD*(T_c) = 0.47 % and *MRD*(P_c) = 3.38 % for the critical locus and *MRD*(P) = 2.90 % and $\Delta y_{\mathrm{C_6H_{14}}}$ = 0.031 for the VLE.

Additionally, we have analyzed the behavior of $CO_2 + n - C_mH_{2m+1}OH$ $(m = 1 - 4)$ mixtures for approximately 2600 points (VLE and critical loci) in a range from 213 to 563 K. In these systems, besides the dispersive interactions and alcohol - alcohol hydrogen bonding, some other specific interactions exist: carbon atom of CO_2 – oxygen atom of alcohol and CO_2 - alcohol hydrogen bonding, between an oxygen atom of CO_2 and the hydrogen atom of the hydroxyl group. Association theories like those of the SAFT family account explicitly for self- and cross-association or solvation phenomena due to the Lewis acid - Lewis base interaction. Thus, we have obtained good results for the CO_2 + methanol mixtures when including solvation phenomena (2C scheme) in CO_2 and association (2B scheme) in methanol, and only one temperature-dependent binary interaction parameter for both VLE and critical locus. For the rest of the alcohols, the net balance of the three types of specific interactions that seem to compete in these systems, in addition to the occasionally opposed effects of temperature, pressure and composition, has lead us to choose a scheme without association; nevertheless, in this case, the temperature-dependent binary interaction parameters when representing the VLE and critical locus are different. For the CO_2 + alkan-1-ol systems the deviations obtained are: $MRD(T_c)$ = 1.91 %, $MRD(P_c)$ = 5.93 %, $MRD(P)$ = 7.07 % and Δy_{CO_2} = 0.022.

Finally, we have represented the ternary critical locus and VLE for *n*-C_6H_{14} + CO_2 + CH_3OH, both found in the literature. To do this, we have used the parameters obtained in this work for the binary interactions CO_2 - CH_3OH and *n*-C_6H_{14} - CH_3OH, and for the CO_2 - alkane interaction those parameters obtained by us in earlier studies. The calculated deviation for the ternary mixture ($MRD(T_c)$ = 3.5 % and $MRD(P_c)$ = 7.1 %) is similar to that obtained for the corresponding binary mixtures determined by the same authors, which indicates that the presence of a third component does not modify the binary interaction between the other two and that a significant ternary interaction does not exist in the mixture.

In this work, the computations were performed using the VLXE software [200] for the PC-SAFT EoS calculations.

Suplementary data

Supplementary data include:

*P_c-T_c, P_c-x and T_c-x representations of experimental data from this work and literature for *n*-hexane + methanol, or + ethanol, or + propan-1-ol, or + butan-1-ol, or + pentan-1-ol, or + hexan-1-ol mixtures (Figures SF1, SF2, SF3, SF4, SF5 and SF6, respectively).

* A comparison between this work experimental data and those from literature for the critical loci of *n*-hexane + alkan-1-ol systems.

*P_c-T_c, P_c-x and T_c-x representations of experimental data from this work and literature for CO_2 + methanol, or + ethanol, or + propan-1-ol, or + butan-1-ol mixtures (Figures SF7, SF8, SF9 and SF10, respectively).

*A comparison between this work experimental data and those from literature for the critical loci of CO_2 + alkan-1-ol systems.

*VLE representations for *n*-hexane + propan-1-ol, or + butan-1-ol, or + pentan-1-ol, or + hexan-1-ol mixtures (Figures SF11, SF12, SF13 and SF14, respectively).

*VLE representations for CO_2 + propan-1-ol and + butan-1-ol mixtures (Figures SF15 and SF16, respectively).

*Table ST1 including values for the temperature-dependent, $k_{ij}(T)$, or temperature-independent, k_{ij}, binary interaction parameters of the studied systems.

*Table ST2 including results from the modelling carried out using either temperature-dependent, $k_{ij}(T)$, or temperature-independent, k_{ij}, binary interaction parameters for the studied systems.

*Table ST3 including deviations obtained in this work and by other authors when modelling the VLE or the critical loci for the *n*-hexane + alkan-1-ol systems.

*Table ST4 including deviations obtained in this work and by other authors when modelling the VLE or the critical loci for the CO_2 + alkan-1-ol systems.

*A video is available in the online version.

Acknowledgments

The authors gratefully acknowledge financial support received from the Ministerio de Educación y Ciencia of Spain (CTQ2005-02213), Ministerio de Ciencia e Innovación (CTQ2008-02037 and CTQ2011-24875) and Convenio La Caixa - Gobierno de Aragón.

Nomenclature

Abbreviations

c.i.	confidence interval
CO_2	carbon dioxide
EDA	electron donor - acceptor
EoS	equation of state
EtOH	ethanol
LA	Lewis acid
LB	Lewis base
$MRD(X) = \frac{100}{N}\sum_{n=1}^{N}\left\|\frac{X_n^{\exp} - X_n^{\mathrm{cal}}}{X_n^{\exp}}\right\|$	mean relative deviation in *X* (generic variable)
$n-\mathrm{C_6H_{14}}$	*n*-hexane
$n-\mathrm{C_mH_{2m+1}OH}$	alkan-1-ol
OF	objective function
PC-SAFT	Perturbed-Chain Statistical Associating Fluid Theory
$scCO_2$	supercritical carbon dioxide
SCF	supercritical fluid
u	uncertainty
VLE	vapor-liquid equilibria
$\Delta y = \frac{1}{N}\sum_{n=1}^{N}\left\|y_n^{\exp} - y_n^{\mathrm{cal}}\right\|$	absolute deviation for the solvent mole fraction in the vapor phase

List of symbols

k_{ij}	binary interaction parameter
m	chain length number
P	pressure
T	temperature
x	liquid-phase mole fraction
y	vapor-phase mole fraction

Greek symbols

ε	segment energy parameter
σ	segment diameter
$\varepsilon^{A_iB_i}$	energy of association
$\kappa^{A_iB_i}$	volume of association

Subscripts

i,j	pure component indexes
c	critical

Superscripts

assoc	association
cal	calculated
DD	dipole-dipole
dis	dispersive
exp	experimental
hc	hard chain
id	ideal
QD	quadrupole-dipole
QQ	quadrupole-quadrupole

REFERENCES

[1] S.C. Tucker, Solvent density inhomogeneities in supercritical fluids, Chemical Reviews 99 (1999) 391-418.

[2] K. Nishikawa, T. Morita, Inhomogeneity of molecular distribution in supercritical fluids, Chemical Physics Letters 316 (2000) 238-242.

[3] S.A. Egorov, Local density augmentation in attractive supercritical solutions: Inhomogeneous fluid approach, Journal of Chemical Physics 112 (2000) 7138-7146.

[4] S.A. Egorov, Preferential solvation in supercritical fluids: An integral equation study, Journal of Chemical Physics 113 (2000) 7502-7510.

[5] W. Song, R. Biswas, M. Maroncelli, Intermolecular interactions and local density augmentation in supercritical solvation: A survey of simulation and experimental results, Journal of Physical Chemistry A 104 (2000) 6924-6939.

[6] Y. Yang, A. Gilbert, C. Xu, Hydrodeoxygenation of bio-crude in supercritical hexane with sulfided CoMo and CoMoP catalysts supported on MgO: A model compound study using phenol, Applied Catalysis A: General 360 (2009) 242-249.

[7] X. Huang, C.W. Curtis, C.B. Roberts, Reaction behavior of Fischer-Tropsch synthesis in near critical and supercritical hexane media, Fuel Chemistry Division Preprints 47 (2002) 151-153.

[8] K. Yokota and K. Fujimoto, Supercritical-phase Fischer-Tropsch synthesis reaction. 2. The effective diffusion of reactant and products in the supercritical-phase reaction, Industrial & Engineering Chemistry Research 30 (1991) 95-100.

[9] T. Jiang, Y. Niu, B. Zhong, Study of process variables for methanol and isobutanol synthesis from syngas under supercritical phase, Journal of Natural Gas Chemistry 8 (1999) 21-24.

[10] S. Masahiro, M. Hiroyasu, W. Daiki, Manufacture of methanol from hydrogen and carbon dioxide in supercritical solvents, JP2000336050, 2000-12-05.

[11] Y. Danten, T. Tassaing, M. Besnard, Vibrational spectra of CO_2-electron donor-acceptor complexes from ab initio, Journal of Physical Chemistry A 106 (2002) 11831-11840.

[12] P. van Ginderen, W.A. Herrebout, B.J. van der Veken, van der Waals complex of dimethyl ether with carbon dioxide, Journal of Physical Chemistry A 107 (2003) 5391-5396.

[13] P. Raveendran, S.L. Wallen, Sugar acetates as novel, renewable CO_2-philes, Journal of the American Chemical Society 124 (2002) 7274-7275.

[14] P. Raveendran, S.L. Wallen, Cooperative C-H···O hydrogen bonding in CO_2 - Lewis base complexes: Implications for solvation in supercritical CO_2, Journal of the American Chemical Society 124 (2002) 12590-12599.

[15] M.A. Blatchford, P. Raveendran, S.L. Wallen, Spectroscopic studies of model carbonyl compounds in CO_2: Evidence for cooperative C-H···O interactions, Journal of Physical Chemistry A 107 (2003) 10311-10323.

[16] A. Fujii, T. Ebata, N. Mikami, Direct observation of weak hydrogen bonds in microsolvated phenol: Infrared spectroscopy of OH stretching vibrations of Phenol - CO and - CO_2 in S_o and D_o, Journal of Physical Chemistry A 106 (2002) 10124-10129.

[17] M. Saharay, S. Balasubramanian, Electron donor-acceptor interactions in ethanol - CO_2 mixtures: An ab initio molecular dynamics study of supercritical carbon dioxide, Journal of Physical Chemistry B 110 (2006) 3782-3790.

[18] W. Xu, J. Yang, Y. Hu, Microscopic structure interaction analysis for supercritical carbon dioxide - ethanol mixtures: A Monte Carlo simulation study, Journal of Physical Chemistry B 113 (200) 4781-4789.

[19] J. Gross, G. Sadowski, Perturbed-Chain SAFT: An equation of state based on a perturbation theory for chain molecules, Industrial & Engineering Chemistry Research 40 (2001) 1244-1260.

[20] J. Gross, G. Sadowski, Application of the Perturbed-Chain SAFT equation of state to associating systems, Industrial & Engineering Chemistry Research 41 (2002) 5510-5515.

[21] J.P. Wolbach, S.I. Sandler, Using molecular orbital calculations to describe the phase behavior of hydrogen-bonding fluids, Industrial & Engineering Chemistry Research 36 (1997) 4041-4051.

[22] J.P. Wolbach, S.I. Sandler, Using molecular orbital calculations to describe the phase behavior of cross-associating mixtures, Industrial & Engineering Chemistry Research 37 (1998) 2917-2928.

[23] S.I. Sandler, J.P. Wolbach, M. Castier, G. Escobedo-Alvarado, Modeling of thermodynamically difficult systems, Fluid Phase Equilibria 136 (1997) 15-29.

[24] F. Llovell, J.C. Pàmies, L.F. Vega, Thermodynamic properties of Lennard-Jones chain molecules: Renormalization-group corrections to a modified statistical associating fluid theory, Journal of Chemical Physics 121 (2004) 10715-10724.

[25] F. Llovell, L.F. Vega, Global fluid phase equilibria and critical phenomena of selected mixtures using the crossover soft-SAFT equation, Journal of Physical Chemistry B 110 (2006) 1350-1362.

[26] M. Cismondi, E.A. Brignole, J. Mollerup, Rescaling of three-parameter equations of state: PC-SAFT and SPHCT, Fluid Phase Equilibria 234 (2005) 108-121.

[27] S.T. Blanco, L. Gil, P. García-Giménez, M. Artal, S. Otín, I. Velasco, Critical properties and high-pressure volumetric behavior of the carbon dioxide + propane system at *T* = 308.15 K. Krichevskii function and related thermodynamic properties, Journal of Physical Chemistry B 113 (2009) 7243-7256.

[28] L. Gil, J.F. Martínez-López, M. Artal, S.T. Blanco, J. Muñoz Embid, J. Fernández, S. Otín, I. Velasco, Volumetric behavior of the {CO_2 (1) + C_2H_6 (2)} system in the subcritical (*T* = 293.15 K), critical, and supercritical (*T* = 308.15 K) regions, Journal of Physical Chemistry B 114 (2010) 5447-5469.

[29] R.A. Heidemann, R.A. Krenz, T. Laursen, Spinodal curves and critical points in mixtures containing polydisperse polymers with many components, Fluid Phase Equilibria 228–229 (2005) 239–245.

[30] S.H. Huang, M. Radosz, Equation of state for small, large, polydisperse, and associating molecules: extension to fluid mixtures, Industrial & Engineering Chemistry Research 30 (1991) 1994-2005.

[31] L.A. Román-Ramírez, F. García-Sánchez, C.H. Ortiz-Estrada, D.N. Justo-García, modeling of vapor–liquid equilibria for CO_2 + 1-alkanol binary systems with the PC-SAFT equation of state using polar contributions, Industrial & Engineering Chemistry Research 49 (2010) 12276-12283.

[32] M. Yarrison, W.G. Chapman, A systematic study of methanol + n-alkane vapor–liquid and liquid–liquid equilibria using the CK-SAFT and PC-SAFT equations of state, Fluid Phase Equilibria 226 (2004) 195-205.

[33] A. Grenner, G.M. Kontogeorgis, N. von Solms, M.L. Michelsen, Modeling phase equilibria of alkanols with the simplified PC-SAFT equation of state and generalized pure compound parameters, Fluid Phase Equilibria 258 (2007) 83-94.

[34] M.B. Oliveira, A.J. Queimada, G.M. Kontogeorgis, J.A.P. Coutinho, Evaluation of the CO_2 behavior in binary mixtures with alkanes, alcohols, acids and esters using the Cubic-Plus-Association equation of state, Journal of Supercritical Fluids 55 (2011) 876-892.

[35] M. Cismondi, J.M. Mollerup, M.S. Zabaloy, Equation of state modeling of the phase equilibria of asymmetric CO2+*n*-alkane binary systems using mixing rules cubic with respect to mole fraction, Journal of Supercritical Fluids 55 (2010) 671-681.

[36] http://webbook.nist.gov

[37] L. Gil, S.F. Otín, J. Muñoz Embid, M.A. Gallardo, S. Blanco, M. Artal, I. Velasco, Experimental setup to measure critical properties of pure and binary mixtures and their densities at different pressures and temperatures. Determination of the precision and uncertainty in the results, Journal of Supercritical Fluids 44 (2008) 123-138.

[38] C-B. Soo, P. Théveneau, C. Coquelet, D. Ramjugernath, D. Richon, Determination of critical properties of pure and multicomponent mixtures using a "dynamic-synthetic" apparatus, Journal of Supercritical Fluids 55 (2010) 545-553.

[39] S. Horstmann, K. Fischer, J. Gmehling, Experimental determination of critical points of pure components and binary mixtures using a flow apparatus, Chemical Engineering and Technology 22 (1999) 839–842.

[40] S. Horstmann, K. Fischer, J. Gmehling, P. Kolár, Experimental determination of the critical line for (carbon dioxide + ethane) and calculation of various thermodynamic properties for (carbon dioxide + *n*-alkane) using the PSRK model, Journal of Chemical Thermodynamics 32 (2000) 451–464.

[41] S. Horstmann, K. Fischer, J. Gmehling, Experimental determination of critical data of mixtures and their relevance for the development of thermodynamic models, Chemical Engineering Science 56 (2001) 6905–6913.

[42] S. Horstmann, K. Fischer, J. Gmehling, Measurement and calculation of critical points for binary and ternary mixtures, AIChE Journal 48 (2002) 2350–2356.

[43] P. Guilbot, P. Théveneau, A. Baba-Ahmed, S. Horstmann, K. Fischer, D. Richon, Vapor–liquid equilibrium data and critical points for the system H_2S + COS. Extension of the PSRK group contribution equation of state, Fluid Phase Equilibria 170 (2000) 193–202.

[44] N. Juntarachat, P.D. Beltran Moreno, S. Bello, R. Privat, J.-N. Jaubert, Validation of a new apparatus using the dynamic and static methods for determining the critical properties of pure components and mixtures, Journal of Supercritical Fluids 68 (2012) 25-30.

[45] N. Juntarachat, S. Bello, R. Privat, J.-N. Jaubert, Validation of a new apparatus using the dynamic method for determining the critical properties of binary mixtures containing CO_2 and a *n*-alkane, Fluid Phase Equilibria 325 (2012) 66-70.

[46] P.H. van Konynenburg, R.L. Scott, Critical lines and phase-equilibria in binary van der Waals mixtures, Philosophical Transactions of the Royal Society of London Series A - Mathematical Physical and Engineering Sciences, 298 (1980) 495-540.

[47] C.G. Savini, D.R. Winterhalter, H.C. van Ness, Heats of mixing for partially miscible systems: Methanol - *n*-hexane and methanol - *n*-heptane, Journal of Chemical & Engineering Data 10 (1965) 171-172.

[48] S.-C. Hwang, R.L. Robinson, Vapor-liquid equilibria at 25°C for nine alcohol - hydrocarbon binary systems, Journal of Chemical & Engineering Data 22 (1977) 319-325.

[49] I.F. Hölscher, G.M. Schneider, J.B. Ott, Liquid-liquid phase equilibria of binary mixtures of methanol with hexane, nonane and decane at pressures up to 150 MPa, Fluid Phase Equilibria 27 (1986) 153-169.

[50] B. C. Oh, Y. Kim, H.Y. Shin, H. Kim, Vapor-liquid equilibria for the system 1-propanol + n-hexane near the critical region, Fluid Phase Equilibria 220 (2004) 41-46.

[51] L.W. Jordan, W.B. Kay, Phase relations of binary systems that form azeotropes: *n*-alkanes - perfluoro-*n*-heptane systems (ethane through *n*-nonane), Chemical Engineering Progress Symposium Series 59 (1963) 46-51.

[52] Th.W. de Loos, W. Poot, J. de Swaan Arons, Vapour-liquid equilibria and critical phenomena in methanol + *n*-alkane systems, Fluid Phase Equilibria 42 (1988) 209-227.

[53] E. Brunner, Fluid mixtures at high pressures VI. Phase separation and critical phenomena in 18 (*n*-alkane + ammonia) and 4 (*n*-alkane + methanol) mixtures, Journal of Chemical Thermodynamics 20 (1988) 273-297.

[54] J. Liu, Z. Qin, G. Wang, X. Hou, J. Wang, Critical properties of binary and ternary mixtures of hexane + methanol, hexane + carbon dioxide, methanol + carbon dioxide, and hexane + carbon dioxide + methanol, Journal of Chemical and Engineering Data 48 (2003) 1610-1613.

[55] A. Zawisza, High-pressure liquid-vapour equilibria, critical state, and $p(V_m,T,x)$ to 448.15 K and 4.053 MPa for $\{x C_6H_{14} + (1-x)CH_3OH\}$, Journal of Chemical Thermodynamics 17 (1985) 941-947.

[56] P. Sauermann, K. Holzapfel, J. Oprzynski, F. Kohler, W. Poot, Th.W. de Loos, The $p\rho T$ properties of ethanol + hexane, Fluid Phase Equilibria 112 (1995) 249-272.

[57] J. Seo, J. Lee, H. Kim, Isothermal vapor-liquid equilibria for the system ethanol and *n*-hexane in the near critical region, Fluid Phase Equilibria 182 (2001) 199-207.

[58] C.L. Young, International Data Series. Selected Data on Mixtures Ser. A 4 (1986) 245-253.

[59] D.W. Morton, M.P.W. Lui, C.L. Young, The (gas + liquid) critical properties and phase behavior of some binary alkanol (C_2-C_5) + alkane (C_5-C_{12}) mixtures, Journal of Chemical Thermodynamics 35 (2003) 1737-1749.

[60] C.L. Young, International Data Series. Selected Data on Mixtures Ser. A 1 (1974) 47-57.

[61] K.M. Bone, C.L. Young, in: C.P. Hicks, C.L. Young, The gas-liquid critical properties of binary mixtures, Chemical Reviews 75 (1975) 119-175.

[62] G. Christou, R.J. Sadus, C.L. Young, Phase behaviour of 1-alkanol + alkane mixtures: Gas-liquid critical temperatures, Fluid Phase Equilibria 67 (1991) 259-271.

[63] E. Laga Lázaro, Determinación de Puntos Críticos y Propiedades *PVT* de Fluidos, TAD Report, 2009, Department of Organic Chemistry and Physical Chemistry, University of Zaragoza, Spain. Unpublished results.

[64] D.H. Lam, A. Jangkamolkulchai, K.D. Luks, Liquid-liquid-vapor phase equilibrium behavior of certain binary carbon dioxide + *n*-alkanol mixtures, Fluid Phase Equilibria 60 (1990) 131-141.

[65] I. Polishuk, J. Wisniak, H. Segura, Simultaneous prediction of the critical and sub-critical phase behavior in mixtures using equation of state I. Carbon dioxide-alkanols, Chemical Engineering Science 56 (2001) 6485-6510.

[66] C. Secuianu, V. Feroiu, D. Geană, Phase equilibria experiments and calculations for carbon dioxide + methanol binary system, Central European Journal of Chemistry 7 (2009) 1-7.

[67] C. Secuianu, V. Feroiu, D. Geană, Phase behavior for carbon dioxide + ethanol system: Experimental measurements and modeling with a cubic equation of state, Journal of Supercritical Fluids 47 (2008) 109-116.

[68] C. Secuianu, V. Feroiu, D. Geană, High-pressure phase equilibria for the carbon dioxide + 1-propanol system, Journal of Chemical & Engineering Data 53 (2008) 2444-2448.

[69] C. J. Peters, K. Gauter, Occurrence of holes in ternary fluid multiphase systems of near-critical carbon dioxide and certain solutes, Chemical Reviews 99 (1999) 419-431.

[70] E. Brunner, Fluid mixtures at high pressures I. Phase separation and critical phenomena of 10 binary mixtures of (a gas + methanol), Journal of Chemical Thermodynamics 17 (1985) 671-679.

[71] E. Brunner, Fluid mixtures at high pressures IV. Isothermal phase equilibria in binary mixtures consisting of (methanol + hydrogen or nitrogen or methane or carbon monoxide or carbon dioxide), Journal of Chemical Thermodynamics 19 (1987) 273-291.

[72] J.W. Ziegler, J.G. Dorsey, Estimation of liquid-vapor critical loci for CO_2 - solvent mixtures using a peak-shape method. Analytical Chemistry 67 (1995) 456-461.

[73] J.W. Ziegler, T.L. Chester, D.P. Innis, S.H. Page, J.G. Dorsey, Supercritical fluid flow injection method for mapping liquid-vapor critical loci of binary mixtures containing CO_2, in: K. W. Hutchenson, N.R. Foster (Eds.),

Innovations in Supercritical Fluids: Science and Technology, ACS Symposium Series 608, American Chemical Society, Washington DC, 1995, pp. 93-110.

[74] A.I. Semenova, E.A. Emelyanova, S.S. Tsimmerman, Phase equilibria in methanol-carbon dioxide system, Zhurnal Fizicheskoi Khimii 53 (1979) 2502-2505.

[75] S.-D. Yeo, S.-J. Park, J.-W. Kim, J.-C. Kim, Critical properties of carbon dioxide + methanol, + ethanol + 1-propanol, and + 1-butanol, Journal of Chemical & Engineering Data 45 (2000) 932-935.

[76] J.-H. Yoon, H.-S. Lee, H. Lee, High pressure vapor-liquid equilibria for carbon dioxide + methanol, carbon dioxide + ethanol, and carbon dioxide + methanol + ethanol, Journal of Chemical & Engineering Data 38 (1993) 53-55.

[77] S.N. Joung, C.W. Yoo, H.Y. Shin, S.Y. Kim, K.-P. Yoo, C.S. Lee, W.S. Huh, Measurements and correlation of high-pressure VLE of binary CO_2 - alcohol systems (methanol, ethanol, 2-methoxyethanol and 2-ethoxyethanol), Fluid Phase Equilibria 185 (2001) 219-230.

[78] G.S. Gurdial, N.R. Foster, S.L.J. Yun, K.D. Tilly, Phase behaviour of supercritical fluid-entrainer, in: E. Kiran, J.F. Brennecke (Eds.), Supercritical Fluid Engineering Science: Fundamentals and Applications, ACS Symposium Series 514, American Chemical Society, Washington DC, 1993, pp. 34-45.

[79] A-D. Leu, S.Y-K. Chung, D.B. Robinson, The equilibrium phase properties of (carbon dioxide + methanol), Journal of Chemical Thermodynamics 23 (1991) 979-985.

[80] J.R. Strubinger, H. Song, J.F. Parcher, High pressure phase distribution isotherms for supercritical fluid chromatographic systems. 2. Binary isotherms of carbon dioxide and methanol, Analytical Chemistry 63 (1991) 104-108.

[81] J. Ke, P.J. King, M.W. George, M. Poliakoff, Method for locating the vapor-liquid critical point of multicomponent fluid mixtures using a shear mode piezoelectric sensor, Analytical Chemistry 77 (2005) 85-92.

[82] Y.L. Tian, M. Han, L. Chen, H.J. Feng, Y. Quin, Study on vapor-liquid phase equilibria for CO_2 - C_2H_5OH system, Acta Physico-Chimica Sinica 17 (2001) 155-160.

[83] S. Sima, V. Feroiu, D. Geană, New high pressure vapor-liquid equilibrium and density predictions for the carbon dioxide plus ethanol system, Journal of Chemical & Engineering Data 56 (2011) 5052-5059.

[84] L.C.W. Baker, T.F. Anderson, Some phase relationships in the three-component liquid system CO_2 - H_2O - C_2H_5OH at high pressures, Journal of the American Chemical Society 79 (1957) 2071-2074.

[85] K. Nagahama, J. Suzuki, T. Suzuki, High pressure vapor-liquid equilibria for the supercritical CO_2 + ethanol + water system, in: M. Perrut (Ed.), Proceedings of the International Symposium on Supercritical Fluids (October 17-19, Nice, France), Lavoisier Tec & Doc, Paris, 1988, pp. 143-150.

[86] J.S. Lim, Y.Y. Lee, Phase equilibria for carbon dioxide - ethanol - water system at elevated pressures, Journal of Supercritical Fluids 7 (1994) 219-230.

[87] H. Tanaka, M. Kato, Vapor-liquid equilibrium properties of carbon dioxide + ethanol mixtures at high pressures, Journal of Chemical Engineering of Japan 28 (1995) 263-266.

[88] J.L. Mendoza de la Cruz, L.A. Galicia-Luna, High pressure vapor-liquid equilibria for the carbon dioxide + ethanol and carbon dioxide + propan-1-ol systems at temperartures from 322.36 K to 391.96 K, ELDATA 5 (1999) 157-164.

[89] L.A. Galicia-Luna, A. Ortega-Rodriguez, New apparatus for the fast determination of high pressure vapor-liquid equilibria of mixtures and of accurate critical pressures, Journal of Chemical & Engineering Data 45 (2000) 265-271.

[90] H. Li, X. Zhang, B. Han, J. Liu, J. He, Z. Liu, Effect of phase bahaviour and pressure on the constant-volume heat capacity and intermolecular interaction of CO_2 - ethanol and CO_2 - *n*-pentane mixtures in the critical region, Chemical European Journal 8 (2002) 451-456.

[91] B. Wang, B. Han, T. Jiang, Z. Zhang, W. Li, W. Wu, Enhancing the rate of the diels−alder reaction using CO2 + ethanol and CO2 + *n*-hexane mixed solvents of different phase regions, Journal of Physical Chemistry B 109 (2005) 24203-24210.

[92] W. Wu, J. Ke, M. Poliakoff, Phase boundaries of CO_2 + toluene, CO_2 + acetone, and CO_2 + ethanol at high temperatures and high pressures, Journal of Chemical & Engineering Data 51 (2006) 1398-1403.

[93] Z.J. Chang, W.X. Yang, C.W. Liang, Study on phase equilibrium properties for CO_2 + cosolvent binary mixtures, Chinese Chemical Letters 12 (2001) 829-832.

[94] O. Elizalde-Solis, L.A. Galicia-Luna, L.E. Camacho-Camacho, High-pressure vapor–liquid equilibria for CO2 + alkanol systems and densities of *n*-dodecane and *n*-tridecane, Fluid Phase Equilibria 259 (2007) 23-32.

[95] G. Silva-Oliver, L.A. Galicia-Luna, Vapor-liquid equilibria near critical points for the CO_2 + 1-butanol and CO_2 + 2-butanol systems at temperatures from 324 to 432 K, Fluid Phase Equilibria 182 (2001) 145-156.

[96] K. Isihara, A. Tsukajima, H. Tanaka, M. Kato, T. Sako, M. Sato, T. Hakuta, Vapor-liquid equilibrium for carbon dioxide + 1-butanol at high pressure, Journal of Chemical & Engineering Data 41 (1996) 324-325.

[97] M. Góral, P. Oracz, S. Warycha, Vapour-liquid equilibria: XIV. The ternary system cyclohexane – methanol - hexane at 293.15 K, Fluid Phase Equilibria 169 (2000) 85-99.

[98] M. Hongo, T. Tsuji, K. Fukuchi, Y. Arai, Vapor-liquid equilibria of methanol + hexane, methanol + heptane, ethanol + hexane, ethanol + heptane, and ethanol + octane at 298.15 K, Journal of Chemical & Engineering Data 39 (1994) 688-691.

[99] A. Iguchi, Kagaku Sochi 20 (1978) 66-68, in: J. Gmehling, U. Onken, W. Arlt, Vapor-Liquid Equilibrium Data Collection, Chemistry Data Series Vol. I, Part 2c, DECHEMA, Frankfurt/Main, 1982, pp. 219, 428, 547.

[100] H. Wolff, H.-E. Hoppel, Die wasserstoffbrückenassoziation von methanol in *n*-hexan nach dampfdruckmessungen, Berichte der Bunsengesellschaft Physikalische Chemie 72 (1968) 710-721.

[101] P. Oracz, S. Warycha, Vapour-liquid equilibria. VII. The ternary system hexane – methanol - acetone at 313.15 K, Fluid Phase Equilibria 108 (1995) 199-211.

[102] C. Alonso, E.A. Montero, C.R. Chamorro, J.J. Segovia, M.C. Martin, M.A. Villamañán, Vapor-liquid equilibrium of octane - enhancing additives in gasolines: 6. Total pressure data and G^E for binary and ternary mixtures containing 1, 1-dimethylethyl methyl ether (MTBE), methanol and *n*-hexane at 313.15 K, Fluid Phase Equilibria 217 (2004) 157-164.

[103] J.S. Choi, D.W. Park, J.N. Rhim, Isothermal phase equilibria for the ternary system (methanol(1) - *n*-hexane(2) - *n*-heptane(3)), Hwahak Konghak 23 (1985) 89-96.

[104] J.B. Ferguson, The system methyl alcohol-*n*-hexane at 45 degrees, Journal of Physical Chemistry, 36 (1931) 1123-1128 (publication date: January 1932).

[105] M. Scheller, H. Schubert, H.G. Konecke, Gas-liquid equilibrium in system normal-hexane – methylcyclohexane - methanol at 60 degrees centigrade, Journal für Praktische Chemie 311 (1969) 974-982.

[106] N. Ishii, Journal of the Society of Chemical Industry of Japan 38 (1935) 659-664.

[107] V.C. Smith, R.L. Robinson, Vapor-liquid equilibria at 25°C in the binary mixtures formed by hexane, benzene, and ethanol, Journal of Chemical & Engineering Data 15 (1970) 391-395.

[108] L.-Z. Zhang, G.-H. Chen, Z.-H. Cao, S.J. Han, New double circulation apparatus for VLE determination: Establishment and applications in the determination of isobars, isotherms, and isoplethes, Thermochimica Acta 169 (1990) 247-261.

[109] H. Wolff, R. Gotz, Association of different deuterated ethanols in hexane (according to vapor-pressure measurements), Zeitschrift für Physikalische Chemie (Frankfurt) 100 (1976) 25-36.

[110] L.S. Kudryavtseva and M. Susarev, Liquid-vapor equilibrium in the systems acetone - hexane and hexane - ethyl alcohol at 35, 45, and 55 deg. and 760 mm of Hg, Zhurnal Prikladnoĭ Khimii (Leningrad, RSFSR) 36 (1963) 1471-1477.

[111] H. Sugi, T. Katayama, Ternary liquid-liquid and miscible binary vapor-liquid-equilibrium data for 2 systems *n*-hexane - ethanol - acetonitrile and water - acetonitrile - ethylacetate, Journal of Chemical Engineering of Japan 11 (1978) 167-172.

[112] B. Janakszewsi, P. Oracz, M. Góral, S. Warycha, Vapour-liquid equilibria. I. An apparatus for isothermal total vapour pressure measurements: Binary mixtures of ethanol and t-butanol with *n*-hexane, *n*-heptane and *n*-octane at 313.15 K, Fluid Phase Equilibria 9 (1982) 295-310.

[113] S.J. O'Shea, R.H. Stokes, Activity coefficients and excess partial molar enthalpies for (ethanol + *n*-hexane) from 283 to 318 K, Journal of Chemical Thermodynamics 18 (1986) 691-696.

[114] M. Díaz Peña, D. Rodríguez Cheda, Equilibrio líquido-vapor I. Los sistemas benceno + ciclohexano a 70°C y metanol + *n*-hexano a 50°C, Anales de Química 66 (1970) 721-735.

[115] K.S. Yuan, J.C.K. Ho, A.K. Koshpande, B.C.-Y. Lu, Vapor-liquid equilibria, Journal of Chemical & Engineering Data 8 (1963) 549-559.

[116] G.W. Lindberg, D. Tassios, Effect of organic and inorganic salts on relative volatility of nonaqueous systems, Journal of Chemical & Engineering Data 16 (1971) 52-55.

[117] N. Van Nhu, A.P. Liu, P. Sauermann, F. Kohler, On the thermodynamics of ethanol + hexane at elevated temperatures and pressures, Fluid Phase Equilibria 145 (1998) 269-285.

[118] J. Schmelzer, M.V. Alekseeva, Vapour-liquid and liquid-liquid equilibria in systems of hexane, perfluorhexane, 1-propanol. (I) Binary systems, Chemische Technik 34 (1982) 424-426.

[119] M.V. Alekseeva, M.F. Moiseenko, Eksperimentalnoe issledovanie i rascheti ravnovesiya zhidkost-par v systeme *n*-propilovij spirt - hexan - *n*-dezilovij spirt, Khimiya i Termodinamica Rastvorov (Leningrad) 5 (1982) 179-195.

[120] A.I. Rusanov, S.A. Levichev, Vestnik Leningradskogo Universiteta Seriya Fizika Khimiya 16 (1967) 124-130, in: J. Gmehling, U. Onken, W. Arlt, Vapor-Liquid Equilibrium Data Collection, Chemistry Data Series Vol. I, Part 2c, DECHEMA, Frankfurt/Main, 1982, pp. 549.

[121] J. Zielkiewicz, (Vapour + liquid) equilibria in (propan-1-ol + *n*-hexane + *n*-heptane) at the temperature 313.15 K, Journal of Chemical Thermodynamics 23 (1991) 605-612.

[122] I. Brown, W. Fock, F. Smith, The thermodynamic properties of normal and branched alcohols in benzene and *n*-hexane, Journal of Chemical Thermodynamics 1 (1969) 273-291.

[123] M. Díaz Peña, D. Rodríguez Cheda, Equilibrio líquido-vapor III. Los sistemas n-propanol + n-hexano a 50°C y *n*-propanol + *n*-heptano a 60°C, Anales de Química 66 (1970) 747-755.

[124] M. Gracia, F. Sánchez, P. Pérez, J. Valero, C. Gutiérrez Losa, Vapour pressures of (butan-1-ol + hexane) at temperatures between 283.10 and 323.12 K, Journal of Chemical Thermodynamics 24 (1992) 463-471.

[125] V. Rodriguez, J. Pardo, M.C. López, F.M. Royo, J.S. Urieta, Vapor pressures of binary mixtures of hexane + 1-butanol, + 2-butanol, + 2-methyl-1-propanol, or 2-methyl-2-propanol at 298.15 K, Journal of Chemical & Engineering Data 38 (1993) 350-352.

[126] C. Berro, M. Rogalski, A. Peneloux, Excess Gibbs energies end excess volumes of 1-butanol - *n*-hexane binary systems, Journal of Chemical & Engineering Data 27 (1982) 352-355.

[127] M. Ronc, G.R. Ratcliff, Measurement of vapor-liquid-equilibria using a semi-continuous total pressure static equilibrium still, Canadian Journal of Chemical Engineering 54 (1976) 326-332.

[128] H. Wolff, A. Shadiakhy, The vapor pressure behaviour and association of mixtures of 1-hexanol and *n*-hexane between 293 and 373 K, Fluid Phase Equilibria 7 (1981) 309-325.

[129] S.A. Wieczorek, J. Stecki, Vapour pressure and thermodynamic properties of hexan-1-ol + *n*-hexane between 298.230 and 342.824 K, Journal of Chemical Thermodynamics 10 (1978) 177-186.

[130] M. Góral, P. Oracz and S. Warycha, Vapour–liquid equilibria: XIII. The ternary system cyclohexane - methanol - hexane at 303.15 K, Fluid Phase Equilibria 152 (1998) 109-120.

[131] S. Tamouza, J.-P. Passarello, P. Tobaly, J.-C. de Hemptinne, Application to binary mixtures of a group contribution SAFT EOS (GC-SAFT), Fluid Phase Equilibria 228-229 (2005) 409-419.

[132] E.K. Karakatsani, G.M. Kontogeorgis, I.G. Economou, Evaluation of the Truncated Perturbed Chain-Polar Statistical Associating Fluid Theory for complex mixture fluid phase equilibria, Industrial & Engineering Chemistry Research 45 (2006) 6063-6074.

[133] P. Arce, M. Aznar, Modeling of critical lines and regions for binary and ternary mixtures using non-cubic and cubic equations of state, Journal of Supercritical Fluids 42 (2007) 1-26.

[134] M. Mourah, D. NguyenHuynh, J.P. Passarello, J.C. de Hemptinne, P. Tobaly, Modelling LLE and VLE of methanol + *n*-alkane series using GC-PC-SAFT with a group contribution k_{ij}, Fluid Phase Equilibria 298 (2010) 154-168.

[135] V. Papaioannou, C.S. Adjiman, G. Jackson, A. Galindo, Simultaneous prediction of vapour–liquid and liquid–liquid equilibria (VLE and LLE) of aqueous mixtures with the SAFT-γ group contribution approach, Fluid Phase Equilibria 306 (2011) 82-96.

[136] G.M. Kontogeorgis, M.L. Michelsen, G.K. Folas, S. Derawi, N. von Solms, E. H. Stenby, Ten years with the CPA (Cubic-Plus-Association) Equation of State. Part 1. Pure Compounds and Self-Associating Systems, Industrial & Engineering Chemistry Research 45 (2006) 4855-4868.

[137] P.C.V. Tyberg, G.M. Kontogeorgis, M.L. Michelsen, E.H. Stenby, Phase equilibria modeling of methanol-containing systems with the CPA and sPC-SAFT equations of state, Fluid Phase Equilibria, 288 (2010), 128-138.

[138] I. Tsivintzelis, G.M. Kontogeorgis, M.L. Michelsen, E.H. Stenby, Modeling phase equilibria for acid gas mixtures using the CPA equation of state. Part II: Binary mixtures with CO_2, Fluid Phase Equilibria 306 (2011) 38-56.

[139] K. Tochigi, T. Namae, T. Suga, H. Matsuda, K. Kurihara, M.C. dos Ramos, C. McCabe, Measurement and prediction of high-pressure vapor–liquid equilibria for binary mixtures of carbon dioxide + *n*-octane, methanol, ethanol, and perfluorohexane, Journal of Supercritical Fluids 55 (2010) 682-689.

[140] J.O. Valderrama, J. Zavaleta, Generalized binary interaction parameters in the Wong–Sandler mixing rules for mixtures containing *n*-alkanols and carbon dioxide, Fluid Phase Equilibria 234 (2005) 136-143.

[141] M. Castier, L.A. Galicia-Luna, S.I. Sandler, Modeling the high-pressure behavior of binary mixtures of carbon dioxide + alkanols using an excess free energy mixing rule, Brazilian Journal of of Chemical Engineering 21 (2004) 659-666.

[142] G. Silva-Oliver, L.A. Galicia-Luna, S.I. Sandler, Vapor–liquid equilibria and critical points for the carbon dioxide + 1-pentanol and carbon dioxide + 2-pentanol systems at temperatures from 332 to 432 K, Fluid Phase Equilibria 200 (2002) 161-172.

[143] M. Artal, J. Muñoz Embid, I. Velasco, C. Berro, E. Rauzy, Representation for bynary mixtures of *n*-alcohols + sub and supercritical CO_2 by a group-contribution method, Fluid Phase Equilibria 178 (2001) 119-130.

[144] J.L. Fulton, G.G. Yee, R.D. Smith, Hydrogen bonding of simple alcohols in supercritical fluids, in: E. Kiran, J.F. Brennecke (Eds.), Supercritical Fluids Engineering Science, Fundamentals and applications, ACS Symposium Series 514, American Chemical Society, Washington DC, 1993, 175-187.

[145] Gmelins Handbuch BD. C. 14, pp. 568, in: H. Knapp, R. Döring, L. Oellrich, U. Plocker, J.M. Prausnitz, Vapor-Liquid Equilibria for Mixtures of Low Boiling Substances, Chemistry Data Series Vol. VI, DECHEMA, Frankfurt/Main, 1982, pp. 621-622.

[146] J.H. Hong, R. Kobayashi, Vapor-liquid equilibriumm studies for the carbon dioxide - methanol system, Fluid Phase Equilibria 41 (1988) 269-276.

[147] W. Weber, S. Zeck, H. Knapp, Gas solubilities in liquid solvents at high pressures: apparatus and results for binary and ternary systems of N_2, CO_2 and CH_3OH, Fluid Phase Equilibria 18 (1984) 253-278.

[148] T. Chang, R.W. Rousseau, Solubilities of carbon dioxide in methanol and methanol - water at high pressures: experimental data and modeling, Fluid Phase Equilibria 23 (1985) 243-258.

[149] J.K. Ferrell, R.W. Rousseau, D.G. Bass, The Solubility of Acid Gases in Methanol, U.S. Department of Commerce, Interagency Energy/Environment R&D Program Report, Ref. PB 296707, 1979, pp. 31-33.

[150] P. Naidoo, D. Ramjugernath, J.D. Raal, A new high-pressure vapour-liquid equilibrium apparatus, Fluid Phase Equilibria 269 (2008) 104-112.

[151] K. Bezanehtak, G.B. Combes, F. Dehghani, N.R. Foster, D.L. Tomasko, Vapor-liquid equilibrium for binary systems of carbon dioxide + methanol, hydrogen + methanol, and hydrogen + carbon dioxide at high pressures, Journal of Chemical & Engineering Data 47 (2002) 161-168.

[152] C.J. Chang, C.-Y. Day, C.-M. Ko, K.-L. Chiu, Densities and *P-x-y* diagrams for carbon dioxide dissolution in methanol, ethanol, and acetone mixtures, Fluid Phase Equilibria 131 (1997) 243-258.

[153] C.J. Chang, K.-L. Chiu, C.-Y. Day, A new apparatus for the determination of *P-x-y* diagrams and Henry constants in high presssure alcohols with critical carbon dioxide, Journal of Supercritical Fluids 12 (1998) 223-237.

[154] K. Ohgaki, T. Katayama, Isothermal vapor-liquid equilibrium data for binary systems containing carbon dioxide at high pressures: Methanol - carbon dioxide, *n*-hexane - carbon dioxide, and benzene - carbon dioxide systems, Journal of Chemical & Engineering Data 21 (1976) 53-55.

[155] T. Katayama, K. Ohgaki, G. Maekawa, M. Goto, T. Nagano, Isothermal vapor-liquid equilibria of acetone - carbon dioxide and methanol - carbon dioxide systems at high pressures, Journal of Chemical Engineering of Japan 8 (1975) 89-92.

[156] T. Laursen, P. Rasmussen, S.I. Andersen, VLE and VLLE measurements of dimethyl ether containing systems, Journal of Chemical & Engineering Data 47 (2002) 198-202.

[157] S. Schwinghammer, M. Siebenhofer, R. Marr, Determination and modelling of the high-pressure vapour-liquid equilibrium carbon dioxide - methyl acetate, Journal of Supercritical Fluids 38 (2006) 1-6.

[158] L.F. Pinto, P.M. Ndiaye, L.P. Ramos, M.L. Corazza, Phase equilibrium data of the system CO_2 + glycerol + methanol at high pressures, Journal of Supercritical Fluids 59 (2011) 1-7.

[159] L.F. Pinto, D.I. Segalen da Silva, F. Rosa da Silva, L.P. Ramos, P.M. Ndiaye, M.L. Corazza, Phase equilibrium data and thermodynamic modeling of the system (CO_2 + biodiesel + methanol) at high pressures, Journal of Chemical Thermodynamics 44 (2012) 57-65.

[160] M.M. Elbaccouch, M.B. Raymond, J.R. Elliott, High-pressure vapor–liquid equilibrium for R-22 + ethanol and R-22 + ethanol + water, Journal of Chemical & Engineering Data 45 (2000) 280-287.

[161] K. Tochigi, T. Namae, T. Suga, H. Matsuda, K. Kurihara, M.C. dos Ramos, C. McCabe, Measurement and prediction of high-pressure vapor-liquid equilibria for binary mixtures of carbon dioxide + *n*-octane, methanol, ethanol, and perfluorohexane, Journal of Supercritical Fluids 55 (2010) 682-689.

[162] X. Xie, J.S. Brown, D. Bush, C.A. Eckert, Bubble and dew point measurements of the ternary system carbon dioxide + methanol + hydrogen at 313.2 K, Journal of Chemical & Engineering Data 50 (2005) 780-783.

[163] K. Suzuki, H. Sue, M. Iotu, R.L. Smith, H. Inomata, K. Arai, S. Saito, Isothermal vapor-liquid equilibrium data for binary systems at high pressures: carbon dioxide - methanol, carbon dioxide - ethanol, carbon dioxide - 1-propanol, methane - ethanol, methane - 1-propanol, ethane - ethanol, and ethane - 1-propanol systems, Journal of Chemical & Engineering Data 35 (1990) 63-66.

[164] S.H. Page, S.R. Goates, M.L. Lee, Methanol/CO_2 phase behavior in supercritical fluid chromatography and extraction, Journal of Supercritical Fluids 4 (1991) 109-117.

[165] T.S. Reighard, S.T. Lee, S.V. Olesik, Determination of methanol/CO_2 and acetonitrile/CO_2 vapor-liquid phase equilibria using a variable-volume view cell, Fluid Phase Equilibria 123 (1996) 215-230.

[166] S. Hirohama, T. Takatsuka, S. Miyamoto, T. Muto, Measurement and correlation of phase equilibria for the carbon dioxide – ethanol - water system, Journal of Chemical Engineering of Japan 26 (1993) 408-415.

[167] H.-Y. Chiu, M.-J. Lee, H.-m. Lin, Vapor-liquid phase boundaries of binary mixtures of carbon dioxide with ethanol and acetone, Journal of Chemical & Engineering Data 53 (2008) 2393-2402.

[168] D. Kodama, M. Kato, High-pressure phase equilibrium for carbon dioxide + ethanol at 291.15 K, Journal of Chemical & Engineering Data 50 (2005) 16-17.

[169] M. Stievano, N. Elvassore, High-pressure density and vapor-liquid equilibrium for the binary systems carbon dioxide - ethanol, carbon dioxide - acetone and carbon dioxide - dichloromethane, Journal of Supercritical Fluids 33 (2005) 7-14.

[170] C.-Y. Day, C.J. Chang, C.-Y. Chen, Phase equilibrium of ethanol + CO_2 and acetone + CO_2 at elevated pressures, Journal of Chemical & Engineering Data 44 (1999) 365-365.

[171] S. Takishima, K. Saiki, K. Arai, S. Saito, Phase equilibria for CO_2 - C_2H_5OH - H_2O system, Journal of Chemical Engineering of Japan 19 (1986) 48-56.

[172] Y.S. Feng, X.Y. Du, C.F. Li, Y.J. Hou, An apparatus for determining high pressure fluid phase equilibria and its applications to supercritical carbon dioxide mixtures, Proceedings of the International Symposium on Supercritical Fluids (October 17-19, Nice, France), Lavoisier Tec & Doc, Paris, 1988, pp. 75-84.

[173] S. Yao, F. Liu, Z. Han, Z. Zhu, High pressure VLE of CO_2 – H_2O – alcohol systems (Part 1. Binary systems), Proceedings of the International Symposium on Thermodynamics in Chemical Engineering and Industry (May 30 - June 2, Beijing, China), Chemical Industry and Engineering Society of China, Beijing, 1988, pp. 688-695.

[174] Z. Shen, F. Tan, J. Yang, J. Wang, Study on the equation of state for supercritical gas-liquid equilibrium, Proceedings of the International Symposium on Supercritical Fluids (October 17-19, Nice, France), Lavoisier Tec & Doc, Paris, 1988, pp. 223-230.

[175] I. Tsivintzelis, D. Missopolinou, K. Kalogiannis, C. Panayiotu, Phase compositions and saturated densities for the binary systems of carbon dioxide with ethanol and dichloromethane, Fluid Phase Equilibria 224 (2004) 89-96.

[176] Ž. Knez, M. Škerget, L. Ilič, C. Lütge, Vapor-liquid equilibrium CO_2 - organic solvent systems (ethanol, tetrahydrofuran, ortho-xilene, meta-xilene, para-xilene), Journal of Supercritical Fluids 43 (2008) 383-389.

[177] W. Bae, S. Kwon, H.-S. Byun, H. Kim, Phase behaviour of the poly(vinyl pyrrolidone) + N-vinyl-2-pyrrolidone + carbon dioxide system, Journal of Supercritical Fluids 30 (2004) 127-137.

[178] A. Vega Gonzalez, R. Tufeu, P. Subra, High pressure vapor-liquid equilibrium for the binary systems carbon dioxide + dimethyl sulfoxide and carbon dioxide + dichloromethane, J Chemical and Engineering Data 47 (2002) 492-495.

[179] D.W. Jennings, R.J. Lee, A.S. Teja, Vapor-liquid equilibria in the carbon dioxide + ethanol and carbon dioxide + 1-butanol systems, Journal of Chemical & Engineering Data 36 (1991) 303-307.

[180] H.-I. Chen, H.-Y. Chang, E.T.S. Huang, T.-C. Huang, A new phase behaviour apparatus for supercritical fluid extraction study, Industrial & Engineering Chemistry Research 39 (2000) 4849-4852.

[181] O. Pfohl, A. Pagel, G. Brunner, Phase equilibria in systems containing o-cresol, p-cresol, carbon dioxide, and ethanol at 323.15–473.15 K and 10–35 Mpa, Fluid Phase Equilibria 157 (1999) 53-79.

[182] T. Laursen, S.I. Andersen, VLE and VLLE measurements of dimethyl ether containing systems. 2, Journal of Chemical & Engineering Data 48 (2003) 1085-1087.

[183] J.E. Gutiérrez, A. Bejarano, J.C. de la Fuente, Measurement and modeling of high-pressure (vapour + liquid) equilibria of (CO_2 + alcohol) binary systems, Journal of Chemical Thermodynamics 42 (2010) 591-596.

[184] J.-H. Yim, J.Y. Geun, L.J. Sung, Vapor-liquid equilibria of carbon dioxide plus *n*-propanol at elevated pressure, Korean Journal of Chemical Engineering 27 (2010) 284-288.

[185] V. Vandana, A.S. Teja, Vapor-liquid equilibria in the carbon dioxide + 1-propanol system, Journal of Chemical & Engineering Data 40 (1995) 459-461.

[186] O. Elizalde-Solis, L.A. Galicia-Luna, L.E. Camacho-Camacho, High-pressure vapor-liquid equilibria for CO_2 + alkanol systems and densities of *n*-dodecane and *n*-tridecane, Fluid Phase Equilibria 259 (2007) 23-32.

[187] C. Secuianu, V. Feroiu, D. Geană, High-pressure vapor-liquid equilibria in the system carbon dioxide + 1-butanol at temperatures from (293.15 to 324.15) K, Journal of Chemical & Engineering Data 49 (2004) 1635-1638.

[188] M.B. King, D.A. Alderson, F.H. Fallah, D.M. Kassim, J.R. Sheldon, R.S. Mahmud, Some vapour/liquid and vapour/solid equilibrium measurements of relevance for supercritical extraction operations, and their correlation, in: M.E. Paulaitis, J.M.L. Penninger, R.D. Gray, P. Davidson (Eds), Chemical Engineering at Supercritical Fluid Conditions, Ann Arbor Science, Ann Arbor, Michigan, 1983, pp. 31-80.

[189] V. Najdanovic-Visak, L.P.N. Rebelo, M.N. da Ponte, Liquid-liquid behaviour of ionic liquid - 1-butanol - water and high pressure CO_2-induced phase changes, Green Chemistry 7 (2005) 443-450.

[190] J.S. Lim, C.H. Yoon, K.-P. Yoo, High-pressure vapor-liquid equilibrium measurement for the binary mixtyres of carbon dioxide + *n*-butanol, Korean Journal of Chemical Engineering 26 (2009) 1754-1758.

[191] M. Kato, D. Kodama, M. Kokubo, K. Ohashi, S. Hashimoto, Volumetric behavior of carbon dioxide + butan-1-ol mixtures at 313.15 K, Journal of Chemical & Engineering Data 56 (2011) 421-425.

[192] T. Hiaki, H. Miyagi, T. Tsuji, M. Hongo, Vapor-liquid equilibria for supercritical carbon dioxide + butanol systems at 323.2 K, Journal of Supercritical Fluids 13 (1998) 23-27.

[193] O. Elizalde-Solís, L.A. Galicia-Luna, Vapor-liquid equilibria and phase densities at saturation of carbon dioxide + 1-butanol and carbon dioxide + 2-butanol from 313 to 363 K, Fluid Phase Equilibria 296 2010 66-71.

[194] C. Borch-Jensen, A. Staby and J. Mollerup, Mutual solubility of 1-butanol and carbon dioxide, ethene, ethane, or propane at a reduced supercritical solvent temperature of 1.03, Journal of Supercritical Fluids 7 (1994) 231-244.

[195] H.-I. Chen, H.-Y. Chang and P.-H. Chen, High pressure phase equilibria of carbon dioxide + 1-butanol, and carbon dioxide + water + 1-butanol systems, Journal of Chemical & Engineering Data 47 (2002) 776-780.

[196] D.R. Lide (Ed.), Handbook of Chemistry and Physics, 89th ed., CRC Press, 2008-2009.

[197] G.M. Kontogeorgis, G.K. Folas, N. Muro-Suñé, F. Roca León, M.L. Michelsen, Solvation phenomena in association theories with applications to oil & gas and chemical industries, Oil & Gas Science and Technology-Revue d' IFP Energies Nouvelles 63 (2008) 305-319.

[198] M. Kleiner and G. Sadowski, Modeling of polar systems using PCP-SAFT: An approach to account for induced-association interactions, Journal of Physical Chemistry C 111 (2007) 15544-15553.

[199] F. Xia, N.S. Li, Y.H. Jin and P.Y. Zhao, Phase behavior of the system *n*-hexane + ethanol + carbon dioxide, Journal of Chemical & Engineering Data 56 (2011) 2583-2586.

[200] T. Laursen, VLXE ApS; Scion-DTU: Diplomvej, Denmark, 2007.

FIGURE CAPTIONS

FIGURE 1. (a), (P_c, T_c); (b), (P_c, x) and (c), (T_c, x) projection for *n*-hexane + alkan-1-ol critical loci. Symbols, experimental values: ⊕, methanol (this work); ■, ethanol (this work); ▲, propan-1-ol (this work); ★, butan-1-ol (this work); ● , pentan-1-ol (ref. [63]);◆, hexan-1-ol (ref. [63]). Lines, calculated with PC-SAFT EoS using the parameters from Tables 5 and 6.

FIGURE 2. (a), (P_c, T_c); (b), (P_c, x) and (c), (T_c, x) projection for CO_2 + alkan-1-ol critical loci. Symbols, experimental values: ⊕, methanol (this work); ■, ethanol (this work); ▲, propan-1-ol (this work); ★, butan-1-ol (this work). Lines, calculated with PC-SAFT EoS using the parameters from Tables 8 and 10.

FIGURE 3. Pressure–mole fraction diagram for $n-\mathrm{C_6H_{14}} + \mathrm{CH_3OH}$ VLE. Symbols, experimental values: ○ , T = 298.15 K (ref. [98]); ★, T = 313.15 K (ref. [102]); ◇, T = 333.15 K (ref. [105]); ▲, T = 348.15 K (ref. [100]); ⌂, T = 423.15 K (ref. [55]); ■, T = 448.15 K (ref. [55]). Lines, calculated with PC-SAFT EoS using the parameters from Tables 5 and 7.

FIGURE 4. Pressure–mole fraction diagram for $n-\mathrm{C_6H_{14}} + \mathrm{C_2H_5OH}$ VLE. Symbols, experimental values: ○ , T = 263.15 K (ref. [106]); ■, T = 293.15 K (ref. [106]); ◇, T = 328.15 K (ref. [115]); ▲, T = 413.15 K (ref. [117]); ★, T = 443.15 K (ref. [117]); ⌂, T = 473.15 K (ref. [117)]. Lines, calculated with PC-SAFT EoS using the parameters from Tables 5 and 7.

FIGURE 5. Pressure–mole fraction diagram for $\mathrm{CO_2} + \mathrm{CH_3OH}$ VLE. Symbols, experimental values: ○ , T = 273.15 K (ref. [145]); ◇, T = 298.15 K (ref. [155]); △, T = 308.15 K (ref. [151]); ▲, T = 323.15 K (ref. [146]); ⌂, T = 348 K (ref. [74]); □, T = 373 K (ref. [74]); ■, T = 423.15 K (ref. [146]); ★, T = 477.6 K (ref. [79]). Lines, calculated with PC-SAFT EoS using the parameters from Tables 9 and 10.

FIGURE 6. Pressure–mole fraction diagram for $\mathrm{CO_2} + \mathrm{C_2H_5OH}$ VLE. Symbols, experimental values: ○ , T = 291.15 K (ref. [168]); ★, T = 304.2 K (ref. [171]). ◇, T = 313.0 K (ref. [89]); ⌂, T = 337.2 K (ref. [179]); ■ , T = 348.40 K (ref. [89]); □, T = 391.96 K (ref. [88]). Lines, calculated with PC-SAFT EoS using the parameters from Tables 9 and 10.

Table 1. Purity, water content (% wt) and supplier of the compounds used in this work. Values of the critical temperatures, T_c, and critical pressures, P_c, obtained in this work for pure compounds and those recommended by the National Institute of Standards and Technology, NIST, ref. [36].

Compound	Purity (%)	% wt water	Supplier	This Work		NIST	
				T_c / K	P_c / MPa	T_c /K	P_c / MPa
CO_2	99.98	≤ 0.0003	Air Liquide	304.21	7.383	304.20 ±0.02	7.3825 ±0.0005
n-C_6H_{14}	99.5	< 0.01	Fluka	507.64	3.044	507.6 ±0.5	3.02 ±0.04
CH_3OH	99.8	< 0.02	Fluka	512.90	8.094	513 ±1	8.1 ±0.1
C_2H_5OH	99.8	< 0.2	Scharlau	514.25	6.168	514 ±7	6.3 ±0.4
C_3H_7OH	99.5	< 0.15	Fluka	537.06	5.179	536.9 ±0.8	5.2 ±0.1
C_4H_9OH	99.8	< 0.005	Aldrich	563.42	4.425	562 ±2	4.5 ±0.4

Table 2. Experimental critical temperatures, T_c, and critical pressures, P_c, for the $\{n-\mathrm{C_6H_{14}}+n-\mathrm{C}_m\mathrm{H}_{2m+1}\mathrm{OH}\}$ mixtures as a function of the $n-\mathrm{C_6H_{14}}$ mole fraction.

$x_{\mathrm{C_6H_{14}}}$	T_c / K	P_c / MPa	$x_{\mathrm{C_6H_{14}}}$	T_c / K	P_c / MPa
***n*-C_6H_{14} + CH_3OH**					
0.0000	512.90	8.094	0.5502	483.79	5.028
0.0499	505.84	7.577	0.6001	486.31	4.876
0.1000	498.87	7.034	0.6496	487.67	4.763
0.1500	493.72	6.682	0.6999	490.40	4.572
0.2000	489.17	6.301	0.7496	493.86	4.321
0.2501	485.92	6.001	0.8001	496.26	4.131
0.2999	483.56	5.767	0.8499	499.99	3.804
0.3499	482.22	5.571	0.8996	502.72	3.556
0.3998	481.85	5.388	0.9502	506.01	3.331
0.4498	481.72	5.282	1.0000	507.64	3.044
0.5000	482.54	5.163			
***n*-C_6H_{14} + C_2H_5OH**					
0.0000	514.25	6.168	0.5501	490.68	4.242
0.0501	511.13	5.921	0.6002	491.09	4.154
0.0999	505.80	5.691	0.6503	492.18	4.048
0.1500	501.43	5.431	0.6999	493.53	3.945
0.2000	498.29	5.230	0.7497	495.45	3.821
0.2499	495.18	5.024	0.7999	498.17	3.696
0.2999	492.49	4.861	0.8497	499.92	3.552
0.3500	491.63	4.700	0.9001	503.41	3.418
0.4001	490.15	4.573	0.9500	505.50	3.256
0.4500	489.89	4.460	1.0000	507.64	3.044
0.4999	489.77	4.349			

n-C_6H_{14} + C_3H_7OH					
0.0000	537.06	5.179	0.5506	502.90	3.612
0.0500	530.79	4.955	0.6001	502.81	3.541
0.0999	525.23	4.756	0.6497	502.87	3.473
0.1501	520.83	4.562	0.7001	503.64	3.412
0.2000	516.21	4.384	0.7497	503.82	3.346
0.2500	512.88	4.245	0.7998	504.58	3.287
0.3001	509.56	4.092	0.8501	505.24	3.226
0.3498	507.59	3.975	0.9002	506.11	3.163
0.4000	505.50	3.867	0.9498	507.02	3.105
0.4501	504.28	3.764	1.0000	507.64	3.044
0.4999	503.52	3.689			
n-C_6H_{14} + C_4H_9OH					
0.0000	563.42	4.425	0.5499	520.81	3.568
0.0500	559.37	4.360	0.5999	518.32	3.495
0.1001	554.84	4.301	0.6501	515.74	3.426
0.1500	550.30	4.227	0.7000	513.59	3.362
0.1999	546.28	4.147	0.7500	511.64	3.301
0.2499	542.06	4.059	0.8000	510.25	3.241
0.3001	538.18	3.976	0.8499	509.19	3.192
0.3501	535.08	3.895	0.9000	508.72	3.142
0.4001	530.76	3.808	0.9500	508.30	3.093
0.4503	526.79	3.725	1.0000	507.64	3.044
0.4999	523.57	3.644			

Table 3. Experimental critical temperatures, T_c, and critical pressures, P_c, for the {$CO_2 + n - C_mH_{2m+1}OH$ } mixtures as a function of the CO_2 mole fraction.

x_{CO_2}	T_c / K	P_c / MPa	x_{CO_2}	T_c / K	P_c / MPa
CO_2 + CH_3OH					
0.0000	512.90	8.094	0.7101	371.44	15.169
0.0501	508.63	8.807	0.7301	363.32	14.487
0.0995	501.64	9.582	0.7502	350.96	13.439
0.1351	495.95	10.133	0.7695	346.18	12.964
0.1997	491.70	10.830	0.7853	339.82	12.112
0.2501	484.72	11.712	0.7998	336.81	11.614
0.3000	480.24	12.249	0.8144	333.74	11.286
0.3505	471.87	13.058	0.8503	328.42	10.345
0.4001	465.25	13.614	0.8701	324.92	10.016
0.4494	455.58	14.389	0.8989	320.75	9.419
0.4999	438.84	15.480	0.9198	317.10	8.878
0.5503	424.25	16.096	0.9601	311.86	8.009
0.6006	408.98	16.388	0.9901	306.25	7.503
0.6505	393.20	16.266	0.9949	305.06	7.402
0.7000	377.29	15.623	1.0000	304.21	7.383
CO_2 + C_2H_5OH					
0.0000	514.25	6.168	0.5505	428.65	14.439
0.0500	507.29	7.309	0.6001	413.32	14.929
0.1000	501.54	8.064	0.6504	400.57	15.077
0.1500	493.23	9.052	0.7199	374.38	14.400
0.1998	486.84	9.579	0.7506	368.18	13.842
0.2504	480.48	10.509	0.8002	348.47	12.429
0.3000	474.58	11.056	0.8504	336.96	11.088

0.3496	466.35	11.865	0.9000	326.90	9.817
0.3999	458.40	12.578	0.9501	319.07	8.605
0.4496	451.14	13.390	1.0000	304.21	7.383
0.5002	436.22	14.086			
$CO_2 + C_3H_7OH$					
0.0000	537.06	5.179	0.5495	447.10	14.602
0.0498	529.39	6.122	0.5998	435.29	15.268
0.0997	523.59	6.862	0.6495	422.60	15.928
0.1495	517.40	7.712	0.6994	398.97	15.975
0.2002	510.88	8.538	0.7498	383.17	15.446
0.2501	502.93	9.383	0.7999	362.07	14.114
0.3000	496.88	10.198	0.8502	344.49	12.177
0.3497	488.68	11.062	0.8999	327.97	10.203
0.4000	480.52	11.901	0.9500	315.45	8.660
0.4494	471.87	12.743	1.0000	304.21	7.383
0.4993	459.09	13.786			
$CO_2 + C_4H_9OH$					
0.0000	563.42	4.425	0.6999	430.26	17.084
0.0496	554.67	5.445	0.7299	419.43	17.271
0.0996	546.59	6.597	0.7501	410.86	17.254
0.1504	538.62	7.800	0.7795	393.78	16.879
0.1995	528.69	8.813	0.8004	384.44	16.538
0.2488	521.54	9.634	0.8099	377.56	16.136
0.3001	513.06	10.826	0.8298	362.32	15.163
0.3500	504.08	11.576	0.8498	351.71	13.885
0.3999	495.90	12.556	0.8601	343.05	12.843
0.4498	487.11	13.338	0.8799	335.74	11.531

0.4994	478.73	13.987	0.9248	323.96	9.868
0.5495	470.59	14.819	0.9599	314.07	8.800
0.5999	458.87	15.596	1.0000	304.21	7.383
0.6495	445.27	16.448			

Table 4. Temperature and pressure ranges of the experimental data (this work and literature critical loci and VLE) used in the modellization with the PC-SAFT model. All the systems have been studied over the whole composition range.

	Critical locus		**VLE**	
System	T_c **/ K**	P_c **/ MPa**	T **/ K**	P **/ MPa**
n-hexane + methanol	480 - 513	3.02 - 8.09	293 - 507	0.013 - 7.40
n-hexane + ethanol	488 - 515	3.01 - 6.17	263 - 514	0.0023 - 6.14
n-hexane + propan-1-ol	502 - 537	3.04 - 5.18	298 - 513	0.0028 - 4.34
n-hexane + butan-1-ol	507 - 563	3.04 - 4.42	288 - 332	0.00041 - 0.076
n-hexane + pentan-1-ol	507 - 588	3.04 - 3.88	303 - 323	0.00044 - 0.054
n-hexane + hexan-1-ol	507 - 545	3.04 - 3.40	293 - 373	0.00006 - 0.245
CO_2 + methanol	304 - 513	7.38 - 18.50	213 - 478	0.10 - 16.46
CO_2 + ethanol	304 - 514	6.15 - 15.30	283 - 494	0.51 - 15.16
CO_2 + propan-1-ol	304 - 537	5.18 - 16.00	293 - 427	0.47 - 16.03
CO_2 + butan-1-ol	304 - 563	4.42 - 17.37	293 - 430	0.52 - 17.35

Table 5.- Association scheme and PC-SAFT EoS pure-compounds parameters used in the *n*-hexane + alkan-1-ol modellization. m, σ, ε: geometric parameters, rescaled in this work from T_c and P_c. $\kappa^{A_iB_i}$ and $\varepsilon^{A_iB_i}$: association parameters taken from reference [20].

Compound	**Association scheme**	***m / M*** **(mol g^{-1})**	σ **(Å)**	ε **(K)**	$\kappa^{A_iB_i}$	$\varepsilon^{A_iB_i}$ **(K)**
n-C_6H_{14}	Non	0.03760	3.8823	225.88		
CH_3OH	2B	0.05273	3.3264	175.20	0.035176	2899.5
C_2H_5OH	2B	0.04924	3.4895	187.51	0.032384	2653.4
C_3H_7OH	2B	0.05560	3.3722	216.80	0.015268	2276.8
C_4H_9OH	2B	0.04079	3.7307	242.47	0.006692	2544.6
$C_5H_{11}OH$	2B	0.04486	3.5439	233.83	0.010319	2252.1
$C_6H_{13}OH$	2B	0.03745	3.7817	247.04	0.005747	2538.9

Table 6.- PC-SAFT EoS temperature-dependent binary interaction parameters, $k_{ij}(T)$, and mean relative deviations in critical temperature and pressure, $MRD(T_c)$ and $MRD(P_c)$, for $\{n-\mathrm{C_6H_{14}} + n-\mathrm{C}_m\mathrm{H}_{2m+1}\mathrm{OH}\ (m=1-6)\}$ systems obtained using the parameters from Table 5. Average deviations for each system are also included.

System	$k_{ij}(T)$	Range T/ K	Nº Points	Range P/ MPa	Range $x_{\mathrm{C_6H_{14}}}$	$MRD(T_c)$/%	$MRD(P_c)$/%	Ref.
n-C_6H_{14} +								
CH_3OH	0.00234 + 1.40x10^{-4}T	481-513	21	3.04-8.09	0-1	0.96	6.82	This work
		481-513	10	3.02-8.06	0-1	0.83	6.92	[52]
		481-513	18	3.02-8.07			4.48	[53]
		480-513	18	3.02-8.12	0-1	1.07	7.37	[54]
		481-507	4	3.05-5.38	0.41-1	0.46	4.65	[55]
		$MRD(T_c)$ = 0.94% ; $MRD(P_c)$ = 6.26%						
C_2H_5OH	0.00187 + 3.70x10^{-5}T	489-515	21	3.04-6.17	0-1	0.42	3.02	This work
		489-514	10	3.03-6.12	0-1	0.43	1.47	[38]
		489-514	11	3.01-6.14	0-1	0.35	2.49	[56]
		493-503	2	3.31-3.93	0.68-0.91	0.59	1.39	[57]
		499-514	6		0-0.8	0.99		[58]
		488-514	8		0-1	0.60		[59]
		$MRD(T_c)$ = 0.50% ; $MRD(P_c)$ = 2.46%						
C_3H_7OH	0.00153 + 6.54x10^{-5}T	502-537	20	3.04-5.18	0-1	0.34	1.21	This work
		503-513	3	3.41-4.34	0.31-0.79	0.10	3.30	[50]
		502-537	10		0-1	0.12		[60]
		502-528	8		0.1-0.89	0.13		[61]
		$MRD(T_c)$ = 0.23% ; $MRD(P_c)$ = 1.48%						
C_4H_9OH	0.00153 + 2.73x10^{-5}T	507-563	21	3.04-4.42	0-1	0.22	0.97	This work
		507-562	10		0-1	0.14		[60]
		508-548	8		0.19-0.93	0.15		[61]
		$MRD(T_c)$ = 0.19% ; $MRD(P_c)$ = 0.97%						
$C_5H_{11}OH$	0.00153 + 1.63x10^{-5}T	507-588	8		0-1	0.85		[59]
		507-588	7		0-1	0.50		[62]
		507-588	21	3.04-3.88	0-1	0.23	1.07	[63]
		$MRD(T_c)$ = 0.42%; $MRD(P_c)$ = 1.07%.						
$C_6H_{13}OH$	0.00153 + 2.12x10^{-5}T	507-545	9	3.04-3.40	0.65-1	0.21	1.12	[63]
		$MRD(T_c)$ = 0.21% ; $MRD(P_c)$ = 1.12%						

Table 7.- PC-SAFT EoS temperature-dependent binary interaction parameters, $k_{ij}(T)$, mean relative deviations in bubble pressure, *MRD* (*P*), and absolute deviations for the solvent mole fraction in the vapor phase, $\Delta y_{C_6H_{14}}$, for $\{ n-C_6H_{14} + n-C_mH_{2m+1}OH\ (m = 1-6)\}$ systems obtained using the parameters from Table 5. Average deviations for each system are also included.

***n*-C_6H_{14} + CH_3OH ; $k_{ij}(T) = 0.00234 + 1.40x10^{-4}T$**													
T / K	**Nº Points**	**Range *P*/ 10^{-3}MPa**	**Range $x_{C_6H_{14}}$**	***MRD (P)/%***	$\Delta y_{C_6H_{14}}$	**Ref.**	***T / K***	**Nº Points**	**Range *P*/ 10^{-3}MPa**	**Range $x_{C_6H_{14}}$**	***MRD (P)/%***	$\Delta y_{C_6H_{14}}$	**Ref.**
293.15	24	13-28	0-1	4.40	0.019	[97]	318.15	13	44-84	0-1	1.88	0.020	[104]
298.15	21	16-35	0-1	4.48		[48]	323.15	24	54-103	0-1	2.02		[100]
298.15	26	31-36	0.06-0.93	2.47	0.011	[98]	333.15	24	76-149	0-1	1.75		[100]
298.15	7	32-35	0.05-0.95	3.43	0.020	[99]	333.15	30	76-194	0-1	1.98	0.026	[105]
303.15	20	22-45	0-1	7.25	0.041	[130]	343.15	25	104-212	0-1	1.68		[100]
308.15	24	28-55	0-1	6.64		[100]	348.15	25	129-251	0-1	1.80		[100]
313.15	25	35-69	0-1	2.52		[100]	398.15	6	450-1040	0-1	0.87		[55]
313.15	55	35-69	0-1	5.73	0.036	[101]	423.15	6	750-1840	0-1	1.42		[55]
313.15	32	35-69	0-1	1.75	0.010	[102]	448.15	6	1200-3100	0-1	1.23		[55]
313.15	14	35-69	0-1	3.78		[103]	402-507	79	500-7400	0-1	1.83		[52]
318.15	25	44-84	0-1	2.22		[100]							
MRD(*P*) = 3.20% ; $\Delta y_{C_6H_{14}}$ = 0.010													
***n*-C_6H_{14} + C_2H_5OH ; $k_{ij}(T) = 0.0187 + 3.70x10^{-5}T$**													
T / K	**Nº Points**	**Range *P*/ 10^{-3}MPa**	**Range $x_{C_6H_{14}}$**	***MRD (P)/%***	$\Delta y_{C_6H_{14}}$	**Ref.**	***T / K***	**Nº Points**	**Range *P*/ 10^{-3}MPa**	**Range $x_{C_6H_{14}}$**	***MRD (P)/%***	$\Delta y_{C_6H_{14}}$	**Ref.**
263.15	19	2.3-4.2	0.05-0.95	4.58	0.058	[106]	323.15	26	29-73	0-1	3.82		[109]
273.15	15	3.8-7.5	0.05-0.95	3.69	0.076	[106]	323.15	20	29-73	0-1	5.59	0.055	[114]
283.15	19	7.2-13	0.05-0.95	2.74	0.067	[106]	328.15	11	37-89	0-1	4.28	0.049	[110]
293.15	19	10-21	0.05-0.95	2.44	0.078	[106]	328.15	17	46-90	0-0.96	2.15	0.038	[115]
298.15	27	7.8-25	0-1	6.49		[48]	333.15	26	47-107	0-1	3.15		[109]
298.15	17	15-27	0.04-0.96	4.19	0.069	[98]	333.15	8	90-110	0.13-0.88	2.35	0.057	[116]
298.15	9	20-25	0.10-0.90	5.18	0.055	[99]	343.15	26	72-152	0-1	2.63		[109]
298.15	9	7.8-25	0-1	4.62	0.055	[107]	353.15	26	108-211	0-1	2.18		[109]
298.15	9	19-26	0.10-0.90	3.72	0.056	[108]	413.15	11	617-1067	0-1	2.32	0.017	[117]

303.15	19	17-33	0.05-0.95	4.37	0.075	[106]	443.15	11	1095-2006	0-1	1.44	0.013	[117]
303.15	26	10-32	0-1	5.48		[109]	473.15	14	1811-3479	0-1	2.46	0.007	[57]
308.15	11	14-40	0-1	6.20	0.046	[110]	473.15	11	1811-3485	0-1	0.79	0.019	[117]
313.15	26	18-49	0-1	4.56		[109]	483.15	12	2109-4130	0-1	1.26	0.015	[57]
313.15	19	18-50	0-1	4.54	0.041	[111]	493.15	7	2334-4885	0-1	1.29	0.008	[57]
313.15	15	18-49	0-1	5.01	0.043	[112]	503.15	5	2838-5561	0-1	0.85	0.001	[57]
318.15	11	22-61	0-1	4.57	0.048	[110]	382-514	127	435-6140	0-1	1.65		[56]
318.15	40	23-60	0-1	5.47	0.049	[113]							
MRD(*P*) = 3.43% ; $\Delta y_{C_6H_{14}}$ = 0.026													
***n*-C_6H_{14} + C_3H_7OH ; $k_{ij}(T)$ = 0.00153 + 6.54x10^{-5}T**													
T* / *K	**Nº Points**	**Range *P*/ 10^{-3}MPa**	**Range $x_{C_6H_{14}}$**	***MRD* (*P*)/%**	$\Delta y_{C_6H_{14}}$	**Ref.**	***T* / *K***	**Nº Points**	**Range *P*/ 10^{-3}MPa**	**Range $x_{C_6H_{14}}$**	***MRD* (*P*)/%**	$\Delta y_{C_6H_{14}}$	**Ref.**
298.15	27	2.8-21	0-1	2.70		[48]	318.15	5	41-48	0.26-0.71	1.04	0.010	[122]
298.15	9	13-21	0.10-0.90	1.77	0.004	[99]	323.15	22	12-58	0-1	2.00	0.008	[123]
298.15	11	2.8-21	0-1	3.12		[118]	483.15	13	2088-2771	0-1	1.79	0.010	[50]
298.15	11	2.8-21	0-1	2.43	0.011	[119]	493.15	14	2451-3215	0-1	1.53	0.015	[50]
308.15	9	5.6-32	0-1	2.56		[120]	503.15	8	2824-3788	0-1	1.04	0.010	[50]
313.15	22	7.0-40	0-1	1.37	0.009	[121]	513.15	4	3554-4340	0-0.24	1.40	0.013	[50]
MRD(*P*) = 2.01% ; $\Delta y_{C_6H_{14}}$ = 0.007													
***n*-C_6H_{14} + C_4H_9OH ; $k_{ij}(T)$ = 0.00153 + 2.73x10^{-5}T**													
T* / *K	**Nº Points**	**Range *P*/ 10^{-3}MPa**	**Range $x_{C_6H_{14}}$**	***MRD* (*P*)/%**	$\Delta y_{C_6H_{14}}$	**Ref.**	***T* / *K***	**Nº Points**	**Range *P*/ 10^{-3}MPa**	**Range $x_{C_6H_{14}}$**	***MRD* (*P*)/%**	$\Delta y_{C_6H_{14}}$	**Ref.**
288.15	15	0.41-13	0-1	2.80	0.006	[124]	313.15	15	2.5-37	0-1	2.41	0.009	[124]
298.15	17	0.82-20	0-1	4.51	0.009	[125]	332.53	26	8.1-76	0-1	3.14	0.010	[126]
MRD(*P*) = 3.25% ; $\Delta y_{C_6H_{14}}$= 0.009													
***n*-C_6H_{14} + $C_5H_{11}OH$; $k_{ij}(T)$ = 0.00153 + 1.63x10^{-5}T**													
T* / *K	**Nº Points**	**Range *P*/ 10^{-3}MPa**	**Range $x_{C_6H_{14}}$**	***MRD* (*P*)/%**	$\Delta y_{C_6H_{14}}$	**Ref.**	***T* / *K***	**Nº Points**	**Range *P*/ 10^{-3}MPa**	**Range $x_{C_6H_{14}}$**	***MRD* (*P*)/%**	$\Delta y_{C_6H_{14}}$	**Ref.**
303.15	15	0.44-24	0-1	2.35	0.004	[127]	323.15	15	1.8-54	0-1	3.02	0.007	[127]
MRD(*P*) = 2.68% ; $\Delta y_{C_6H_{14}}$= 0.005													
***n*-C_6H_{14} + $C_6H_{13}OH$; $k_{ij}(T)$ = 0.00153 + 2.12x10^{-5}T**													

T / K	**№ Points**	**Range *P*/ 10^{-3}MPa**	**Range $x_{C_6H_{14}}$**	***MRD (P)/%***	$\Delta y_{C_6H_{14}}$	**Ref.**	*T / K*	**№ Points**	**Range *P*/ 10^{-3}MPa**	**Range $x_{C_6H_{14}}$**	***MRD (P)/%***	$\Delta y_{C_6H_{14}}$	**Ref.**
293.15	23	0.06-16	0-1	3.70		[128]	328.21	11	0.95-65	0-1	1.17		[129]
298.23	11	0.11-20	0-1	2.42	0.000	[129]	333.15	23	1.3-76	0-1	1.51		[128]
303.15	23	0.14-25	0-1	2.82		[128]	333.16	11	1.3-76	0-1	1.58		[129]
303.15	11	0.16-25	0-1	2.11		[129]	338.18	11	1.8-90	0-1	1.94		[129]
308.15	11	0.23-31	0-1	2.56		[129]	342.82	11	2.3-104	0-1	2.28	0.004	[129]
313.15	23	0.32-37	0-1	1.68		[128]	343.15	23	2.3-105	0-1	1.86		[128]
313.22	11	0.33-37	0-1	0.82		[129]	353.15	23	4.1-142	0-1	2.18		[128]
318.21	11	0.48-45	0-1	0.31		[129]	363.15	22	6.9-188	0-1	2.38		[128]
323.15	23	0.65-54	0-1	1.40		[128]	373.15	23	11-245	0-1	2.46		[128]
323.16	11	0.68-54	0-1	0.67	0.001	[129]							
MRD(*P*) = 1.81% ; $\Delta y_{C_6H_{14}}$ = 0.002													

Table 8.- PC-SAFT EoS temperature-dependent binary interaction parameters, $k_{ij}(T)$, and mean relative deviations in critical temperature and pressure, $MRD(T_c)$ and $MRD(P_c)$, for $\{CO_2 + n - C_mH_{2m+1}OH\ (m = 1 - 4)\}$ systems obtained using the parameters from Table 10. Average deviations for each system are also included.

System	$k_{ij}(T)$	Range T/ K	Nº Points	Range P/ MPa	Range x_{CO_2}	$MRD(T_c)$/%	$MRD(P_c)$/%	Ref.
CO_2 +								
CH_3OH	-0.0323 + 2.88x10^{-4}T	304-513	30	7.38-16.39	0-1	1.17	5.97	This work
		304-513	18	7.42-16.34	0-1	2.86	6.30	[54]
		304-492	20	7.39-16.41			3.45	[70]
		323-473	4	9.55-16.13	0.27-0.84	3.10	11.0	[71]
		321-473	19	9.5-16.5			2.90	[72], [73]
		323-408	4	9.80-18.50	0.42-0.75	12.5	28.2	[74]
		307-422	11	7.35-16.41	0.49-0.98	5.49	15.7	[75]
		313.2	1	8.21	0.968	2.97	0.49	[76]
		313-343	5	8.15-12.40	0.76-0.94	2.53	15.0	[77]
		305-320	8	7.62-9.35	0.93-0.99	0.69	2.04	[78]
		323-478	4	9.50-16.50	0.25-0.85	2.54	7.17	[79]
		304-317	4	7.38-9.24	0.96-1	0.72	7.53	[80]
		304-328	6	7.38-10.49	0.79-1	1.78	10.8	[81]
		$MRD(T_c)$ = 2.67% ; $MRD(P_c)$ = 7.17%						
C_2H_5OH	2.60x10^{-4}T	304-514	21	6.17-15.08	0-1	0.77	3.93	This work
		323-483	15	9.6-15.4			4.25	[73]
		310-410	7	7.77-15.17	0.60-0.96	1.16	2.62	[75]
		313.2	1	8.15	0.970	1.70	4.30	[76]
		313-345	5	8.16-11.97	0.80-0.96	0.87	5.06	[77]
		306-325	8	7.65-9.74	0.93-0.99	0.54	4.41	[78]
		304-514	6	6.15-15.30	0-1	5.63	15.5	[82]
		321-364	10	9.10-13.86	0.83-0.93	2.06	14.1	[83]
		304-321	5	7.38-9.27	0.93-1	0.31	3.49	[84]
		313-333	2	8.03-10.71	0.89-0.97	0.74	9.27	[85]
		313-343	4	8.1-11.9			7.68	[86]
		308.15	1	7.794	0.9940	0.80	4.60	[87]
		333.53	1	10.75	0.850	0.60	8.80	[88]
		313-373	5	8.15-14.34	0.72-0.97	1.19	4.70	[89]
		308.15	1	7.702	0.9797	0.60	0.38	[90]
		318.15	1	8.80	0.9649	1.60	11.4	[91]
		383-493	2	8.87-14.72	0.20-0.70	1.18	3.85	[92]

		$MRD(T_c)$ = 1.37% ; $MRD(P_c)$ = 6.17%						
C_3H_7OH	$2.65x10^{-4}T$	304-537	21	5.18-15.97	0-1	0.97	3.48	This work
		313-353	3	8.19-13.40	0.87-0.98	1.46	13.4	[68]
		323-513	18	8.4-16.0			2.62	[73]
		314-424	9	8.44-16.00	0.64-0.97	1.53	2.08	[75]
		307-320	6	7.58-9.00	0.96-0.99	0.27	2.35	[78]
		352.83	1	13.33	0.833	1.50	10.8	[88]
		426.68	1	15.335	0.540	5.78	4.28	[94]
		$MRD(T_c)$ = 1.16% ; $MRD(P_c)$ = 3.53%						
C_4H_9OH	$2.90x10^{-4}T$	304-563	27	4.42-17.27	0-1	1.88	6.92	This work
		323-533	17	8.5-17.4			2.58	[73]
		315-427	6	8.71-17.37	0.71-0.97	2.78	5.00	[75]
		305-329	8	7.58-10.81	0.967-0.997	0.43	5.19	[78]
		324-427	5	9.80-17.03	0.75-0.93	3.74	5.06	[95]
		313.15	1	8.23	0.987	0.78	3.40	[96]
		$MRD(T_c)$ = 1.92% ; $MRD(P_c)$ = 5.17%						

Table 9.- PC-SAFT EoS temperature-dependent binary interaction parameters, $k_{ij}(T)$, mean relative deviations in bubble pressure, *MRD* (*P*), and absolute deviations for the solvent mole fraction in the vapor phase, $\Delta y_{\mathrm{CO_2}}$, for $\{\mathrm{CO_2} + n - \mathrm{C}_m\mathrm{H}_{2m+1}\mathrm{OH}\ (m = 1 - 4)\}$ systems obtained using the parameters from Table 10. Average deviations for each system are also included.

CO_2 + CH_3OH ; $k_{ij}(T)$ = -0.0323 + 2.88x10^{-4}T													
***T* / K**	**Nº Points**	**Range *P*/ MPa**	**Range $x_{\mathrm{CO_2}}$**	***MRD (P)/%***	$\Delta y_{\mathrm{CO_2}}$	**Ref.**	***T* / K**	**Nº Points**	**Range *P*/ MPa**	**Range $x_{\mathrm{CO_2}}$**	***MRD (P)/%***	$\Delta y_{\mathrm{CO_2}}$	**Ref.**
213.15	4	0.10-0.43	0.09-0.58	16.9	0.001	[145]	313.14	17	1.32-8.03	0.07-0.88	4.62	0.002	[152]
228.15	7	0.10-0.71	0.05-0.45	11.7	0.001	[145]	313.14	17	1.32-7.72	0.07-0.88	4.97	0.002	[153]
230.00	6	0.69-0.88	0.38-0.96	9.37	0.000	[146]	313.14	16	0.57-7.78	0.03-0.74	2.69	0.007	[139]
233.15	6	0.30-0.89	0.11-0.54	8.53		[147]	313.15	11	0.69-8.12	0.04-0.94	4.16	0.010	[77]
237.15	9	0.10-1.01	0.03-0.47	8.78	0.001	[145]	313.15	8	1.29-6.76	0.07-0.47	6.9	0.004	[150]
243.15	6	0.20-1.33	0.06-0.71	11.0		[148]	313.15	9	0.58-8.06	0.03-0.90	4.07	0.002	[154]
247.15	10	0.10-1.16	0.02-0.62	5.42	0.001	[145]	313.15	5	4.20-7.82	0.24-0.87	4.65		[158]
248.15	7	0.33-1.69	0.08-1	5.61		[147]	313.15	5	4.20-7.82	0.24-0.87	4.65		[159]
250.00	7	0.69-1.75	0.16-0.93	4.52	0.000	[146]	313.2	13	0.70-8.07	0.04-0.87	2.81	0.003	[76]
253.15	6	0.55-1.52	0.11-0.49	10.2		[147]	313.2	7	0.93-7.93	0.05-0.79	4.04		[162]
258.15	6	0.22-2.13	0.04-0.72	5.55		[148]	313.4	8	0.68-7.71	0.03-0.62	9.31	0.006	[163]
258.15	4	0.51-1.65	0.09-0.35	1.20	0.042	[149]	320.15	10	0.60-8.93	0.03-0.88	5.22	0.004	[77]
263.15	4	0.79-2.53	0.12-0.67	2.10	0.003	[150]	323	14	0.50-9.00	0.02-0.64	11.5	0.009	[74]
273.15	10	0.69-3.45	0.08-0.99	2.57	0.000	[146]	323.15	10	1.03-9.51	0.04-0.81	8.55	0.015	[66]
273.15	9	0.45-3.30	0.06-0.76	3.54		[147]	323.15	13	0.99-9.53	0.04-0.82	5.14		[71]
273.15	20	0.66-3.49	0.08-1	1.55		[147]	323.15	13	0.99-9.53	0.04-0.82	5.77	0.010	[146]
273.15	6	0.19-3.19	0.02-0.65	1.74		[148]	323.15	5	5.06-9.24	0.24-0.87	6.73		[159]
273.15	4	0.89-3.27	0.11-0.67	1.22	0.002	[150]	323.2	10	0.06-9.42	0-0.79	7.83	0.008	[79]
278.15	8	1.50-3.93	0.12-0.82	10.3	0.001	[151]	330.00	11	0.78-10.57	0.03-0.82	4.94	0.014	[77]
288.15	7	1.50-4.95	0.11-0.83	10.3	0.001	[151]	330.00	13	0.69-10.65	0.02-0.85	5.57	0.009	[146]
290.00	9	0.69-5.16	0.05-0.97	2.96	0.001	[146]	333	12	9.51-10.90	0.78-0.96	7.08		[164]
291.1	12	0.56-4.93	0.06-0.88	23.6	0.005	[152]	333.15	5	5.70-10.78	0.24-0.87	6.08		[159]
291.2	11	0.56-4.33	0.06-0.76	25.5	0.004	[153]	335.65	11	0.84-11.45	0.03-0.79	5.61	0.022	[77]
293.15	6	0.79-5.03	0.06-0.61	5.54	0.003	[66]	342.8	13	0.67-12.39	0.02-0.76	5.38	0.030	[77]
298.1	6	1.30-5.42	0.09-0.54	3.25	0.003	[156]	343	12	9.45-12.58	0.80-0.95	5.75		[164]
298.15	30	0.50-5.99	0.03-0.83	6.38	0.001	[66]	343.15	5	6.44-12.16	0.24-0.87	6.49		[159]

298.15	17	1.73-6.23	0.12-0.97	4.05		[71]	348	16	0.05-11.00	0.01-0.43	7.44	0.007	[74]
298.15	13	1.73-5.75	0.12-0.65	4.95	0.001	[146]	352.6	9	0.82-13.53	0.02-0.65	8.09	0.021	[79]
298.15	11	0.78-5.08	0.06-0.56	5.41		[147]	353	10	8.11-13.89	0.80-0.95	2.55		[164]
298.15	8	0.26-5.38	0.02-0.57	2.94		[148]	363	10	11.74-14.78	0.77-0.93	6.22		[164]
298.15	9	1.50-6.08	0.10-0.88	8.00	0.002	[151]	363.15	8	0.97-8.56	0.03-0.27	8.20	0.013	[150]
298.15	8	0.79-5.95	0.06-0.90	2.59	0.001	[154]	373	16	0.50-11.00	0.005-0.32	7.95	0.027	[74]
298.15	13	0.22-6.13	0.01-0.96	1.41	0.002	[155]	373	10	10.79-15.28	0.77-0.91	7.16		[164]
298.16	17	0.92-5.71	0.07-0.88	3.85	0.004	[152]	373.15	11	2.01-15.42	0.04-0.67	10.6		[71]
298.16	17	0.92-5.71	0.07-0.88	3.98	0.004	[153]	373.15	10	3.81-15.42	0.09-0.67	9.85	0.023	[146]
303.1	7	1.24-5.51	0.07-0.45	6.93	0.002	[156]	373.15	9	2.16-12.07	0.04-0.36	12.7	0.023	[150]
303.15	6	0.84-5.40	0.05-0.42	6.15	0.003	[157]	383	6	11.76-15.56	0.77-0.84	6.58		[164]
303.15	5	3.24-6.41	0.24-0.87	2.41		[158]	393	17	1.00-13.00	0.01-0.31	10.0	0.012	[74]
303.15	5	3.24-6.41	0.24-0.87	2.41		[159]	393	5	11.00-14.71	0.80-0.84	7.42		[164]
303.18	16	0.89-6.32	0.07-0.88	4.29	0.004	[152]	394.2	9	1.03-16.29	0.01-0.55	7.74	0.036	[79]
303.18	16	0.89-6.32	0.07-0.88	4.22	0.003	[153]	423.15	10	3.67-16.08	0.05-0.47	6.53		[71]
308.15	9	1.54-7.43	0.09-0.89	7.54	0.006	[151]	423.15	10	3.67-16.13	0.05-0.52	6.53	0.046	[146]
308.15	16	1.32-7.01	0.09-0.88	3.57	0.002	[152]	473.15	3	7.52-12.80	0.07-0.24	5.55		[71]
308.15	16	1.32-7.01	0.09-0.88	3.57	0.003	[153]	473.15	3	7.52-12.80	0.07-0.24	5.58	0.047	[146]
310.00	19	0.69-7.74	0.03-0.97	3.70	0.002	[146]	477.6	8	5.29-12.51	0.02-0.21	4.63	0.031	[79]
310.15	19	0.48-7.60	0.020-0.97	5.08	0.003	[66]	298-373	70	1.54-15.55	0.10-0.91	6.82		[165]
313.0	11	1.14-7.53	0.07-0.60	2.83		[160]	298-423	46	6.08-16.46	0.49-0.98	2.10		[75]
313.1	5	1.59-6.34	0.09-0.42	3.98	0.004	[156]							
MRD(*P*) = 6.04% ; Δy_{CO_2} = 0.008													
CO_2 + C_2H_5OH ; $k_{ij}(T)$ = 0.0625 + 1.23x10^{-4}*T*													
***T* / K**	**Nº Points**	**Range *P*/ MPa**	**Range x_{CO_2}**	***MRD* (*P*)/%**	**Δy_{CO_2}**	**Ref.**	***T* / K**	**Nº Points**	**Range *P*/ MPa**	**Range x_{CO_2}**	***MRD* (*P*)/%**	**Δy_{CO_2}**	**Ref.**
283	5	1.14-4.14	0.10-0.73	3.47	0.010	[166]	313.4	10	0.51-7.91	0.03-0.87	8.23	0.035	[163]
288	5	0.86-4.67	0.07-0.68	2.89	0.014	[166]	313.40	10	0.57-8.11	0.03-0.97	7.84	0.023	[77]
291.15	10	1.16-4.36	0.16-0.73	30.9	0.005	[152]*	313.46	10	1.74-8.02	0.10-0.93	6.59	0.027	[85]
291.15	13	2.45-5.53	0.19-0.98	7.64		[167]	314.2	8	5.54-7.92	0.34-0.87	8.27		[177]
291.15	9	2.09-5.40	0.18-0.99	3.69	0.005	[168]	314.45	6	7.07-8.30	0.55-0.95	7.09		[178]
291.15	3	3.30-4.73	0.24-0.49	12.4		[169]	314.5	6	5.55-7.89	0.34-0.84	9.92	0.021	[179]
291.15	10	1.16-4.36	0.16-0.73	39.5	0.004	[170]*	318.15	3	8.60-8.75	0.90-0.98	6.39		[91]
292	5	1.63-5.08	0.12-0.79	3.69	0.013	[166]	322.5	11	0.57-9.18	0.03-0.92	9.78	0.029	[77]

293.1	8	0.68-5.27	0.05-0.81	4.83	0.017	[67]	323.1	11	2.94-9.17	0.19-0.79	11.1	0.031	[173]
298.17	8	1.16-5.82	0.13-0.81	25.9	0.008	[152]*	323.1	4	5.03-8.20	0.25-0.51	13.0	0.013	[180]
298.17	13	2.79-6.37	0.19-0.98	5.61		[167]	323.15	3	4.93-8.11	0.24-0.49	10.8		[169]
298.17	8	1.16-5.82	0.13-0.81	32.2	0.008	[170]*	323.2	7	5.03-9.24	0.27-0.88	7.76	0.016	[86]
303.1	9	0.91-6.52	0.06-0.91	4.28	0.020	[67]	323.4	5	4.40-7.32	0.21-0.42	7.50	0.035	[172]
303.12	11	1.16-6.48	0.10-0.85	12.2	0.012	[152]	324.17	1	8.22	0.55	4.50		[178]
303.12	13	2.99-7.04	0.19-0.98	5.78		[167]	325.2	9	6.27-9.35	0.33-0.77	9.95	0.026	[179]
303.12	11	1.16-6.48	0.10-0.85	16.4	0.012	[170]	328.2	12	1.65-9.42	0.08-0.63	9.40	0.033	[175]
303.15	3	3.60-5.62	0.24-0.49	5.26		[169]	333.1	9	0.95-10.07	0.05-0.65	9.56	0.047	[67]
304.2	12	3.75-7.22	0.27-0.996	3.12	0.012	[171]	333.2	8	2.15-10.50	0.11-0.69	6.02		[83]
304.2	9	3.31-7.33	0.23-0.997	4.26	0.017	[172]	333.2	7	8.20-10.53	0.41-0.81	7.46	0.023	[86]
304.6	12	2.22-6.98	0.18-0.89	11.3	0.018	[173]	333.2	13	1.35-10.66	0.06-0.73	10.9	0.027	[176]
308.11	16	1.57-7.17	0.11-0.83	6.69	0.016	[152]	333.27	14	0.53-10.63	0.02-0.85	7.46	0.056	[85]
308.11	13	3.27-7.69	0.19-0.98	6.58		[167]	333.4	13	0.54-10.65	0.02-0.82	9.69	0.052	[163]
308.11	16	1.57-7.17	0.12-0.83	14.0	0.014	[170]	333.40	10	0.66-10.61	0.03-0.83	10.00	0.039	[77]
308.15	19	1.55-7.75	0.11-0.99	5.89	0.019	[87]	333.53	5	1.74-10.01	0.08-0.64	3.37	0.044	[88]
308.15	2	7.16-7.44	0.92-0.95	4.79		[90]	333.8	15	0.93-10.84	0.03-0.82	8.46	0.038	[89]
308.2	2	5.83-7.14	0.48-0.82	5.12	0.015	[166]	333.80	13	0.61-11.28	0.03-0.86	15.2	0.030	[77]
308.2	7	7.12-7.67	0.77-0.99	5.73	0.013	[171]	337.2	8	6.22-10.84	0.27-0.70	6.65	0.042	[179]
308.2	6	4.15-7.60	0.28-0.98	4.39	0.009	[174]	343.2	9	1.44-9.35	0.08-0.49	18.8		[83]
308.6	7	3.31-7.27	0.21-0.91	3.99	0.021	[172]	343.2	8	9.00-11.80	0.42-0.76	3.63	0.103	[86]
313.0	14	1.66-7.47	0.10-0.67	4.71	0.037	[89]	344.75	11	0.80-11.93	0.03-0.80	7.93	0.063	[77]
313.1	10	3.02-7.63	0.23-0.82	12.0	0.024	[173]	348.40	7	1.51-12.30	0.06-0.73	4.54	0.063	[89]
313.14	15	0.91-7.92	0.05-0.82	8.76	0.023	[152]	353.15	12	0.52-11.08	0.02-0.49	8.01	0.070	[67]
313.14	16	0.61-7.72	0.05-0.73	12.1	0.030	[139]	353.2	12	3.46-13.90	0.10-0.75	12.0	0.059	[176]
313.14	12	3.51-8.18	0.19-0.95	7.23		[167]	363.2	14	1.12-14.15	0.06-0.77	17.7		[83]
313.14	15	0.91-7.92	0.05-0.82	5.52	0.023	[170]	373.00	7	2.18-14.11	0.06-0.66	1.62	0.085	[89]
313.15	8	0.53-7.18	0.03-0.56	4.27	0.039	[67]	373.15	3	7.10-13.30	0.22-0.54	3.81	0.068	[181]
313.15	3	4.38-6.96	0.24-0.49	10.9		[169]	373.2	5	3.40-12.36	0.13-0.55	12.5		[83]
313.2	10	0.60-8.07	0.03-0.95	6.89	0.031	[76]	391.96	9	1.32-14.62	0.03-0.60	5.79	0.091	[88]
313.2	7	6.35-8.03	0.43-0.95	6.85	0.015	[86]	298-413	26	6.18-15.16	0.65-0.96	5.56		[75]
313.2	10	3.40-7.96	0.19-0.91	5.82	0.027	[172]	323-333	22	0.73-9.46	0.03-0.64	6.19	0.042	[160]
313.2	10	1.60-7.82	0.09-0.84	10.2	0.022	[175]	333-494	75	6.74-14.84	0.20-0.96	4.45		[92]
313.2	8	1.31-7.68	0.10-0.78	16.1	0.008	[176]							

MRD(*P*) = 7.85% ; Δy_{CO_2} = 0.031													
CO_2 + C_3H_7OH ; $k_{ij}(T)$ = 0.118 - 2.15x10^{-5}T													
***T* / K**	**Nº Points**	**Range *P*/ MPa**	**Range x_{CO_2}**	***MRD* (*P*)/%**	**Δy_{CO_2}**	**Ref.**	***T* / K**	**Nº Points**	**Range *P*/ MPa**	**Range x_{CO_2}**	***MRD* (*P*)/%**	**Δy_{CO_2}**	**Ref.**
293.1	8	0.74-5.26	0.05-0.81	4.18	0.005	[68]	333.0	9	2.16-10.46	0.10-0.73	6.59	0.043	[183]
303.1	8	0.64-6.52	0.04-0.79	6.23	0.010	[68]	333.1	10	0.94-9.97	0.04-0.61	7.79	0.030	[68]
305.6	10	2.10-7.20	0.17-0.88	8.87	0.009	[173]	333.15	8	1.83-11.01	0.09-0.78	6.10	0.064	[184]
308.1	9	0.47-6.91	0.02-0.68	9.95	0.020	[182]	333.4	9	0.67-10.82	0.03-0.81	4.13	0.051	[163]
313.0	9	2.15-8.03	0.12-0.83	3.57	0.007	[183]	337.2	10	3.30-8.98	0.14-0.45	9.19	0.021	[185]
313.1	7	2.94-8.04	0.23-0.84	8.62	0.013	[173]	343.15	8	1.39-12.74	0.05-0.77	3.67	0.058	[184]
313.15	8	0.69-7.86	0.03-0.74	5.04	0.016	[68]	344.82	3	11.46-12.32	0.61-0.80	5.92	0.083	[186]
313.15	9	1.41-8.19	0.09-0.92	9.10	0.015	[184]	353.1	12	0.75-12.64	0.03-0.63	8.20	0.046	[68]
313.4	10	0.52-8.18	0.04-0.96	4.56	0.013	[163]	373.16	7	12.06-14.98	0.49-0.77	5.22	0.081	[186]
315.0	8	2.64-7.17	0.14-0.56	6.64	0.014	[185]	397.48	5	12.34-15.77	0.42-0.70	4.76	0.050	[186]
318.15	11	0.54-8.33	0.02-0.70	10.2	0.027	[182]	426.68	6	10.60-15.33	0.18-0.54	20.6	0.120	[186]
323.0	10	2.33-9.57	0.12-0.77	5.42	0.060	[183]	298-423	37	6.27-16.03	0.64-0.94	5.42		[75]
323.15	8	1.53-9.82	0.10-0.76	7.54	0.018	[184]							
MRD(*P*) = 6.89% ; Δy_{CO_2} = 0.033													
CO_2 + C_4H_9OH ; $k_{ij}(T)$ = 0.190 - 1.93x10^{-4}T													
***T* / K**	**Nº Points**	**Range *P*/ MPa**	**Range x_{CO_2}**	***MRD* (*P*)/%**	**Δy_{CO_2}**	**Ref.**	***T* / K**	**Nº Points**	**Range *P*/ MPa**	**Range x_{CO_2}**	***MRD* (*P*)/%**	**Δy_{CO_2}**	**Ref.**
293.1	7	0.63-5.46	0.04-0.74	8.61	0.002	[187]	333.15	3	8.00-10.76	0.44-0.77	9.61		[189]
298.15	1	5.72	0.60	1.10		[189]	333.15	10	1.43-9.82	0.06-0.60	18.9	0.015	[190]
303.1	14	0.52-6.74	0.03-0.84	10.5	0.003	[187]	333.15	11	5.02-11.90	0.26-0.83	9.26	0.052	[195]
313.1	23	0.57-8.11	0.03-0.78	7.65	0.010	[187]	333.58	2	10.76-11.30	0.73-0.86	8.53	0.120	[95]
313.1	8	2.84-8.93	0.22-0.83	6.33	0.009	[188]	337.2	11	6.18-11.78	0.30-0.78	9.36	0.024	[179]
313.15	7	6.70-8.18	0.49-0.95	3.73	0.060	[96]	343.15	10	1.68-10.98	0.05-0.66	33.3	0.021	[190]*
313.15	3	6.39-7.79	0.10-0.65	3.50		[189]	343.15	8	5.02-12.02	0.24-0.64	11.4	0.023	[195]
313.15	8	1.67-7.68	0.09-0.65	11.1	0.009	[190]	353.15	8	5.02-12.02	0.22-0.57	13.8	0.023	[195]
313.15	10	1.69-8.31	0.10-0.95	7.87		[191]	354.06	9	2.07-12.98	0.10-0.68	7.71	0.026	[186]
313.2	8	6.02-7.96	0.41-0.87	5.88		[192]	355.38	2	13.91-14.20	0.75-0.82	4.43	0.082	[95]
313.22	7	2.14-8.06	0.13-0.85	10.3	0.008	[193]	363.17	9	3.09-14.89	0.12-0.76	12.4	0.028	[193]
313.4	9	2.73-8.31	0.16-0.72	11.3		[194]	383.1	11	2.02-16.50	0.08-0.77	7.00	0.024	[188]

314.8	8	4.63-7.98	0.28-0.70	8.14	0.024	[179]	392.72	5	14.57-16.78	0.60-0.81	1.17	0.069	[95]
323.15	3	7.17-9.45	0.44-0.77	9.65		[189]	398.98	10	2.12-15.53	0.08-0.62	7.97	0.000	[186]
323.15	8	2.03-9.27	0.10-0.67	13.8	0.017	[190]	426.95	5	11.89-16.94	0.42-0.70	3.84	0.067	[95]
324.1	15	1.65-10.09	0.09-0.88	7.90	0.094	[187]	430.25	10	2.37-16.13	0.07-0.61	11.0	0.070	[186]
324.16	4	9.63-9.77	0.80-0.90	11.2	0.218	[95]	303-428	28	7.06-17.35	0.71-0.97	4.37		[75]
325.3	9	5.23-9.87	0.29-0.81	10.4	0.051	[179]							
MRD(*P*) = 8.76% ; Δy_{CO_2} = 0.034													

*Data not included in the means due to their high deviations.

Table 10.- Association scheme and PC-SAFT EoS pure-compounds parameters used in the CO_2 + alkan-1-ol modellization. m, σ, ε: geometric parameters; for CO_2, obtained in a previous work [27]; for the alkan-1-ols, rescaled in this work from T_c and P_c. $\kappa^{A_iB_i}$ and $\varepsilon^{A_iB_i}$: association parameters extracted from reference [20].

Compound	**Association scheme**	***m / M*** **(mol g^{-1})**	σ**(Å)**	ε**(K)**	$\kappa^{A_iB_i}$	$\varepsilon^{A_iB_i}$**(K)**
CO_2	+ CH_3OH: 2C	0.04834	2.8251	163.76		
CH_3OH	2B	0.05273	3.3264	175.20	0.035176	2899.5
C_2H_5OH	Non	0.06554	3.1612	235.72		
C_3H_7OH	Non	0.05510	3.2881	236.77		
C_4H_9OH	Non	0.04208	3.6000	254.48		

FIGURE 1a

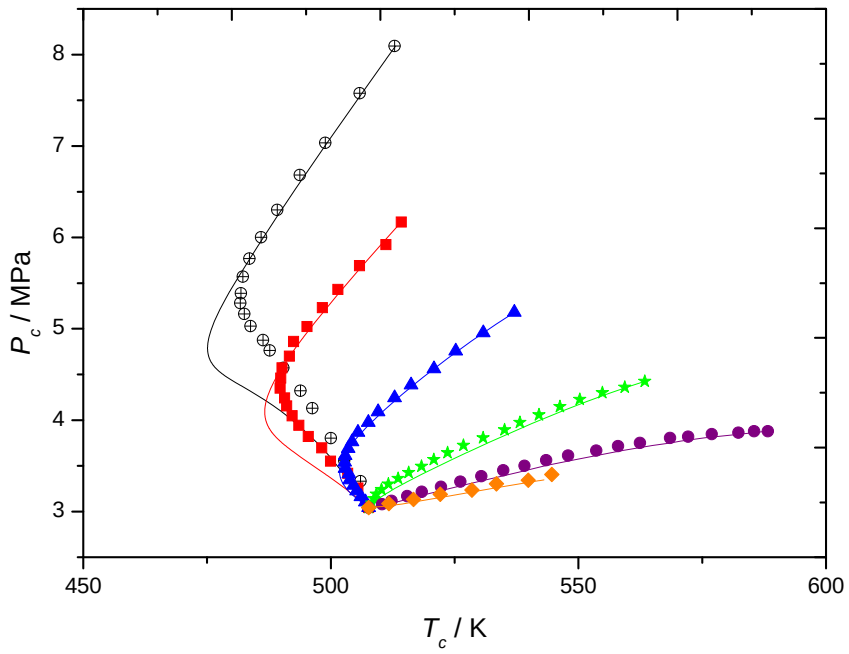

FIGURE 1b

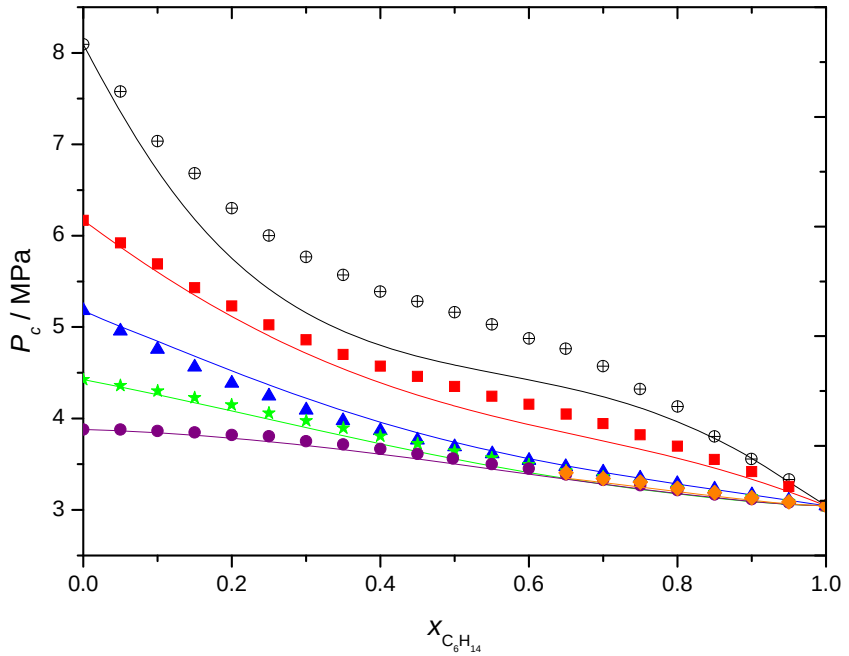

FIGURE 1c

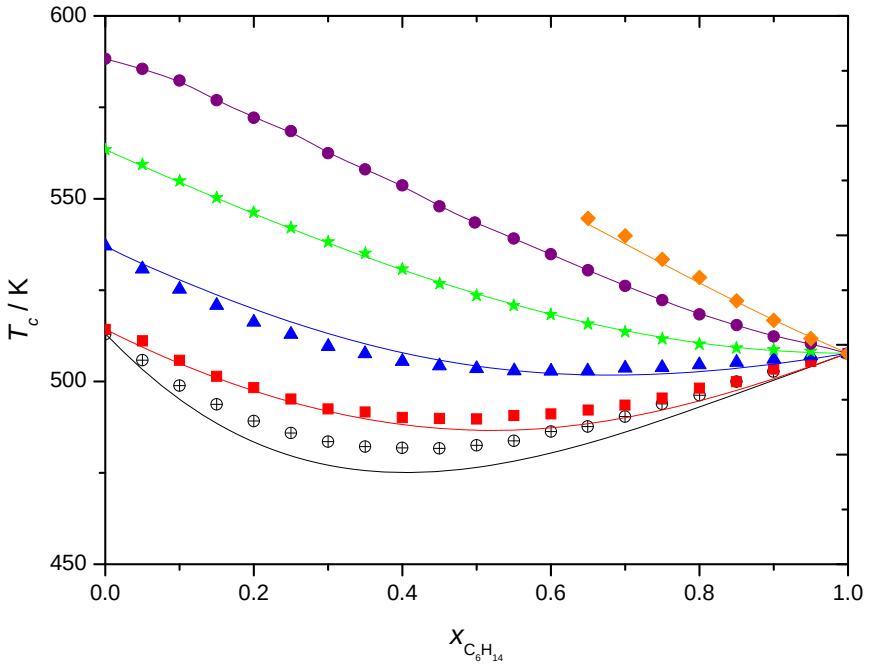

FIGURE 2a

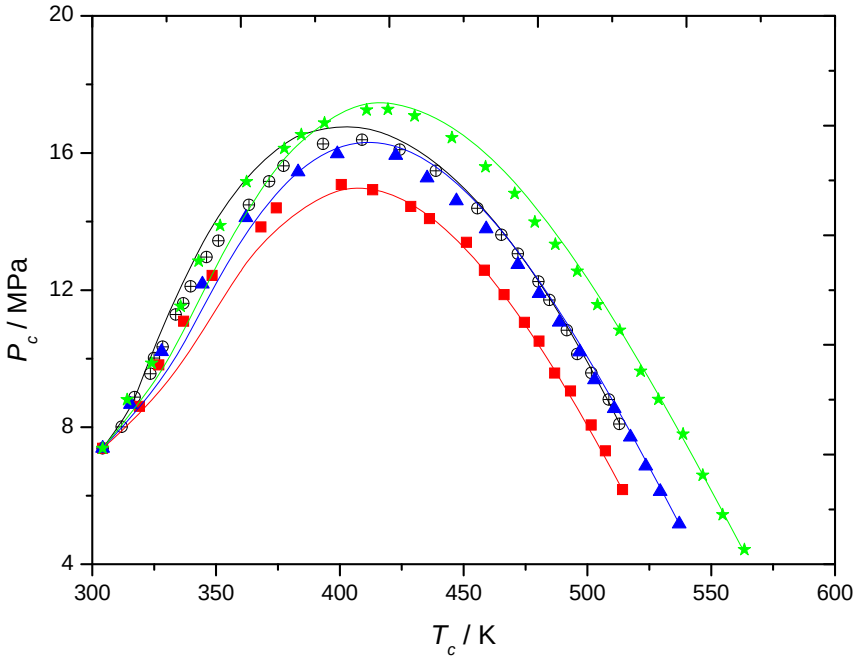

FIGURE 2b

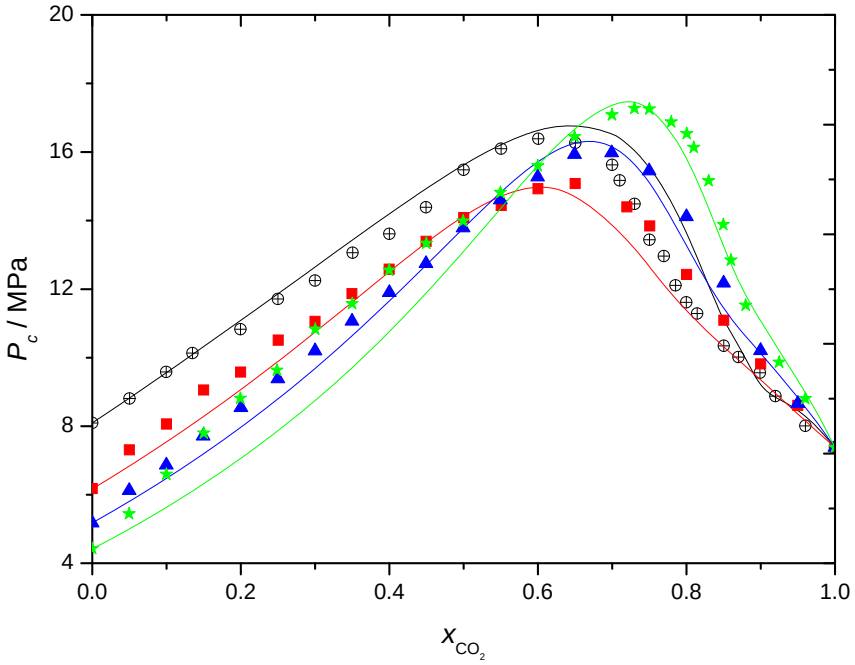

FIGURE 2c

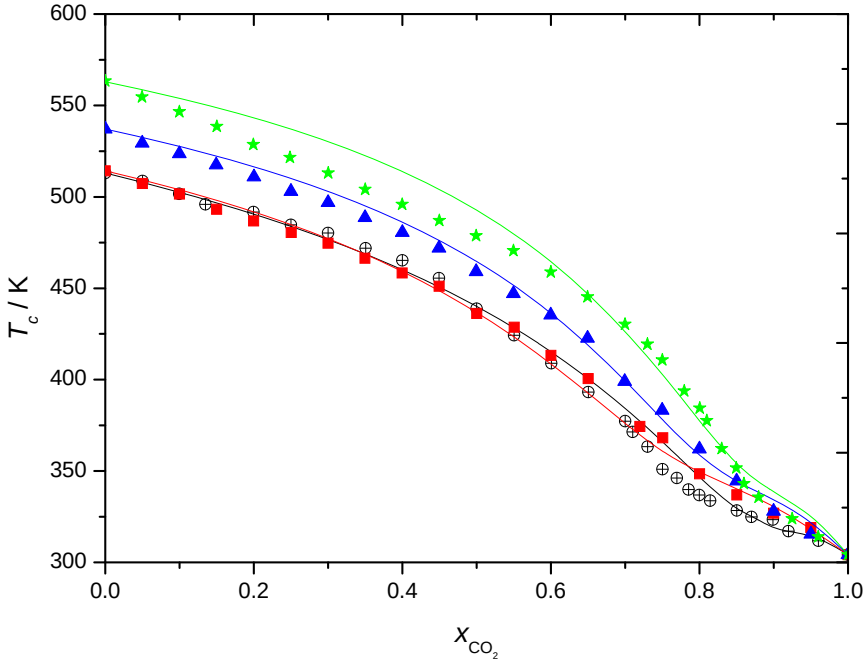

FIGURE 3

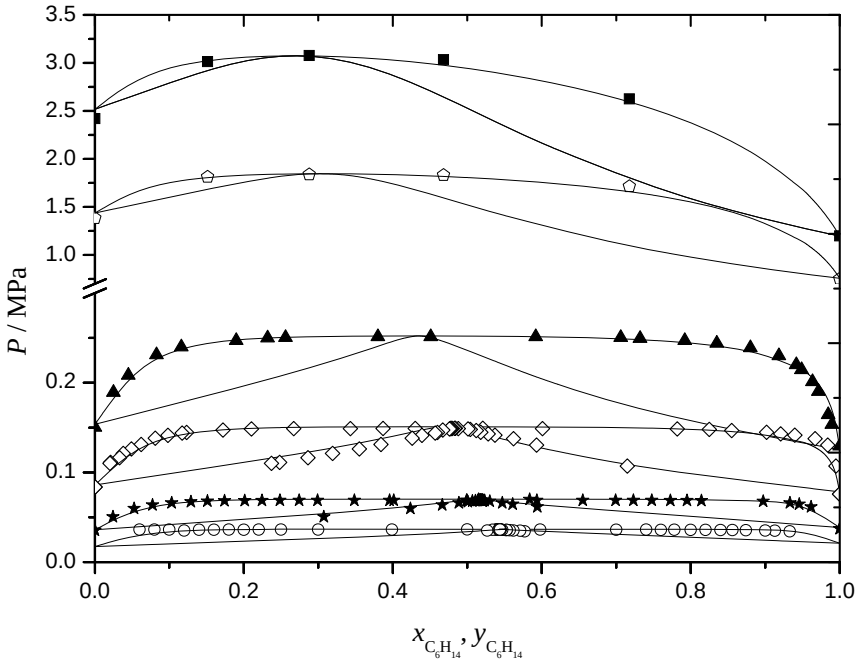

FIGURE 4

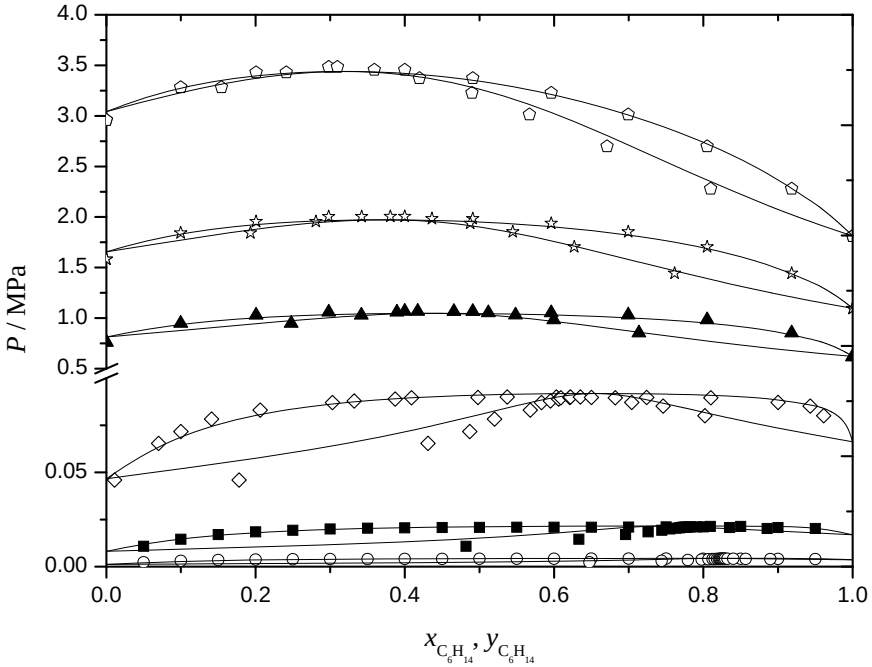

FIGURE 5

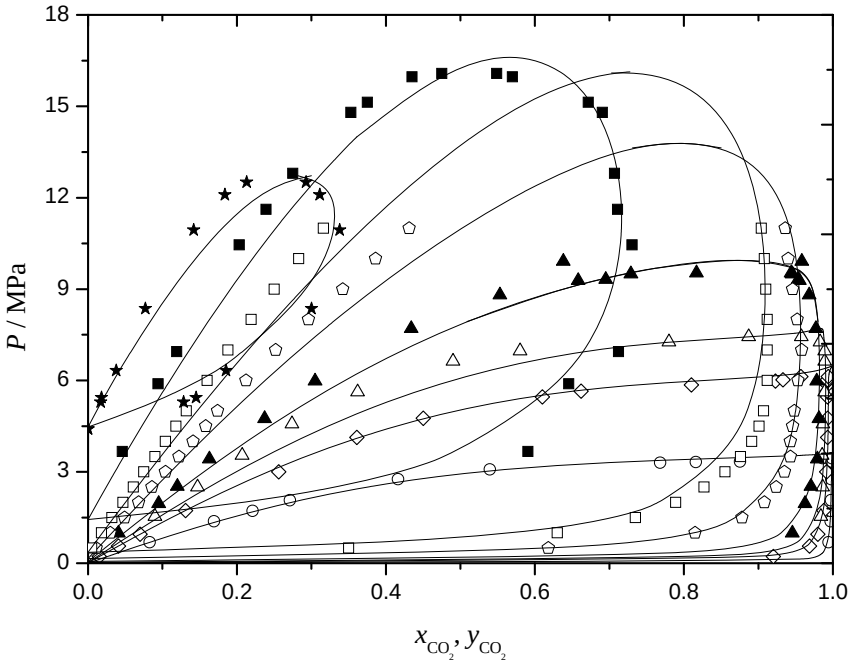

FIGURE 6

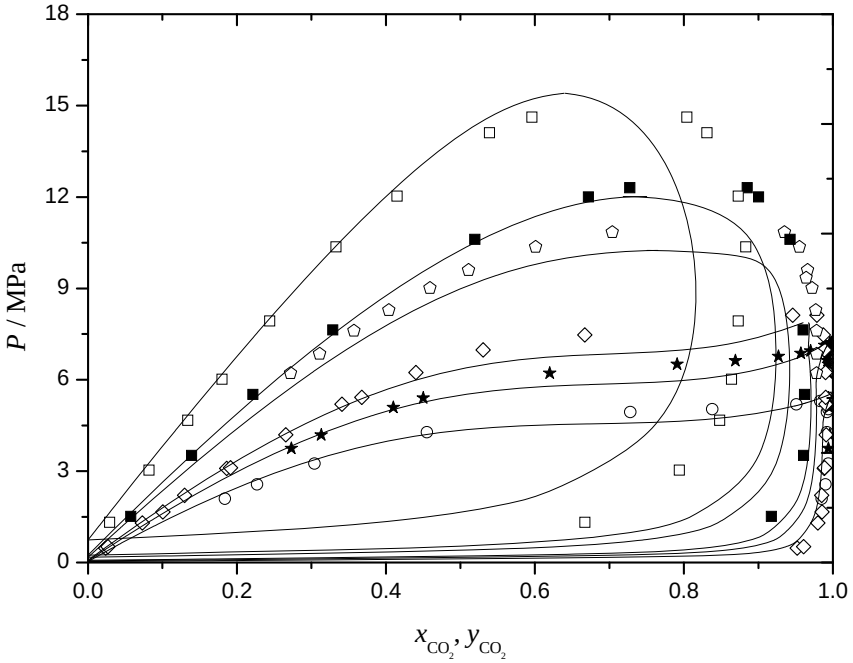

SUPPLEMENTARY DATA

Experimental determination of the critical loci for {*n*-C_6H_{14} or CO_2 + alkan-1-ol} mixtures. Evaluation of their critical and subcritical behavior using PC-SAFT EoS.

Laura Gil, Sofía Blanco, Clara Rivas, Eduardo Laga, Javier Fernández, Manuela Artal*, Inmaculada Velasco

Departamento de Química Física, Facultad de Ciencias, Universidad de Zaragoza, 50009 – Zaragoza, Spain

*Corresponding author: martal@unizar.es

Figure SF1. (a), (P_c, T_c); (b), (P_c, x) and (c), (T_c, x) projections for *n*-hexane + methanol critical locus. Experimental results from this work and literature: ● , this work; ◆, ref. [52]; × , ref. [53]; ■ , ref. [54]; ▲, ref. [55].

Figure SF1a

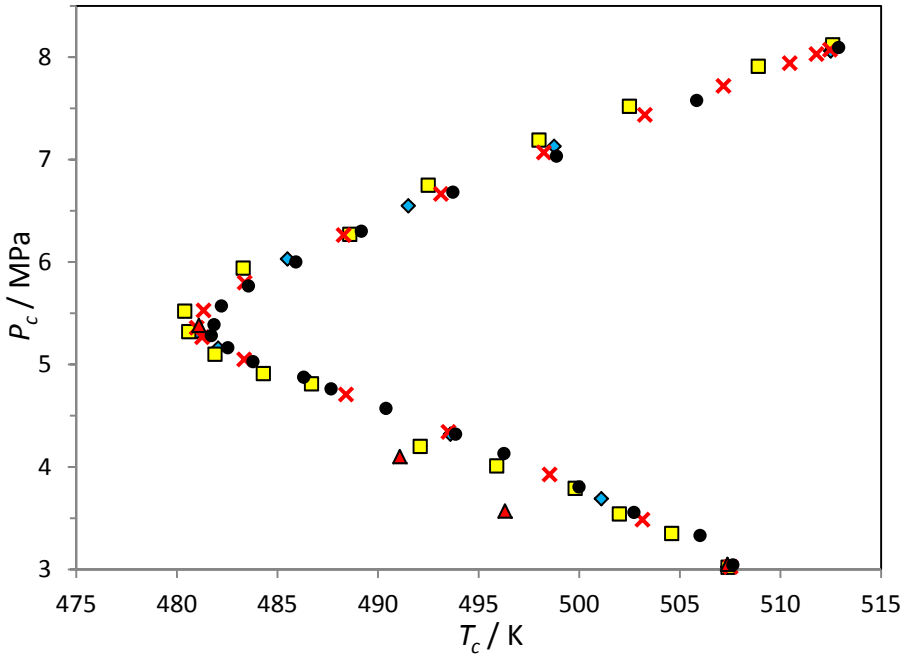

Figure SF1b

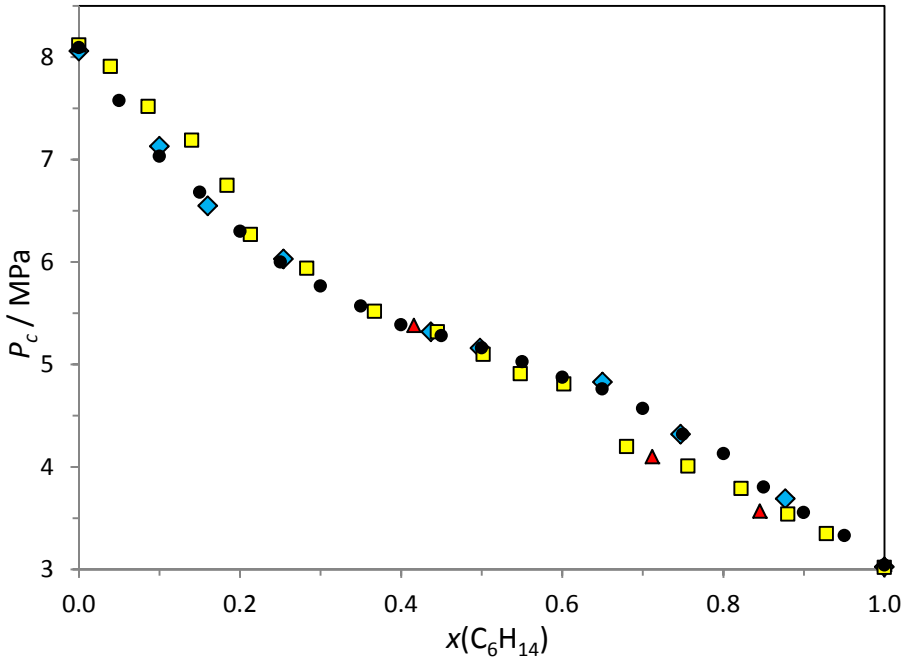

Figure SF1c

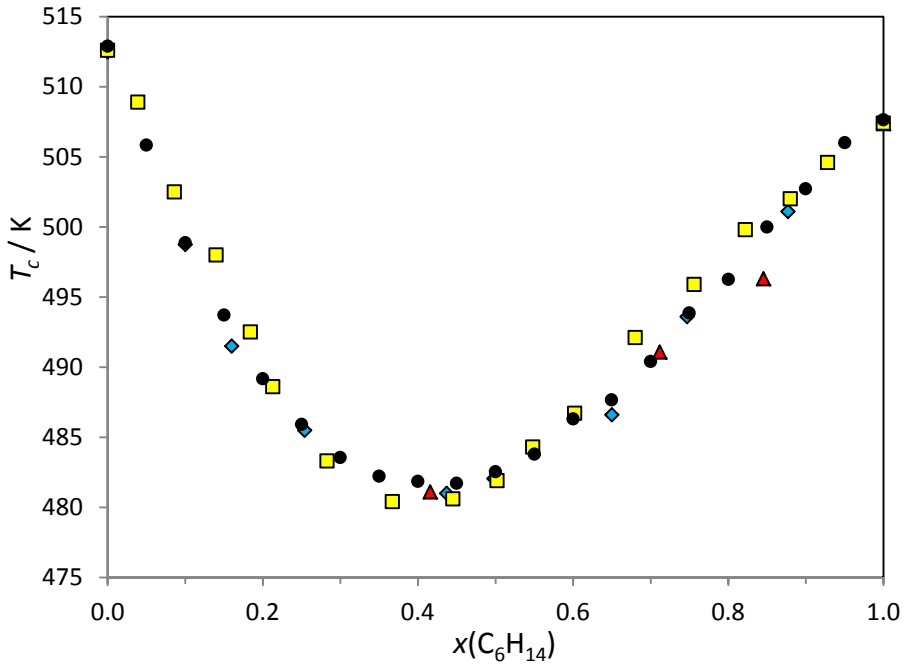

Figure SF2. (a), (P_c, T_c); (b), (P_c, x) and (c), (T_c, x) projections for *n*-hexane + ethanol critical locus. Experimental results from this work and literature: ●, this work; ◆, ref. [38]; □, ref. [56]; ▲, ref. [57]; +, ref. [58]; ×, ref. [59].

Figure SF2a

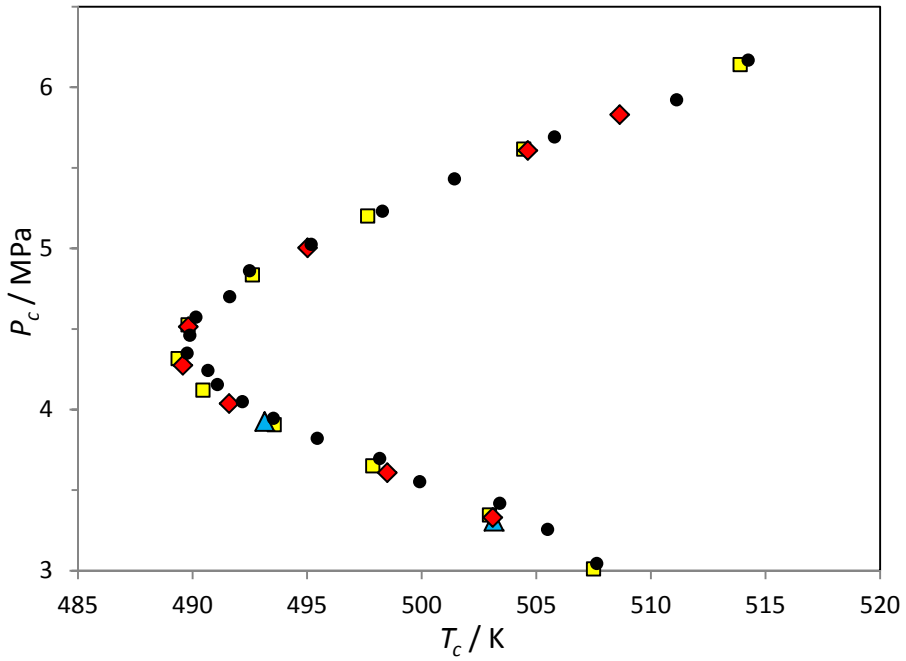

Figure SF2b

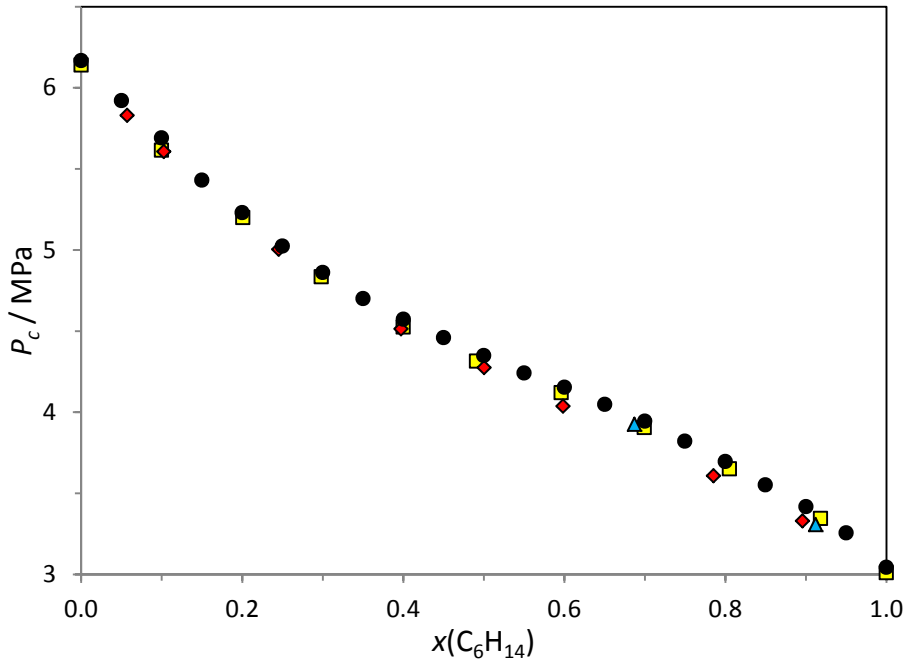

Figure SF2c

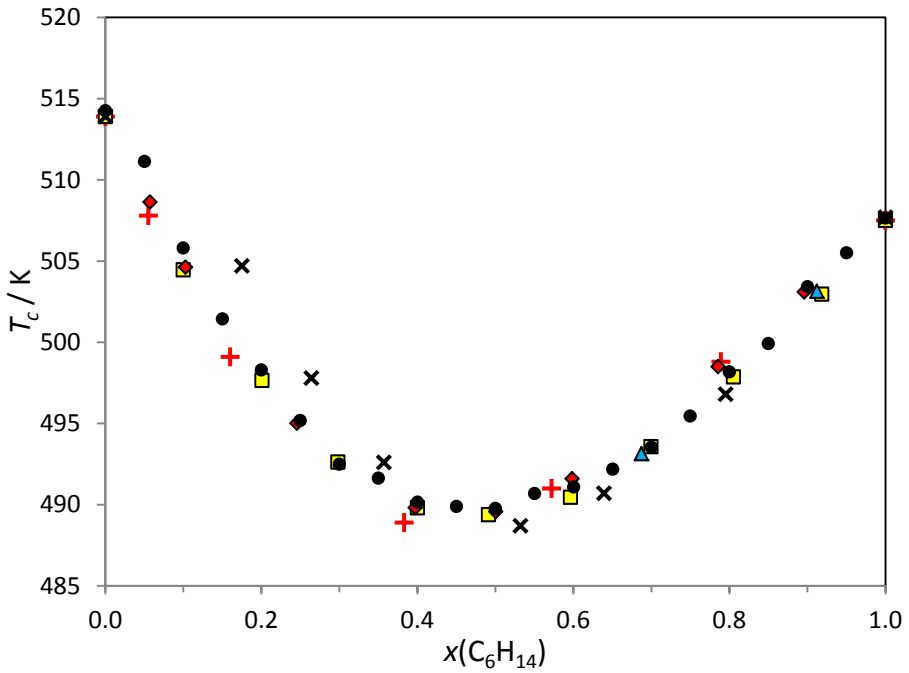

Figure SF3. (a), (P_c, T_c); (b), (P_c, x) and (c), (T_c, x) projections for *n*-hexane + propan-1-ol critical locus. Experimental results from this work and literature: ●, this work; ◻, ref. [50]; ◆, ref. [60,61].

Figure SF3a

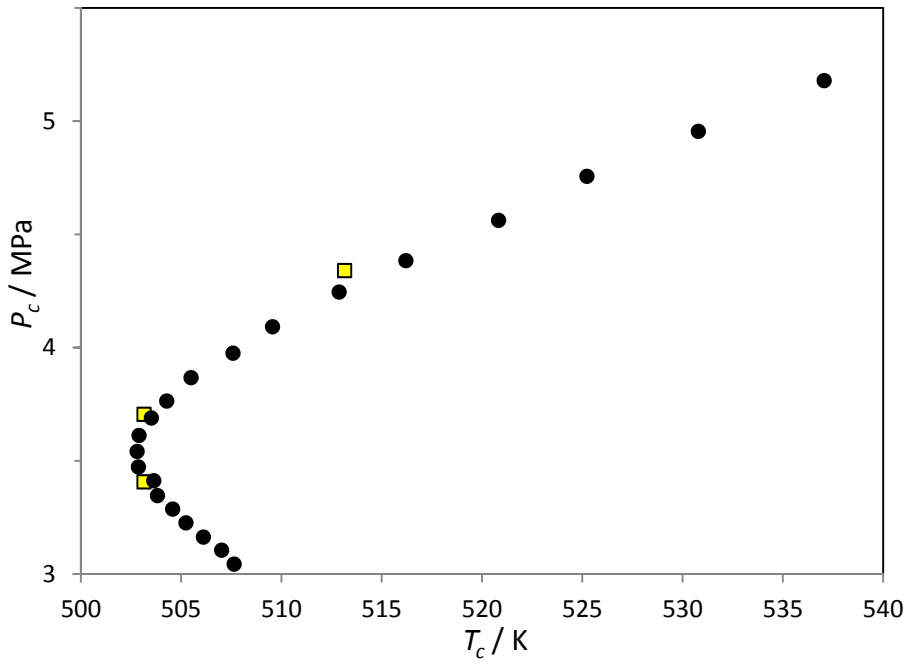

Figure SF3b

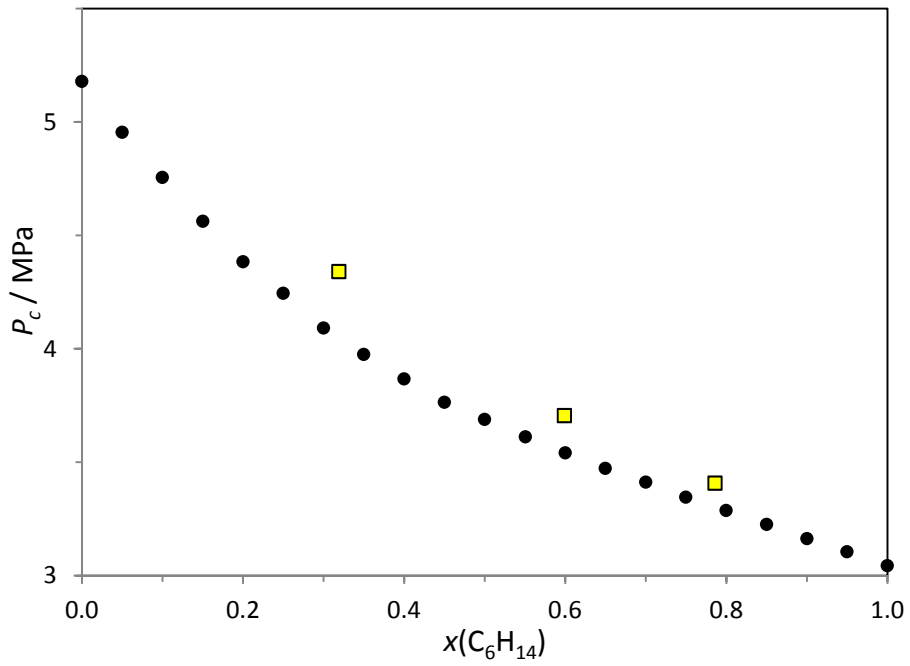

Figure SF3c

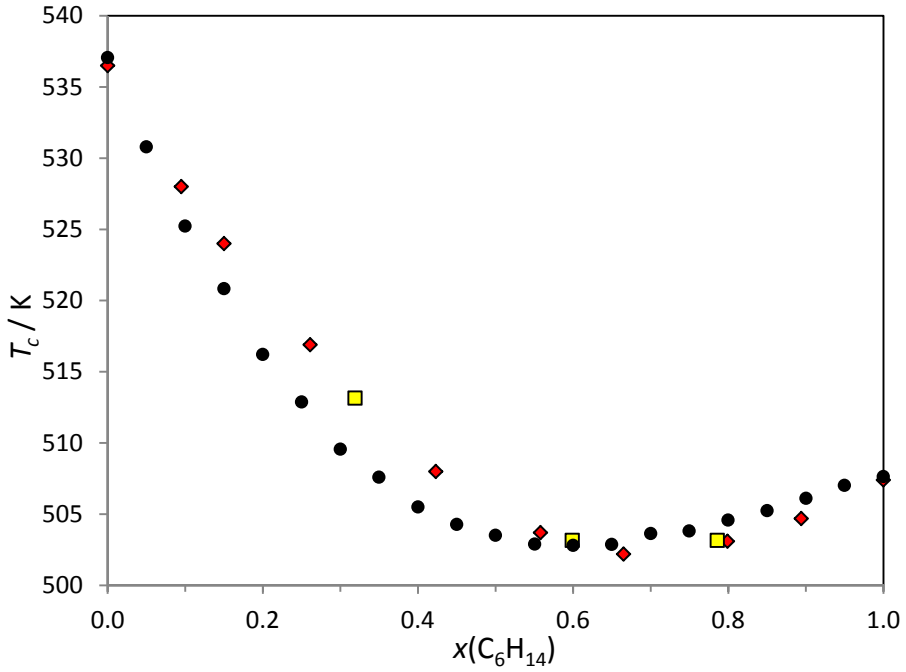

Figure SF4. (a), (P_c, T_c); (b), (P_c, x) and (c), (T_c, x) projections for *n*-hexane + butan-1-ol critical locus. Experimental results from this work and literature: ●, this work; ◆, ref. [60,61].

Figure SF4a

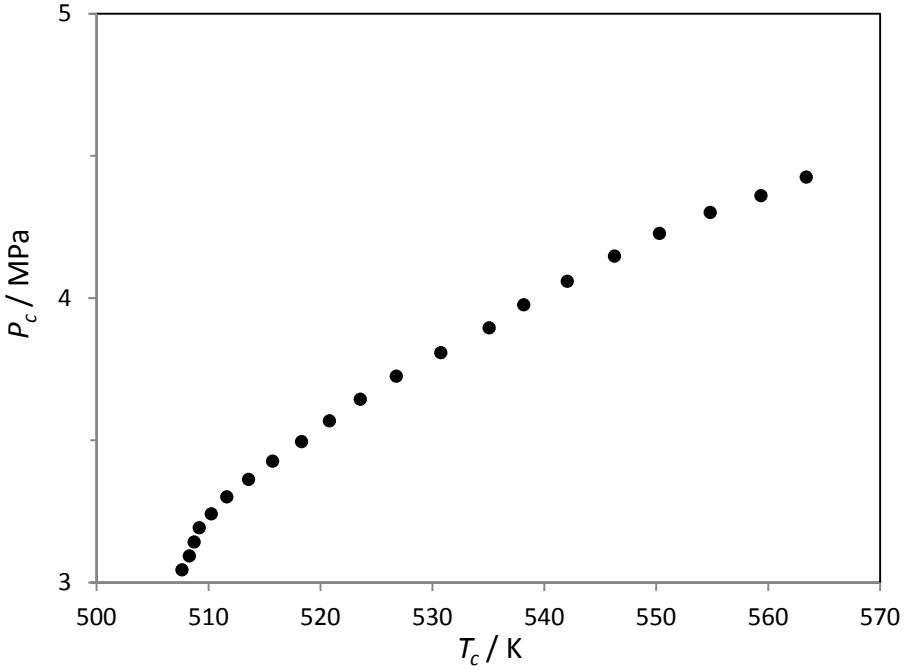

Figure SF4b

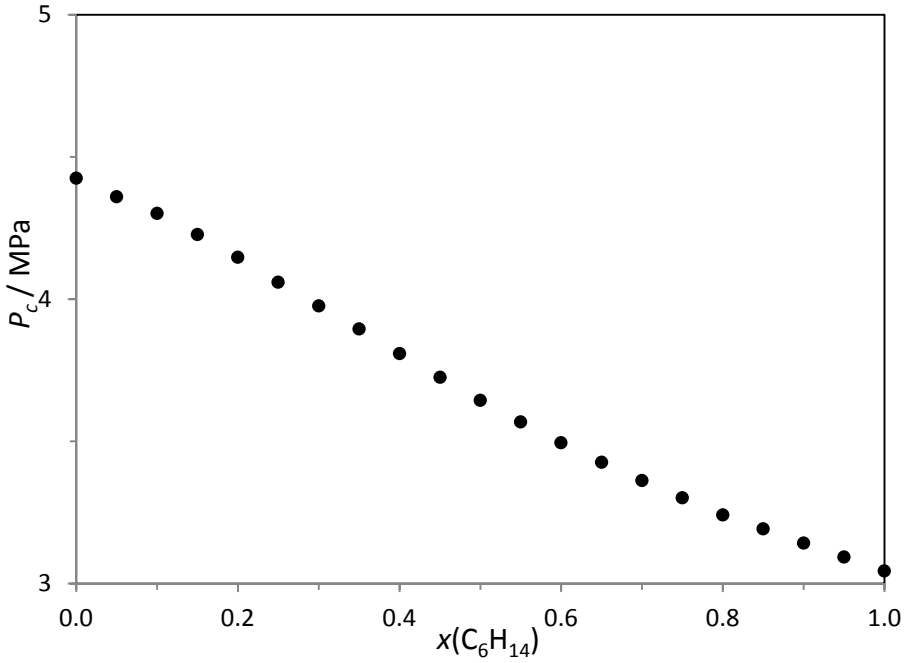

Figure SF4c

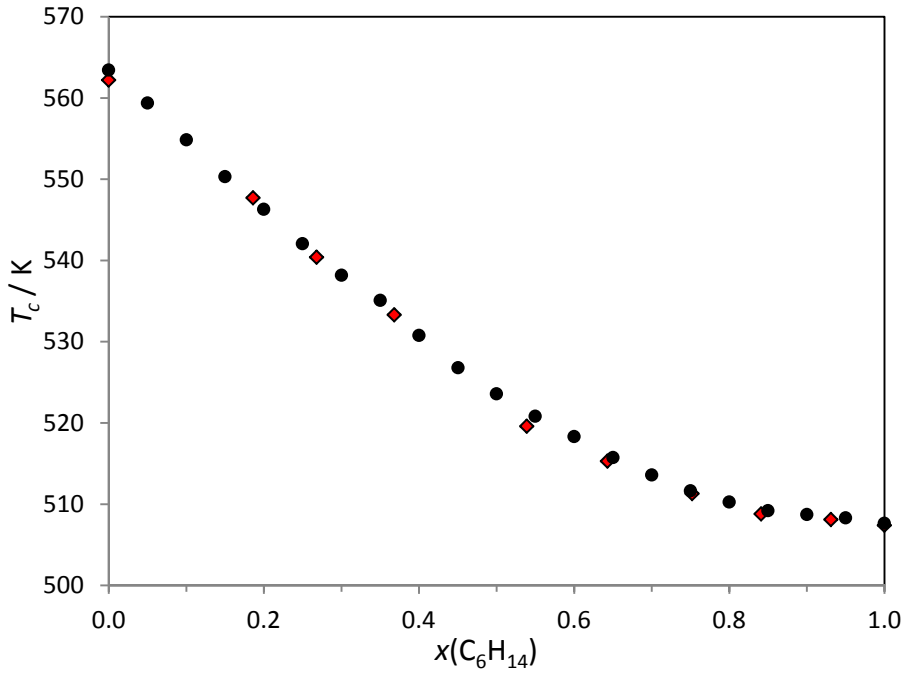

Figure SF5. (a), (P_c, T_c); (b), (P_c, x) and (c), (T_c, x) projections for *n*-hexane + pentan-1-ol critical locus. Experimental results from literature: ✕, ref. [59]; ☐, ref. [62]; ●, ref. [63] (unpublished data).

Figure SF5a

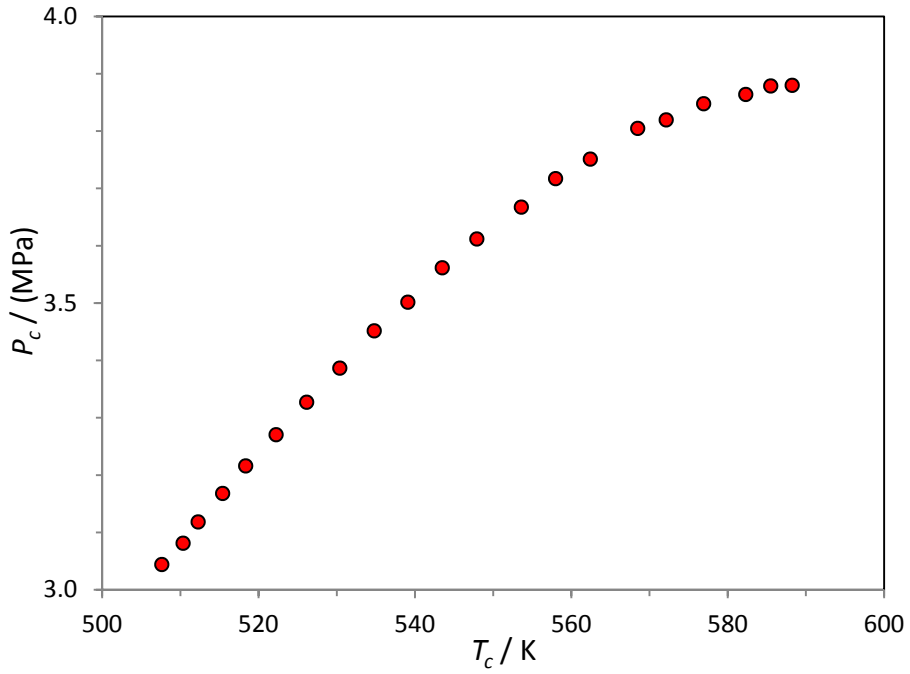

Figure SF5b

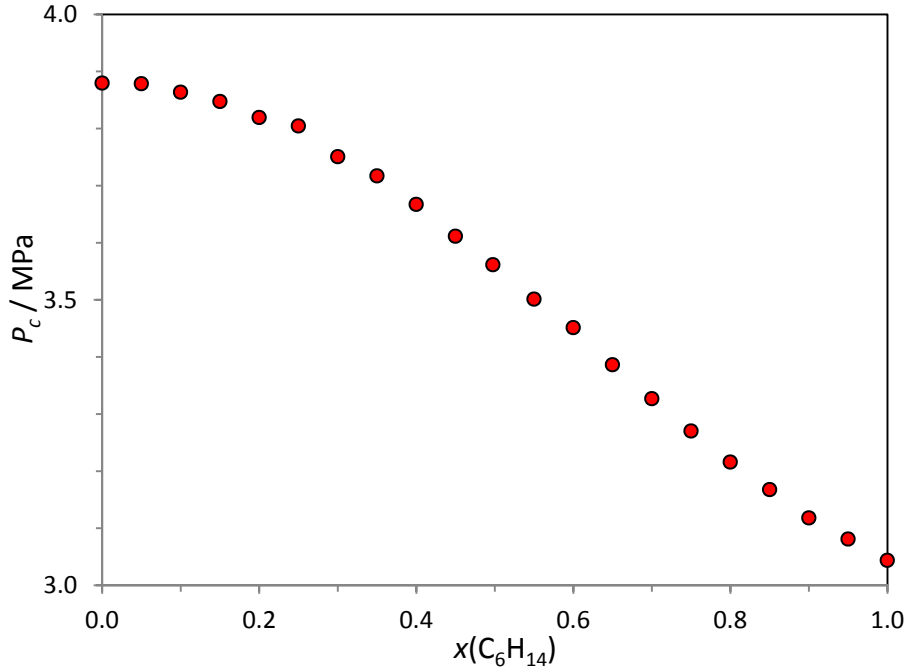

Figure SF5c

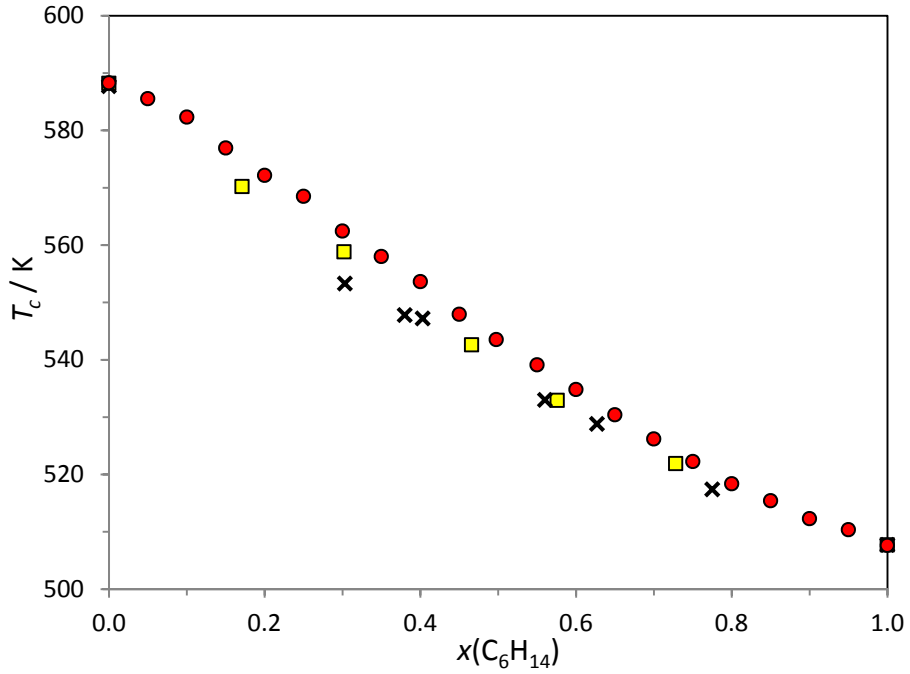

Figure SF6. (a), (P_c, T_c); (b), (P_c, x) and (c), (T_c, x) projections for *n*-hexane + hexan-1-ol critical locus. Experimental results from literature: ●, ref. [63] (unpublished data).

Figure SF6a

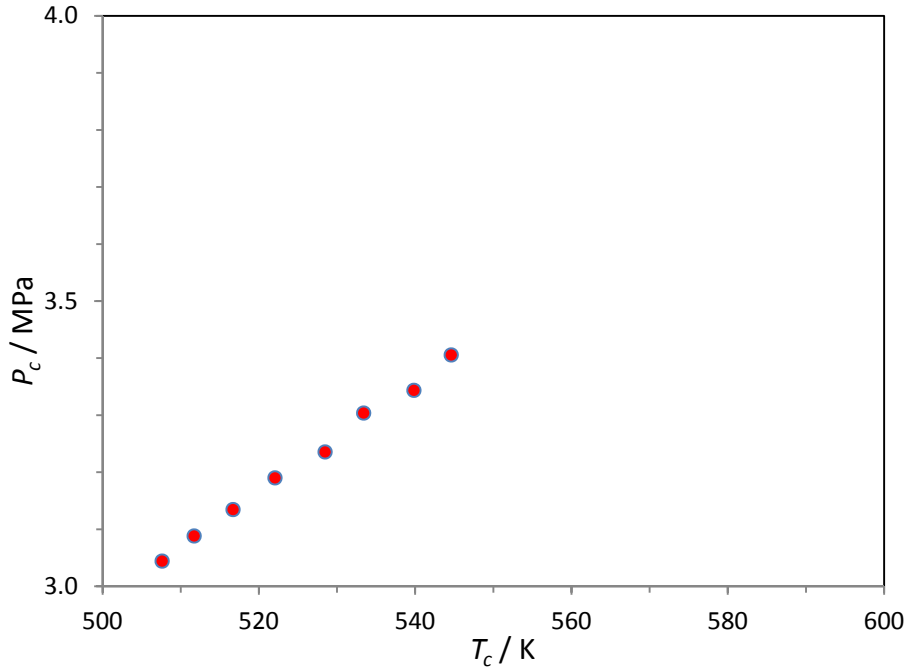

Figure SF6b

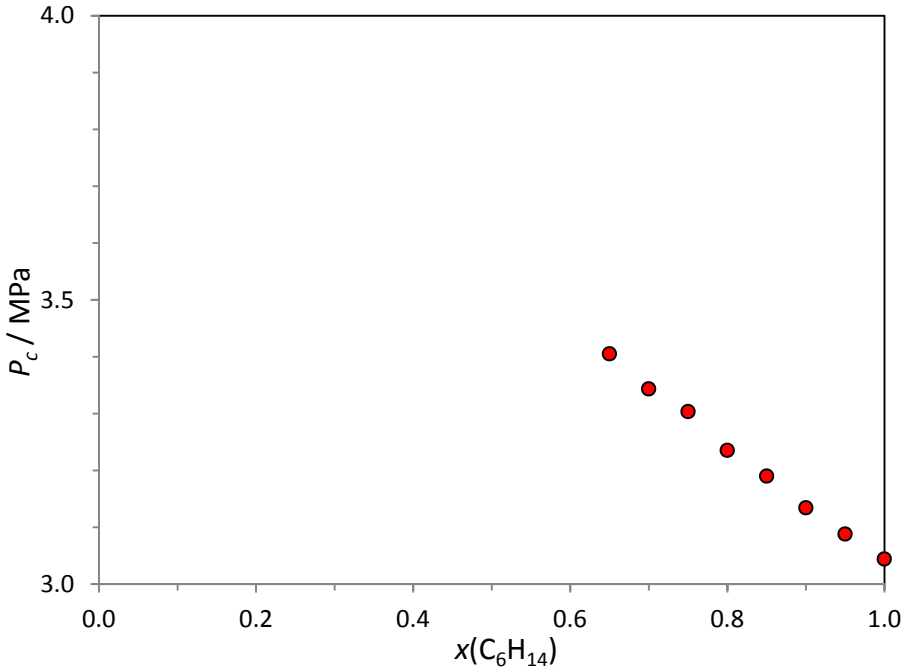

Figure SF6c

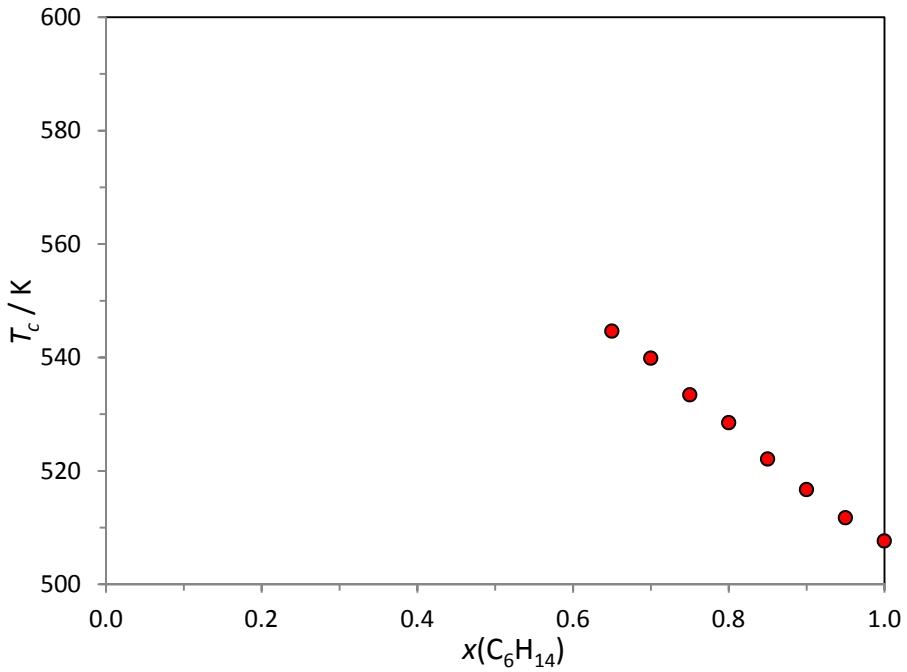

Comparison between this work experimental data and those from literature for the critical loci of *n*-hexane + alkan-1-ol systems.

The results of our current investigation for *n*-hexane + methanol system are in good agreement with those from de Loos et al. [52] (x, T_c, P_c) and Brunner [53] (P_c, T_c). Liu et al.'s [54] data are also in good agreement with ours in the P_c-T_c projection; however, in T_c-x and P_c-x planes such agreement only holds for the central range of concentrations. Two of the three (x, T_c, P_c) points from Zawisza [55] agree with ours in the T_c-x projection, but the agreement in P_c-T_c and P_c-x is less marked.

For *n*-hexane + ethanol mixtures, Sauermann et al. [56], Seo et al. [57] and Soo et al. [38] provide (x, T_c, P_c) data in very good agreement with our study. The agreement with Young [58] is a little worse and it is even worse compared with Morton et al. [59], whose results differ from those from this study and from other authors', especially in the alcohol-rich region, where the differences reach up to 6 K.

Oh et al.'s [50] is the only investigation in which (x, T_c, P_c) were determined for the *n*-hexane + propan-1-ol system, but only at three compositions. P_c-T_c projection is in good agreement with our current work, but P_c-x and T_c-x plots present some differences with ours, which become greater as the mixture becomes richer in propan-1-ol. Young [60] and Bone and Young [61] provide identical (x, T_c) data, in good agreement with Oh [50].

For *n*-hexane + butan-1-ol, we have only found two references, Young [60] and Bone and Young [61] which give identical data (x, T_c), in very good agreement with this work.

Christou, Sadus and Young [62] and Morton et al. [59] provide whole-composition (x, T_c) data for *n*-hexane + pentan-1-ol. Laga [63] (unpublished data), with the same apparatus that we used in our investigation, provides whole-composition (x, T_c, P_c) data. T_c results from Christou et al. are slightly lower than Laga's data and those proposed by Morton are even lower than Christou values.

Unpublished results from Laga [63] were the only data found for *n*-hexane + hexan-1-ol system.

Figure SF7. (a), (P_c, T_c); (b), (P_c, x) and (c), (T_c, x) projections for CO_2 + methanol critical locus. Experimental results from this work and literature: ●, this work; ◆, ref. [54]; △, ref. [70]; □, ref. [71]; ■, ref. [72,73]; +, ref. [73]; ◆, ref. [74]; ○, ref. [75]; ◆, ref. [76]; ×, ref. [77]; □, ref. [78]; ×, ref. [79]; ○, ref. [80]; ▲, ref. [81]; +, ref. [93].

Figure SF7a

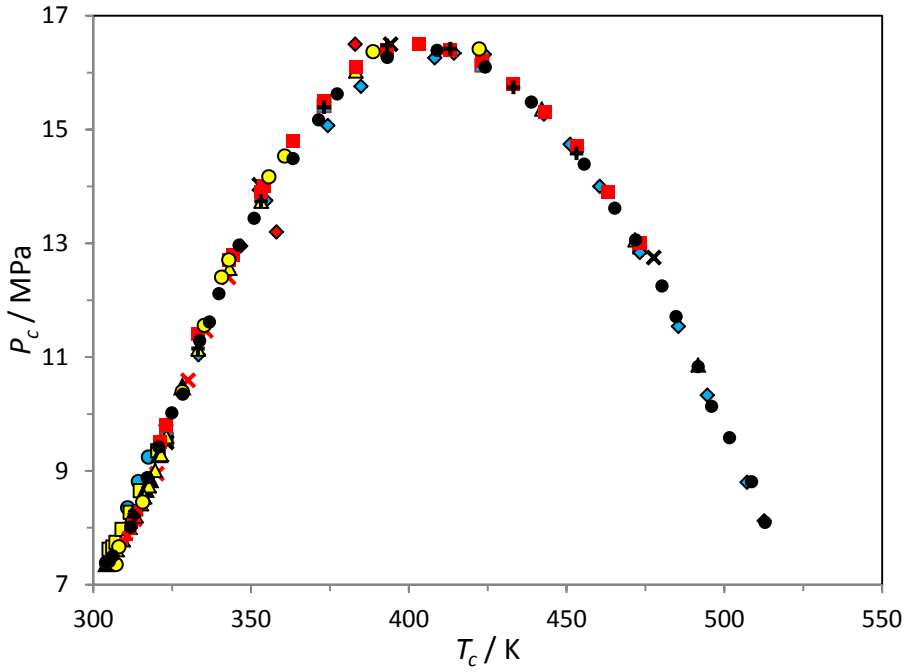

Figure SF7b

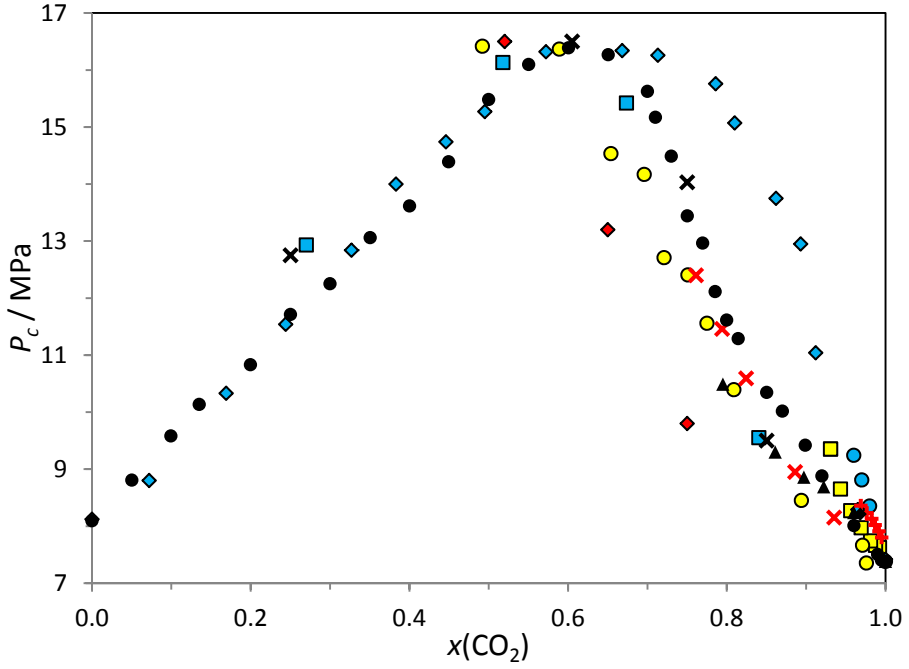

Figure SF7c

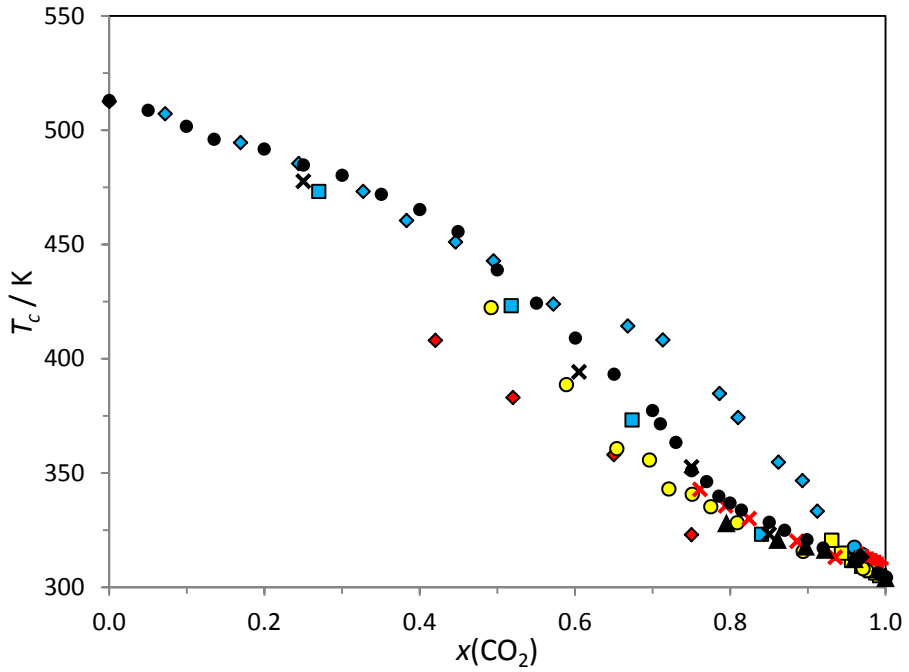

Figure SF8. (a), (P_c, T_c); (b), (P_c, x) and (c), (T_c, x) projections for CO_2 + ethanol critical locus. Experimental results from this work and literature: ●, this work; ■ , ref. [73]; ○ , ref. [75]; ◆, ref. [76]; ×, ref. [77]; □ , ref. [78]; ◇, ref. [82]; △ , ref. [83]; ▲, ref. [84]; ● , ref. [85]; +, ref. [86]; ×, ref. [87]; △ , ref. [88]; ◇, ref. [89]; ◆, ref. [90]; ■ , ref. [91]; ○ , ref. [92]; +, ref. [93].

Figure SF8a

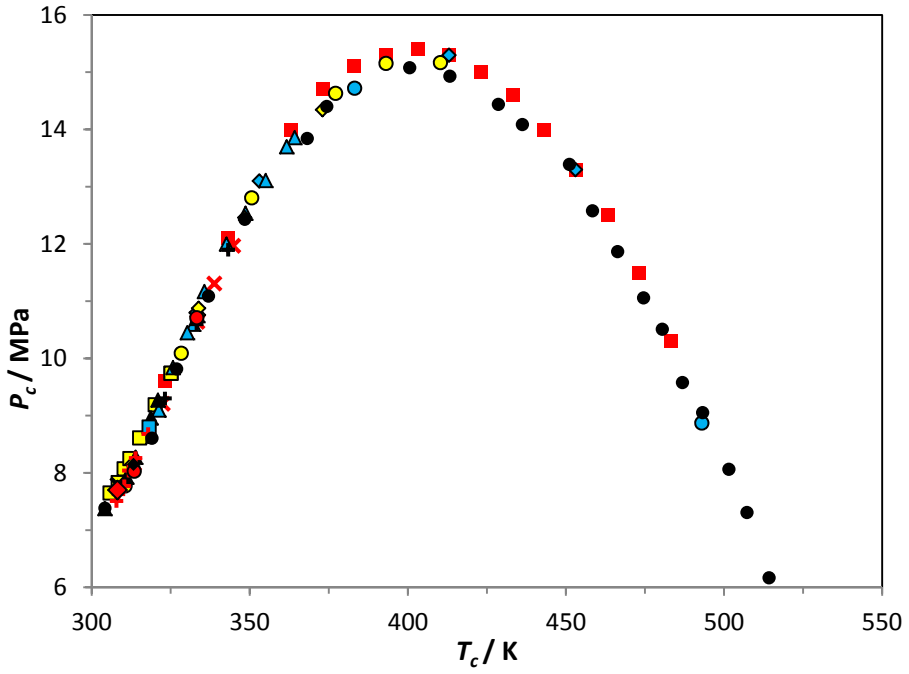

Figure SF8b

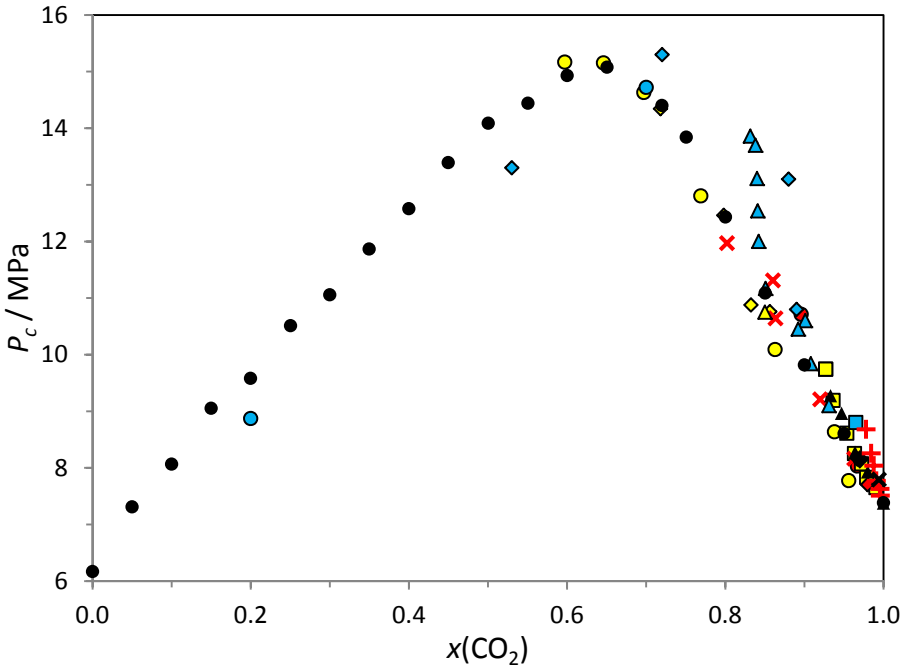

Figure SF8c

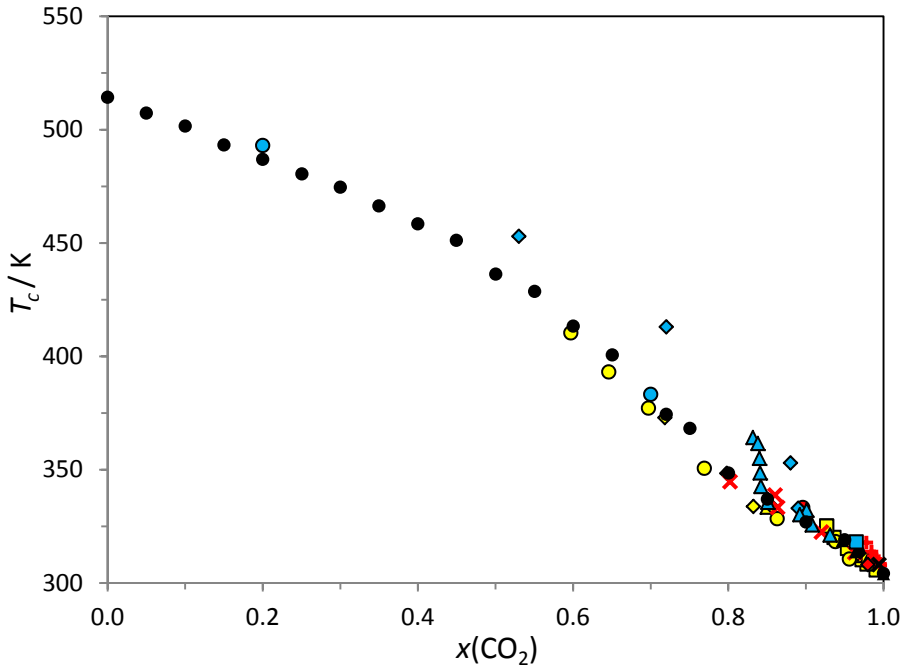

Figure SF9. (a), (P_c, T_c); (b), (P_c, x) and (c), (T_c, x) projections for CO_2 + propan-1-ol critical locus. Experimental results from this work and literature: ●, this work; ×, ref. [68]; ■, ref. [73]; ○, ref. [75]; □, ref. [78]; △, ref. [88]; ▲, ref. [94].

Figure SF9a

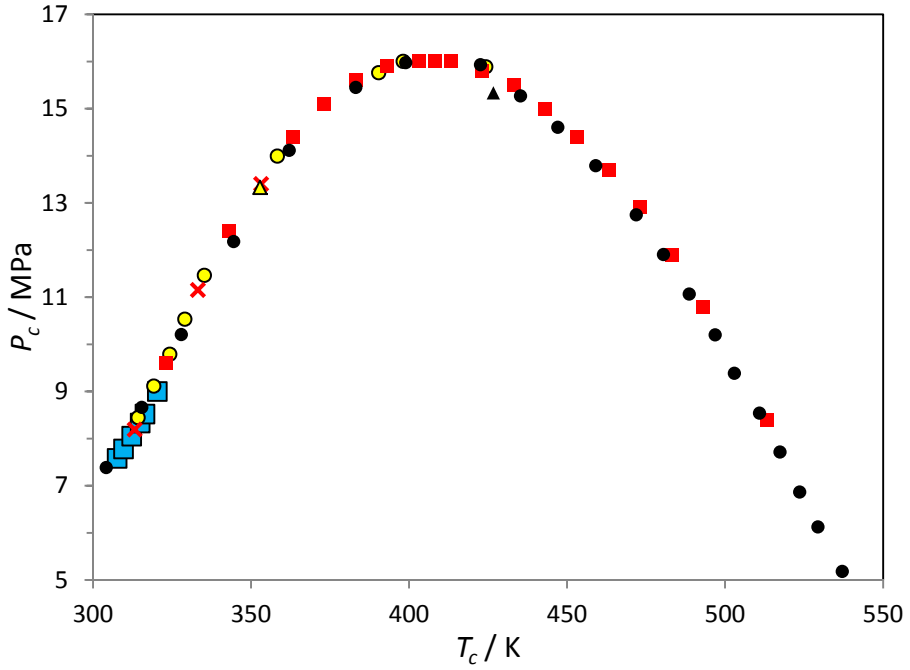

Figure SF9b

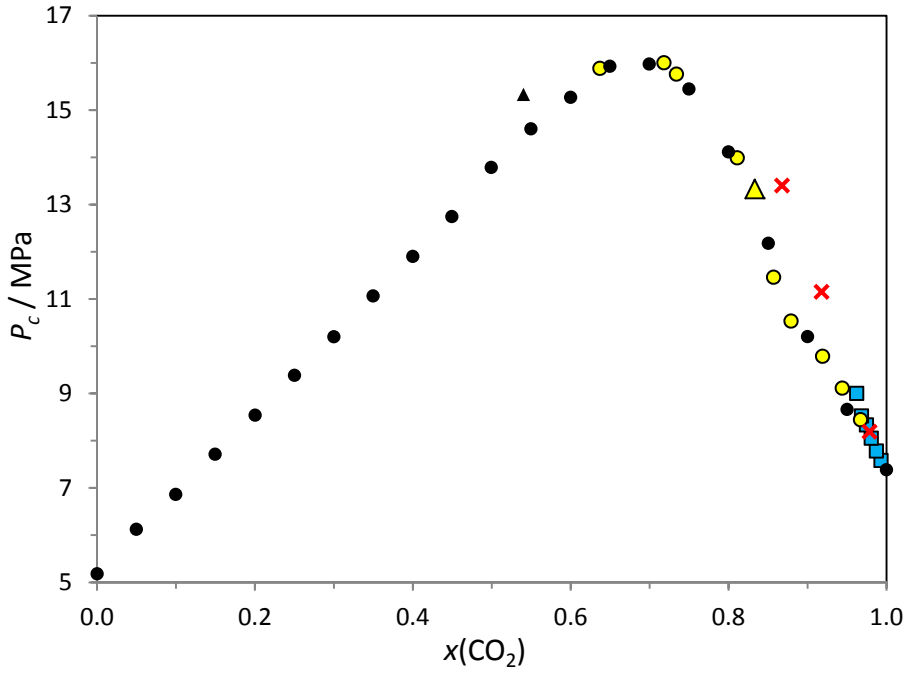

Figure SF9c

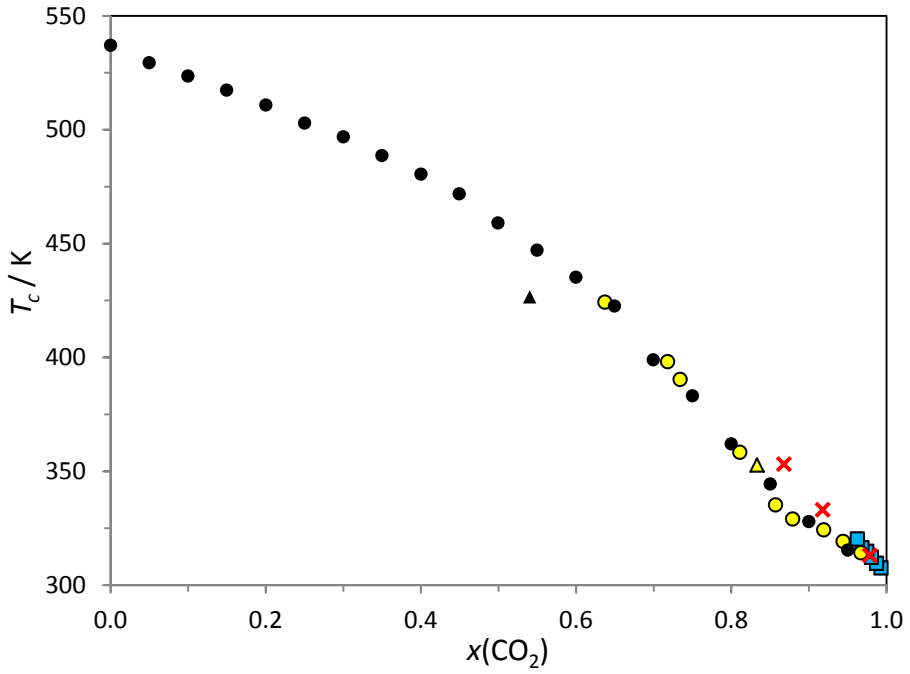

Figure SF10. (a), (P_c, T_c); (b), (P_c, x) and (c), (T_c, x) projections for CO_2 + butan-1-ol critical locus. Experimental results from this work and literature: ●, this work; ■, ref. [73]; ○, ref. [75]; □, ref. [78]; +, ref. [95]; ×, ref. [96].

Figure SF10a

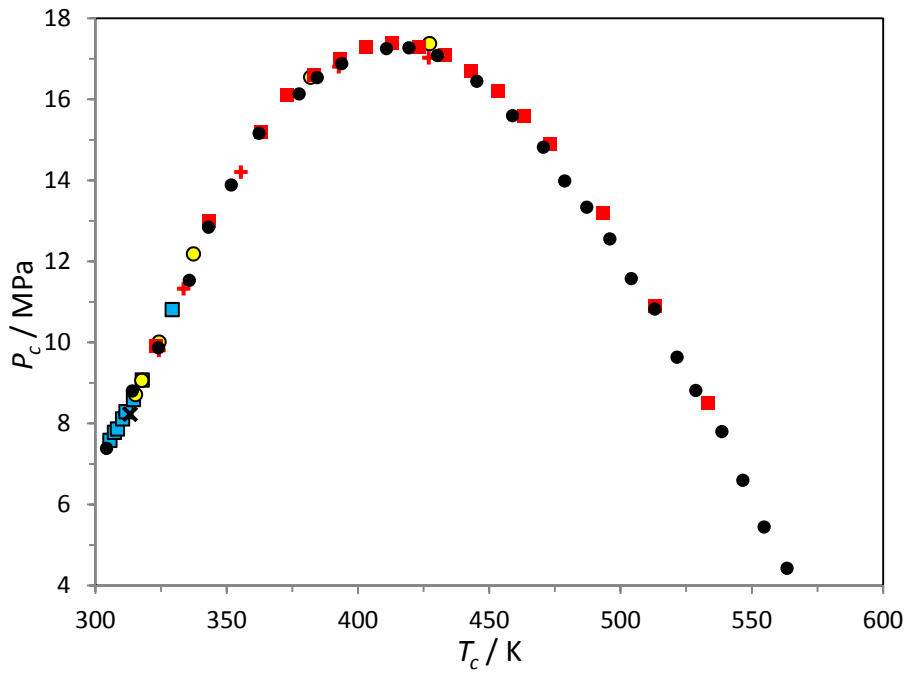

Figure SF10b

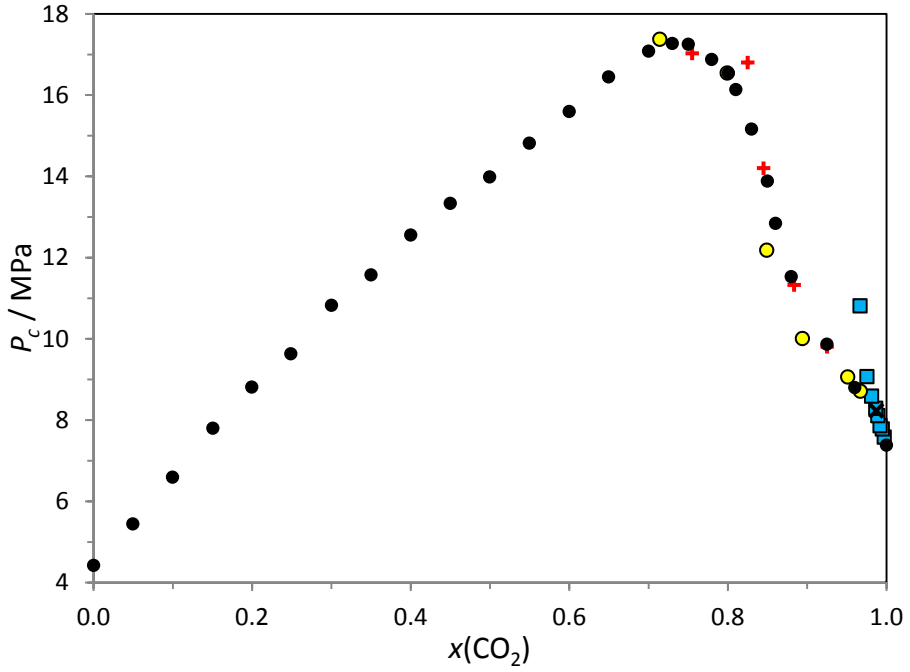

Figure SF10c

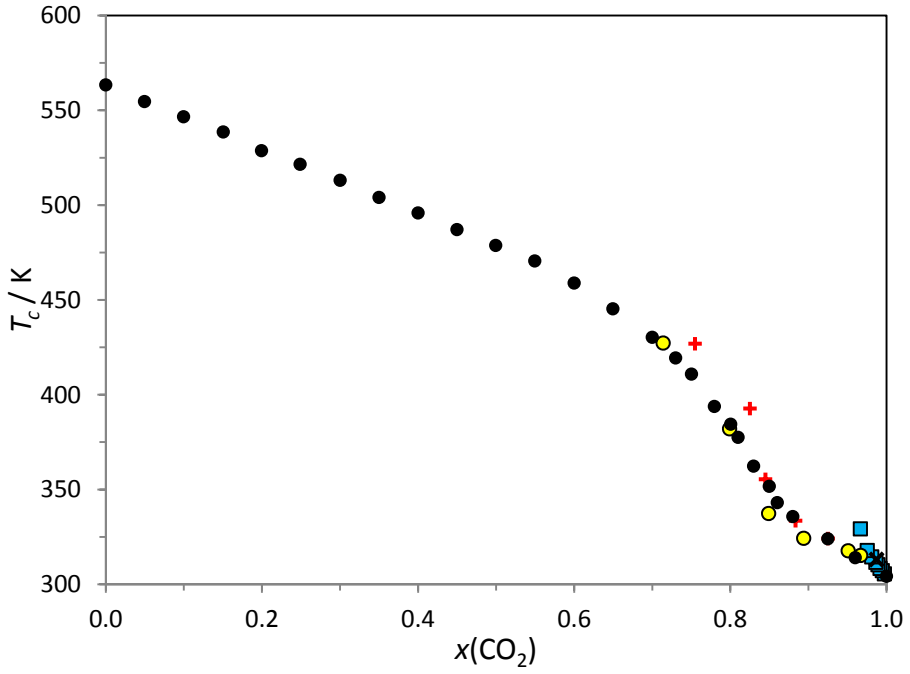

Comparison between this work experimental data and those from literature for the critical loci of CO_2 + alkan-1-ol systems.

For the CO_2 + methanol system, Brunner [70,71], Ziegler et al. [72,73] and Liu et al. [54] give data over the whole range of compositions. The latter author determines (x, T_c, P_c) properties while the others just offer (T_c, P_c) values. The rest of the references provide data in the rich or very rich zone in CO_2. The agreement is very good amongst all authors for the P_c-T_c projection, including our current work (except for Semenova et al. [74], whose data show higher deviations when increasing methanol concentration). Nevertheless, T_c-x and P_c-x projections show strong discrepancies: Liu et al. [54] (for x_{CO_2} > 0.6), Semenova et al. [74] and Yeo et al.'s [75] data are the most disperse, showing differences of up to 60 degrees and 6 MPa. Our T_c-x and P_c-x results are in good agreement with Yoon et al. [76] and Joung et al. [77], as well as with Liu et al. [54] in the rich-alcohol zone (x_{CO_2} < 0.6) and with Gurdial et al. [78] for its CO_2 richest points; Brunner [71] and Leu et al. [79] report similar data, slightly lower than ours, but in agreement when it comes to the shape of the curve in T_c-x, while this shape is a little displaced in P_c-x values.

Only Ziegler et al. [73] provide data along the whole range of compositions for CO_2 + ethanol (T_c, P_c) measurements. The rest of the authors present data for CO_2-rich mixtures. Overall agreement is in general good, except with Tian et al. [82] and with Sima et al. [83] for x_{CO_2}< 0.842. The agreement is better in the P_c-T_c projection (where even Tian et al. [82] and Sima et al. [83] are in good agreement with the others) than in T_c-x or P_c-x planes, though Ziegler and Dorsey's [72] data present P_c vs. T_c values higher than ours.

Chang et al. [93] give only graphic data for CO_2 + methanol or + ethanol systems, both in the very rich zone in CO_2. Their results are slightly higher than ours in the P_c-x and T_c-x projections but they are in good agreement in the P_c-T_c plane.

For CO_2 + propan-1-ol, Ziegler et al. [73] give data along the whole range of compositions providing (T_c, P_c) measurements. The rest of the references provide (x, T_c, P_c) data for 0.5 < x_{CO_2}< 0.85. Our results are in very good agreement with Ziegler et al. [73] and Yeo et al. [75]. Secuianu et al. [68] and Gurdial et al.'s [78] data show good agreement with our work in the P_c-T_c projection, but this agreement is worse in T_c-x and P_c-x.

Again, Ziegler et al. [73] are the only authors who give data covering the whole range of compositions for CO_2 + butan-1-ol, while other studies concentrate on CO_2-rich mixtures. Results from all of the authors, including ours, show very good agreement in the P_c-T_c projection. In the T_c-x and P_c-x planes our results are in very good agreement with several of the points from Yeo et al. [75] and Silva-Oliver and Galicia-Luna [95].

Figure SF11. Pressure–mole fraction diagram for *n*-hexane + propan-1-ol VLE. Symbols, experimental data: ○, T = 298.15 K, ref. [119]; ★, T = 313.15 K, ref. [121]; ◇, T = 323.15 K, ref. [123]; ▲, T = 483.15 K, ref. [50]; ■, T = 493.15 K, ref. [50]. Lines, calculated with PC-SAFT EoS using the parameters from Tables 5 and 7.

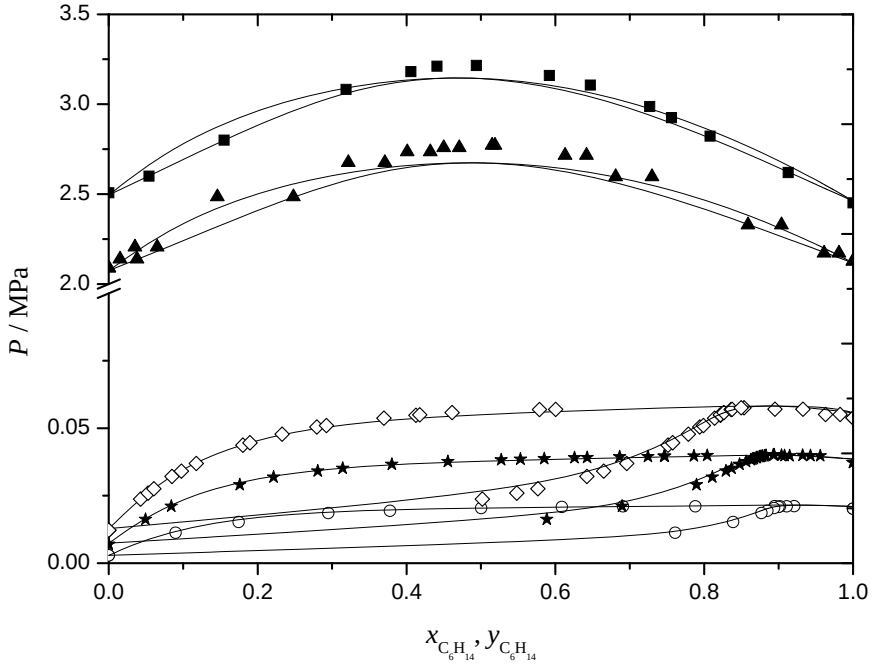

Figure SF12. Pressure–mole fraction diagram for *n*-hexane + butan-1-ol VLE. Symbols, experimental data: ○ , T = 288.15 K, ref. [124]; ★, T = 298.15 K, ref. [125]; ◇, T = 313.15 K, ref. [124]; ■, T = 333.15 K, ref. [126]. Lines, calculated with PC-SAFT EoS using the parameters from Tables 5 and 7.

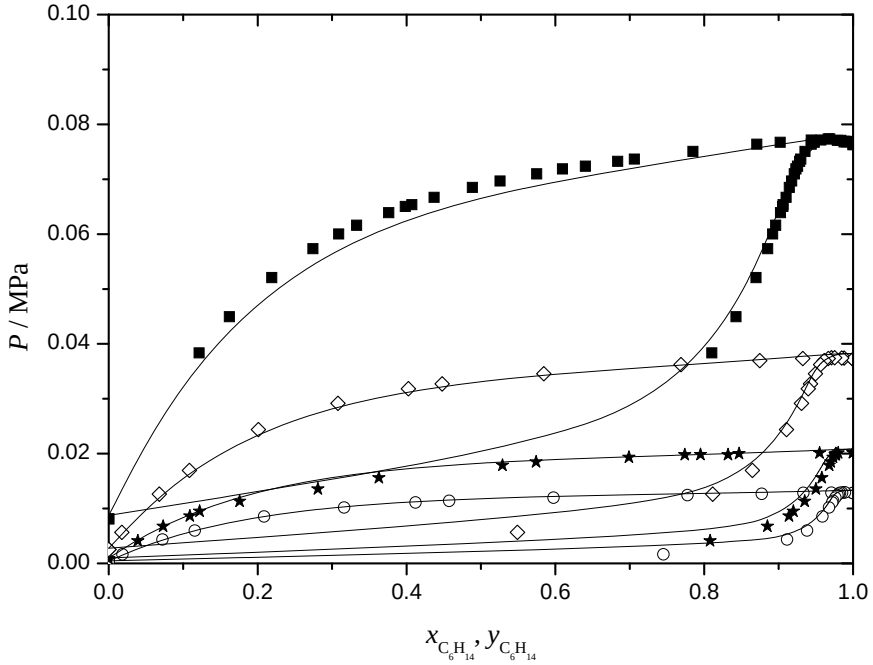

Figure SF13. Pressure–mole fraction diagram for *n*-hexane + pentan-1-ol VLE. Symbols, experimental data: ○ , *T* = 303.15 K, ref. [127]; ★, *T* = 323.15 K, ref. [127]. Lines, calculated with PC-SAFT EoS using the parameters from Tables 5 and 7.

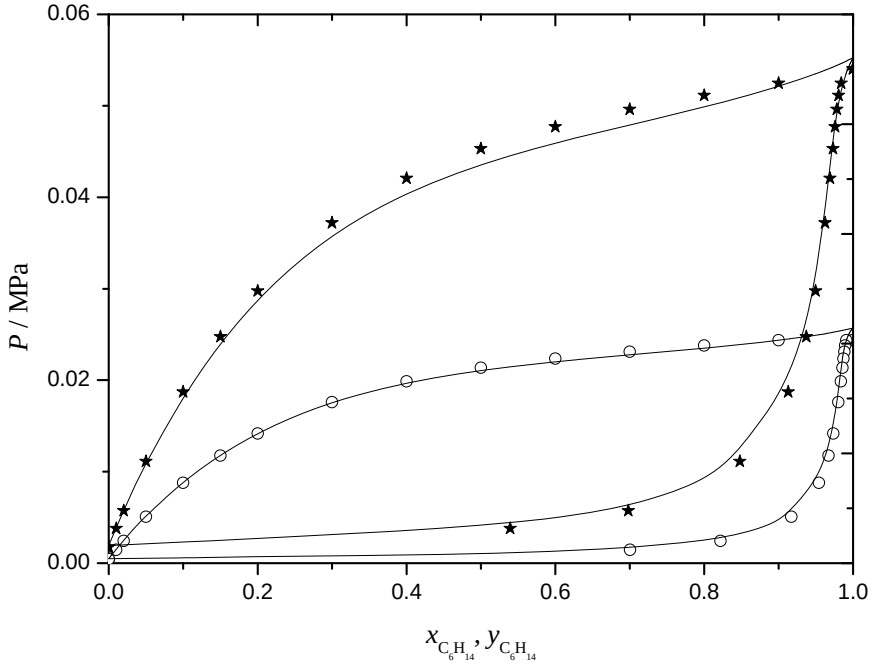

Figure SF14. Pressure–mole fraction diagram for *n*-hexane + hexan-1-ol VLE. Symbols, experimental data: ○ , *T* = 298.15 K, ref. [129]; ★, *T* = 323.15 K, ref. [128]; ◇, *T* = 343.15 K, ref. [129]; ■, *T* = 363.15 K, ref. [128]. Lines, calculated with PC-SAFT EoS using the parameters from Tables 5 and 7.

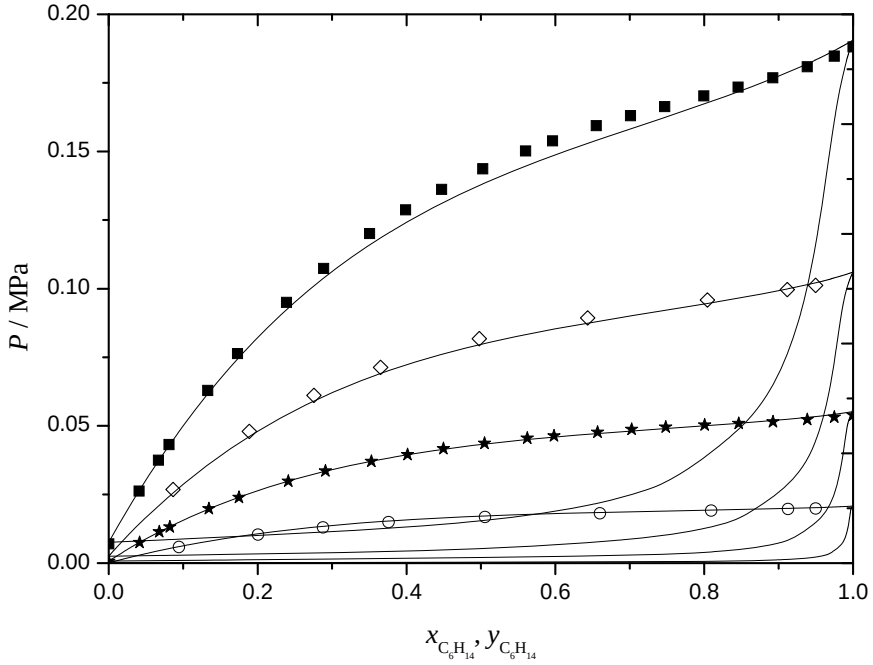

Figure SF15. Pressure–mole fraction diagram for CO_2 + propan-1-ol VLE. Symbols, experimental data: ○, T = 293.15 K, ref. [68]; ★, T = 303.15 K, ref. [68]; ◇, T = 313 K, ref. [183]; ⌂, T = 333.15 K, ref. [184]; ■, T = 353.15 K, ref. [68]; □, T = 397.48 K, ref. [186]. Lines, calculated with PC-SAFT EoS using the parameters from Tables 9 and 10.

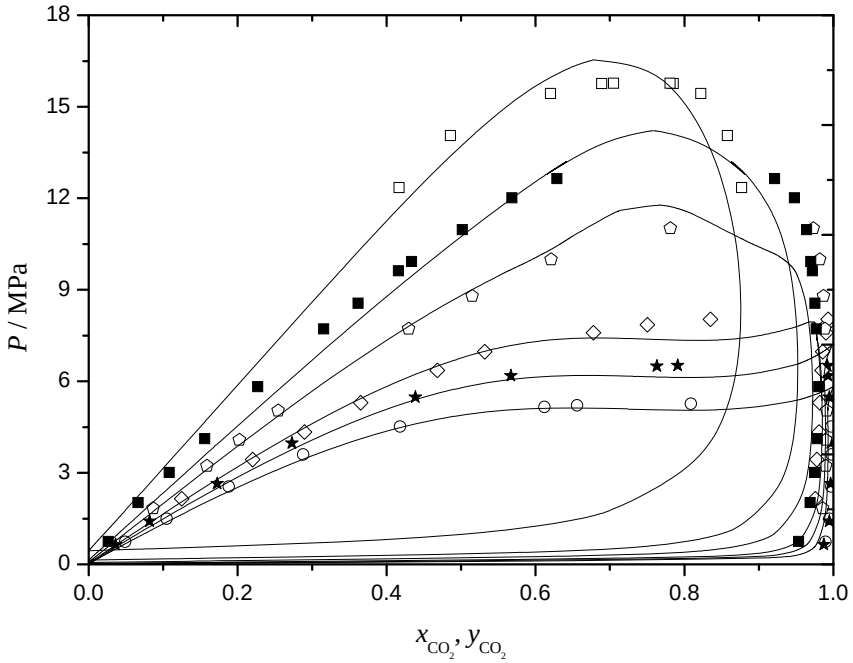

Figure SF16. Pressure–mole fraction diagram for CO_2 + butan-1-ol VLE. Symbols, experimental data: ○, T = 293.15 K, ref. [187]; ★, T = 313.15 K, ref. [187]; ◇, T = 337.2 K, ref. [179]; ⌂, T = 392.72 K, ref. [95]; □, T = 426.95 K, ref. [95]. Lines, calculated with PC-SAFT EoS using the parameters from Tables 9 and 10.

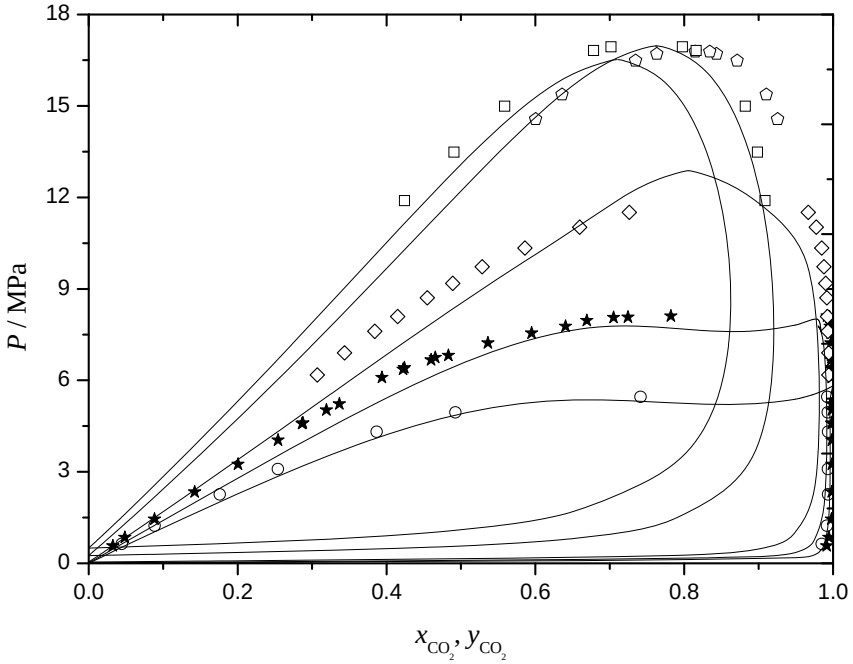

Table ST1. Temperature range covered by the data used in the modellization of the studied systems; range of the temperature-dependent binary interaction parameters, $k_{ij}(T)$, obtained for these temperatures and temperature-independent binary interaction parameters, k_{ij}.

System	VLE and critical locus		
	Range T / K	**Range $k_{ij}(T)$**	**k_{ij}**
n-C_6H_{14}+CH_3OH	293-513	0.0434-0.0742	0.0470
n-C_6H_{14}+C_2H_5OH	263-515	0.0116-0.0209	0.0163
n-C_6H_{14}+C_3H_7OH	298-537	0.0210-0.0366	0.0289
n-C_6H_{14}+C_4H_9OH	288-563	0.00939-0.0169	0.0132
n-C_6H_{14}+$C_5H_{11}OH$	303-588	0.00647-0.0111	0.00900
n-C_6H_{14}+$C_6H_{13}OH$	293-545	0.00774-0.0131	0.0104
CO_2+CH_3OH	213-513	0.0290-0.115	0.0720

	VLE			**Critical locus**		
	Range T / K	**Range $k_{ij}(T)$**	**k_{ij}**	**Range T / K**	**Range $k_{ij}(T)$**	**k_{ij}**
CO_2+C_2H_5OH	283-494	0.0973-0.123	0.104	304-514	0.0790-0.134	0.0910
CO_2+C_3H_7OH	293-427	0.112-0.108	0.109	304-537	0.0806-0.142	0.0949
CO_2+C_4H_9OH	293-430	0.133-0.107	0.120	304-563	0.0882-0.163	0.110

Table ST2. Mean relative deviations in critical temperature, *MRD(Tc)*, critical pressure, *MRD(Pc)*, and bubble pressure, *MRD(P)*, and absolute deviations for the solvent mole fraction in the vapor phase, Δy, obtained using the pure-compounds parameters from Tables 5 and 10 and the temperature-dependent or temperature-independent binary interaction parameters for the modelled systems.

System	Binary Interaction Parameters	Critical locus		VLE	
		MRD(Tc)/%	***MRD(Pc)/%***	***MRD(P)/%***	$\Delta y_{C_6H_{14}}$
n-C_6H_{14}+CH_3OH	$k_{ij}(T)=0.00234+1.40\times10^{-4}T$	0.94	6.26	3.20	0.010
	$k_{ij}=0.0470$	0.45	6.47	3.86	0.030
n-C_6H_{14}+C_2H_5OH	$k_{ij}(T)=0.00187+3.70\times10^{-5}T$	0.50	2.46	3.43	0.026
	$k_{ij}=0.0163$	0.36	2.28	3.38	0.049
n-C_6H_{14}+C_3H_7OH	$k_{ij}(T)=0.00153+6.54\times10^{-5}T$	0.23	1.48	2.01	0.007
	$k_{ij}=0.0289$	0.26	1.34	4.47	0.014
n-C_6H_{14}+C_4H_9OH	$k_{ij}(T)=0.00153+2.73\times10^{-5}T$	0.19	0.97	3.25	0.009
	$k_{ij}=0.0132$	0.24	0.90	4.29	0.013
n-C_6H_{14}+$C_5H_{11}OH$	$k_{ij}(T)=0.00153+1.63\times10^{-5}T$	0.42	1.07	2.68	0.005
	$k_{ij}=0.0090$	0.44	1.05	3.83	0.003
n-C_6H_{14}+$C_6H_{13}OH$	$k_{ij}(T)=0.00153+2.12\times10^{-5}T$	0.21	1.12	1.81	0.002
	$k_{ij}=0.0104$	0.12	0.89	2.56	0.002
System	**Binary Interaction Parameters**	**Critical locus**		**VLE**	
		MRD(Tc)/%	***MRD(Pc)/%***	***MRD(P)/%***	Δy_{CO_2}
CO_2+CH_3OH	$k_{ij}(T)=-0.0323+2.88\times10^{-4}T$	2.67	7.17	6.04	0.008
	$k_{ij}=0.072$	2.92	9.11	11.04	0.010
CO_2+C_2H_5OH	$k_{ij}(T)=2.60\times10^{-4}T$	1.37	6.17	----	----
	$k_{ij}=0.091$	1.32	8.62		
	$k_{ij}(T)=0.0625+1.23\times10^{-4}T$	----	----	7.85	0.031
	$k_{ij}=0.104$			9.23	0.034
CO_2+C_3H_7OH	$k_{ij}(T)=2.65\times10^{-4}T$	1.16	3.53	----	----
	$k_{ij}=0.095$	1.20	6.23		
	$k_{ij}(T)=0.118-2.15\times10^{-5}T$	----	----	6.89	0.033
	$k_{ij}=0.109$			7.87	0.038
CO_2+C_4H_9OH	$k_{ij}(T)=2.90\times10^{-4}T$	1.92	5.17	----	----
	$k_{ij}=0.110$	1.56	7.91		
	$k_{ij}(T)=0.190-1.93\times10^{-4}T$	----	----	8.76	0.034
	$k_{ij}=0.120$			12.2	0.023

Table ST3. Comparison between the results from this work modellization and those from literature for *n*-hexane + alkan-1-ol systems.

System	Model	Binary Interaction Parameters	Range *T*/K	*MRD(P)*/%	$\Delta y_{C_6H_{14}}$	*MRD(T_c)*/%	*MRD(P_c)*/%	Ref.
n-C_6H_{14}+CH_3OH	PC-SAFT	*Temperature dependent*	293-513	3.20	0.010	0.94	6.26	This work
	tPC-PSAFT	*Non temperature dependent*	313-348	4.0	----	----	----	[132]
	GC-PC-SAFT	*Non temperature dependent*	293-448	6-7	----	----	----	[134]
	CPA	*Temperature dependent*	298-333	2.6	0.018	----	----	[136]
alkane+CH_3OH	sPC-PSAFT	*Fitted*	273-423	2.8	0.015	----	----	[137]
	PC-SAFT	*Temperature dependent*	313-463	3-8	----	----	----	[32]
n-C_6H_{14} + C_2H_5OH	PC-SAFT	*Temperature dependent*	263-515	3.43	0.026	0.50	2.46	This work
	PC-SAFT	*Non temperature dependent*	488-514	----	----	0.15	----	[133]
	sPC-PSAFT	*Non temperature dependent*	273.15	3.5	0.009	----	----	[33]
	SAFT-VR	0	263-303	9.7	0.027	----	----	[131]
	CPA	*Non temperature dependent*	298.15	1.2	0.005	----	----	[136]
n-C_6H_{14} + C_3H_7OH	PC-SAFT	*Temperature dependent*	298-537	2.01	0.007	0.23	1.48	This work
	sPC-PSAFT	0	348.15	5.8	0.024	----	----	[33]
	SAFT-VR	0	318-348	10.3	0.030	----	----	[131]
	CPA	*Non temperature dependent*	298-323	1.3	0.005	----	----	[136]
n-C_6H_{14} + C_4H_9OH	PC-SAFT	*Temperature dependent*	288-563	3.25	0.009	0.19	0.97	This work
	SAFT-VR	0	323-348	7.67	----	----	----	[131]
	CPA	*Non temperature dependent*	298-333	3.5	0.005	----	----	[136]
n-C_6H_{14} +$C_5H_{11}OH$	PC-SAFT	*Temperature dependent*	303-588	2.68	0.005	0.42	1.07	This work
	PC-SAFT	*Non temperature dependent*	507-587	----	----	0.10	----	[133]
	SAFT-VR	0	303-545	6.30	----			[131]
n-C_6H_{14} +$C_6H_{13}OH$	PC-SAFT	*Temperature dependent*	293-545	1.81	0.002	0.21	1.12	This work
	sPC-PSAFT	0	323.15	6.3	----	----	----	[33]
	SAFT-γ	0	323.15	4.08	----	----	----	[135]
	SAFT-VR	0	293-373	5.69	----	----	----	[131]

Table ST4. Comparison between the results from this work modellization and those from literature for CO_2 + alkan-1-ol systems.

System	Model	Binary Interaction Parameters	Range *T*/K	*MRD(P)/%*	Δy_{CO_2}	*MRD(T_c)/%*	*MRD(P_c)/%*	Ref.
CO_2+CH_3OH	PC-SAFT	*Temperature dependent*	213-513	6.04	0.008	2.67	7.17	This work
	PC-SAFT	*Non temperature dependent*	291-492	----	----	0.08	0.01	[133]
	PC-SAFT	*Temperature dependent*	230-478	7.9	0.027	----	----	[31]
	PC-SAFT-QD	*Temperature dependent*	230-478	11.4	0.033	----	----	[31]
	SAFT-VR	*Non temperature dependent*	313	0.46	0.005	----	----	[139]
	CPA	*Non temperature dependent*	273-290	1.3	0.001	----	----	[138]
	CPA	*Temperature dependent*	291-313	----	0.003	----	----	[34]
	PR-WS-VL	*Temperature dependent*	313-343	2.92	< 0.02	----	----	[140]
CO_2+C_2H_5OH	PC-SAFT	*Temperature dependent*	283-514	7.85	0.031	1.37	6.17	This work
	PC-SAFT	*Non temperature dependent*	291-373	----	----	0.12	0.02	[133]
	PC-SAFT	*Temperature dependent*	291-373	15.9	0.020	----	----	[31]
	PC-SAFT-QD	*Temperature dependent*	291-373	15.0	0.021	----	----	[31]
	sPC-SAFT	*Temperature dependent*	291-313	10.2	0.007	----	----	[33]
	SAFT-VR	*Non temperature dependent*	313	4.03	0.002	----	----	[139]
	CPA	*Temperature dependent*	291-313	----	0.020	----	----	[34]
	CPA	*Non temperature dependent*	291	1.0	0.004	----	----	[138]
	PR-WS-VL	*Temperature dependent*	313-345	1.65	< 0.02	----	----	[140]
	PR-VL	*Temperature dependent*	283-337	3.08	0.006	----	----	[143]
CO_2+C_3H_7OH	PC-SAFT	*Temperature dependent*	293-537	6.89	0.033	1.16	3.53	This work
	PC-SAFT	*Non temperature dependent*	313-333	----	----	0.20	0.01	[133]
	PC-SAFT	*Temperature dependent*	308-337	12.9	0.003	----	----	[31]

	PC-SAFT-QD	*Temperature dependent*	308-337	8.2	0.003	----	----	[31]
	CPA	*Temperature dependent*	315-337	----	0.002	----	----	[34]
	CPA	*Non temperature dependent*	313-333	7.4	0.002	----	----	[138]
	PR-WS	*Temperature dependent*	344-427	1.2	0.010	----	----	[94]
	PR-WS-VL	*Temperature dependent*	313-337	3.5	< 0.02	----	----	[140]
	PR-VL	*Temperature dependent*	313-337	1.52	0.001	----	----	[143]
CO_2+C_4H_9OH	PC-SAFT	*Temperature dependent*	293-563	8.76	0.034	1.92	5.17	This work
	PC-SAFT	*Non temperature dependent*	303-428	----	----	0.18	0.01	[133]
	PC-SAFT	*Temperature dependent*	293-427	12.1	0.014	----	----	[31]
	PC-SAFT-QD	*Temperature dependent*	293-427	10.3	0.010	----	----	[31]
	CPA	*Temperature dependent*	293-324	----	0.005	----	----	[34]
	PT-NRTL	*Temperature dependent*	324-427	0.9	0.017	----	----	[95]
	PR-WS	*Temperature dependent*	354-430	1.4	0.008	----	----	[94]
	PR-WS-VL	*Temperature dependent*	314-337	3.5	< 0.02	----	----	[140]
	PR-VL	*Temperature dependent*	298-337	1.12	0.012	----	----	[143]